

**Methodologies for Mixing Zone Model Validation of
Surface Thermal Discharges in Large Rivers**

Chengjung Wu

B.S., Environmental Engineering, National Chung-Hsing University, Taiwan (2000)

**A thesis (dissertation) presented to the faculty of the
OGI School of Science & Engineering
at Oregon Health & Science University
in partial fulfillment of the
requirements for the degree
Master in Science
in
Environmental Science and Engineering**

The dissertation "Methodologies of Mixing Zone Model Validation of Surface Thermal Discharge in Large Rivers" by Chengjung Wu has been examined by the following Examination Committee:

Dr. Robert L. Doneker, Thesis Advisor
Assistant Professor, OGI School of Science & Engineering

Dr. Antonio M. Baptista
Professor, OGI School of Science & Engineering

Dr. David A. Jay
Associate Professor, OGI School of Science & Engineering

Table of Contents

TABLE OF CONTENTS	III
LIST OF FIGURES.....	V
LIST OF TABLES.....	VIII
ABSTRACT.....	IX
1 INTRODUCTION.....	1
1.1 CURRENT ISSUES IN ENERGY DEMAND AND THERMAL POLLUTION	1
1.2 DEFINITION OF TERMS IN THIS STUDY.....	3
1.3 PURPOSE.....	3
2 THERMAL PLUME FIELD DATA ACQUISITION AND DATA QUALITY.....	6
2.1 FIELD DATA COLLECTION.....	6
3 THERMAL PLUME TEMPERATURE SIMULATION.....	10
3.1 HYDRODYNAMIC MIXING PROCESSES.....	10
3.2 INTRODUCTION OF CORNELL MIXING ZONE EXPERT SYSTEM (CORMIX)..	12
3.3 SURFACE DISCHARGE FLOW CLASSIFICATION.....	14
3.4 PARAMETERIZATION FOR CORMIX SIMULATION	17
3.5 APPLICATION OF THE FAR FIELD LOCATOR (FFL)	38
4 FIELD DATA PROCESSING AND UTILITY DEVELOPMENT	42
4.1 FIELD DATA PRE-PROCESSING.....	42
4.2 ARCVIEW MAPPING METHODOLOGY DEVELOPMENT.....	61
4.3 CORMIX-RELATED SOFTWARE DEVELOPMENTS	62
5 MODEL VALIDATION	73
5.1 COOPER NUCLEAR STATION	73
5.2 FORT CALHOUN GENERATING STATION.....	83
5.3 NEBRASKA CITY POWER STATION	91
5.4 NORTH OMAHA POWER STATION	96
5.5 OVERALL RESULTS AND STATISTICS ANALYSIS.....	101
6 REGULATORY MIXING ZONES FOR THERMAL DISCHARGES AT STUDY SITES.....	109
6.1 INTERPRETING THE MEAN VELOCITY, AVERAGE WATER DEPTH, AND DEPTH AT DISCHARGE.....	109
6.2 THERMAL DISCHARGE ASSESSMENT BASED ON THE CORMIX SIMULATION	113
7 SATELLITE THERMAL IMAGERY	127

7.1	INTRODUCTION OF MULTI-SPECTRAL THERMAL IMAGER	127
7.2	ANALYSIS OF THE MTI REMOTE SENSED DATA	129
8	CONCLUSIONS AND RECOMMENDATIONS.....	132
8.1	CONCLUSIONS.....	132
8.2	RECOMMENDATIONS FOR FIELD SURVEYS.....	134
	REFERENCES.....	136
	APPENDIX A.....	140
	APPENDIX B.....	153

List of Figures

Figure 2.1 Thermal survey sites along the Missouri River	7
Figure 2.2 Screen Shot of WinRiver Program and ADCP data visualizatio	9
Figure 3.1 CORMIX3 Classification	18
Figure 3.2 Upstream Thermistor String Data	19
Figure 3.3 CORMIX Schematization Created by Field ADCP data	22
Figure 3.4 Channel entry bottom slope estimation from ADCP profile	23
Figure 3.5 Illustrations of CORMIX Schematization at Cooper Nuclear Station	32
Figure 3.6 Illustrations of CORMIX Schematization at Fort Calhoun Nuclear Station	34
Figure 3.7 Illustrations of CORMIX Schematization at Nebraska City Power Station	35
Figure 3.8 Illustrations of CORMIX Schematization at North Omaha Power Station	37
Figure 3.9 Illustration of the cumulative discharge method for translating the CORMIX predicted far-field plume to the actual flow characteristics in winding irregular rivers or estuaries [15]	41
Figure 4.1 Illustration of the Boxcar Filtering technique on an input signal	44
Figure 4.2 Trends of Unprocessed and Boxcar-processed Data	45
Figure 4.3 The processed data by applying Boxcar window with different rectangle lengths	46
Figure 4.4 Transversal Excess Temperature Profiles at Cooper Nuclear Station	49
Figure 4.5 The Transversal Excess Temperature Profiles at Fort Calhoun	52
Figure 4.6 Transversal Excess Temperature Profiles at Nebraska City Power Station	55
Figure 4.7 The Transversal Excess Temperature Profiles in North Omaha Power Station	58
Figure 4.8 Cross-sectional distributions of CORMIX predicted jet/plume sections[15]	64
Figure 4.9 Scheme of the Conversion between CORMIX and Geographical Coordinates	66
Figure 4.10 Control Flow of CorGC	70
Figure 4.11 Scheme of Avenue Script in ArcView	72
Figure 5.1 CorVue Plume Visualization for Flow Class SA1 at Cooper Nuclear Station	76
Figure 5.2 Vertical Temperature Profiles of Thermal Surveys and CORMIX Predictions (Cooper Nuclear Station)	77

Figure 5.3 Excess Temperature Lateral Profiles of Field Surveys and CORMIX Predictions (Cooper Nuclear Station)	80
Figure 5.4 CorVue Plume Visualization for Flow Class PL2 at Fort Calhoun Nuclear Station	86
Figure 5.5 Averaged Excess Temperature Profiles in of Averaged Field Surveys and CORMIX Predictions (Fort Calhoun Power Station)	87
Figure 5.6 Excess Temperature Profiles in of Field Surveys and CORMIX Predictions (Nebraska City Power Station)	94
Figure 5.7 Excess Temperature Profiles of Field Surveys and CORMIX Predictions (North Omaha Power Station)	98
Figure 5.8 Overall Comparison of CORMIX Prediction and Field Observation in Temperature, Width, and Thickness – Cooper Station	101
Figure 5.9 Comparison of CORMIX Prediction and Field Observation in Temperature, Width, and Thickness – Ft. Calhoun Station	102
Figure 5.10 Comparison of CORMIX Prediction and Field Observation in Temperature, Width, and Thickness – Nebraska City Station	103
Figure 5.11 Comparison of CORMIX Prediction and Field Observation in Temperature, Width, and Thickness – North Omaha Station	104
Figure 5.12 Regression and Correlation of Flow Class PL2	106
Figure 5.13 Regression and Correlation of Flow Class SA1 in Near-Field Simulation	107
Figure 5.14 Regression and Correlation of Flow Class SA1 in Far-Field Simulation	108
Figure 6.1 Illustration of the Thermal Plume Pattern and Excess Temperature Distribution in 7Q10 Discharge Condition at Cooper Nuclear Power Plant	115
Figure 6.2 Illustration of the Thermal Plume Pattern and Excess Temperature Distribution in mm7Q10 Discharge Condition at Cooper Nuclear Power Plant	116
Figure 6.3 Illustration of the Thermal Plume Pattern and Excess Temperature Distribution in w7Q10 Discharge Condition at Cooper Nuclear Power Plant .	117
Figure 6.4 Illustration of the Thermal Plume Pattern and Excess Temperature Distribution in 7Q10 Discharge Condition at Ft. Calhoun Nuclear Power Plant	118
Figure 6.5 Illustration of the Thermal Plume Pattern and Excess Temperature Distribution in mm7Q10 Discharge Condition at Ft. Calhoun Nuclear Power Plant	119
Figure 6.6 Illustration of the Thermal Plume Pattern and Excess Temperature Distribution in w7Q10 Discharge Condition at Ft. Calhoun Nuclear Power Plant	120

Figure 6.7 Illustration of the Thermal Plume Pattern and Excess Temperature Distribution in 7Q10 Discharge Condition at Nebraska City Coal Fired Power Plant	121
Figure 6.8 Illustration of the Thermal Plume Pattern and Excess Temperature Distribution in mm7Q10 Discharge Condition at Nebraska City Coal Fired Power Plant	122
Figure 6.9 Illustration of the Thermal Plume Pattern and Excess Temperature Distribution in w7Q10 Discharge Condition at Nebraska City Coal Fired Power Plant	123
Figure 6.10 Illustration of the Thermal Plume Pattern and Excess Temperature Distribution in 7Q10 Discharge Condition at North Omaha Coal Fired Power Plant	124
Figure 6.11 Illustration of the Thermal Plume Pattern and Excess Temperature Distribution in mm7Q10 Discharge Condition at North Omaha Coal Fired Power Plant	125
Figure 6.12 Illustration of the Thermal Plume Pattern and Excess Temperature Distribution in w7Q10 Discharge Condition at North Omaha Coal Fired Power Plant	126
Figure 7.1 MTI Thermal Imagery at North Omaha Station, Sept. 9, 2001	131

List of Tables

Table 3.1 Settings in WinRiver for Near-bank Discharge Estimates	25
Table 3.2 Input Parameters for CORMIX Simulations	31
Table 4.1 List of Algorithms Created in CorGC.....	71
Table 6.1 HA and HD under Different Discharges.....	112
Table 6.2 WQ Standards and the Predicted Temperature at 5000 ft (1524 m) Downstream of the Outfall.....	114

Abstract

Methodologies for Mixing Zone Model Validation of Surface Thermal Discharges in
Large Rivers

Chengjung Wu, B.S.

M.S., OGI School of Science & Engineering
Oregon Health & Science University

December 2002

Thesis Advisor: Dr. R. L. Doneker

To meet the increased demand for electricity it will be necessary to expand the capacity of current generating facilities and to build new power plants over the next few decades. The public is concerned with several associated environmental issues, such as air-borne emissions, waste disposal, and water quality impacts from cooling water discharges. Cooling water discharges from steam condensation units can have significant adverse impact on water quality by creating unfavorable habitat for wildlife in the receiving water. To assure protection of a balanced population of aquatic organisms, cooling water discharges from power plants are often regulated with the application of a mixing zone requirement within an allocated impact zone.

The USEPA-approved water quality model CORMIX (Cornell Mixing Zone Expert System) is used to simulate thermal plume dimensions and dilution for four power plants discharges on the Missouri river in Nebraska. A series of methods and techniques are developed to create representative model input for thermal discharge simulation in large rivers. Ambient parameterization is based upon measured field survey data including thermistor string data and Acoustic Doppler Current Profiler (ADCP) river profiling measurements. Discharge conditions are parameterized based on the daily motoring records at power plant facilities and plant construction plans.

CORMIX model validation was conducted on observed plume dimensions, temperatures, and dilution using field data sets from conventional boat surveys and remotely sensed satellite imagery. Advanced remote sensing technology may be preferable to conventional boat surveys for thermal discharge monitoring due to its high synoptic capability and relatively low cost. In this study, Multispectral Thermal Imager (MTI) remote sensed satellite data is analyzed and compared with field observations to evaluate the technology for future model thermal plume validation studies.

The overall results support the CORMIX model predictive capability in simulating plume trajectory and dilution. Statistical analysis also indicates that forecasting of dilution characteristics are well-correlated and correspond to observed field data. The reasonable quantitative agreement shown in this study demonstrates the dilution (temperature) predictability of CORMIX for surface thermal discharges in large rivers. In regards to plume dimensions, there is some under-prediction of plume lateral extent and some mismatches in vertical plume profiles, particularly for unstable near-field flows. In regards to the evaluation of MTI satellite remote sensing data, this technology is not presently applicable to power plant plume monitoring in the Missouri river. This is due to the coarse resolution of imagery and inappropriate atmospheric corrections applied to thermal plume sensor data measurements.

1

Introduction

1.1 Current Issues In Energy Demand and Thermal Pollution

With increasing global energy demand and electricity market deregulation, numerous new electric power plants are being constructed while existing plants are being expanded or are operating at full design capacity. Currently, several environment-related issues, such as air pollution, nuclear waste disposal, and cooling water discharge are of concern in the permit processing for the electricity industry.

More than 75 % of utility-derived power in the United States is generated by the steam electric power industry. Presently, at 3250 US steam-electric utilities the fossil-fuel fired station is the majority whereas only 66 nuclear power stations are commissioned[1, 2]. Conceptually, for this steam-electric power generation, water is heated in a boiler by the combustion of fossil fuels or through a nuclear reaction to generate steam to run steam turbines which drive electric generators. In the cooling system, a large volume of the cool water absorbs the heat of turbine exhaust steam for condensation. Sequentially, the condensed steam (water) is re-circulated to the boiler for reuse while the temperature of the cooling water rises.

Commonly, two types of cooling systems- once-through and closed-cycle- are used for cooling purposes in most power plants. Once-through cooling systems intake large volumes of water from a river, lake, or estuary. This water is pumped through

the condenser and returned at higher temperature to the water body. Therefore, most power plants using one-through cooling system are built on large rivers. The excess temperature can be quickly dissipated by the river current and turbulence. Closed-cycle systems receive smaller volumes and after the condenser return it to a cooling tower, basin, cooling pond, or cooling lake. Make-up water is needed because evaporation removes a portion of the cooling water from the closed-cycle system[2]. About 50% of US generating capacity utilize closed-cycle cooling systems, whereas once-through systems account for 44%[3, 4]. Commonly, the closed-cycle cooling systems are thought to have less environmental impact because of reuse and storage of the heated water, but construction cost are much higher than once-through cooling systems and there is consumptive use through evaporative losses.

For once-through cooling systems, cooling water alters the physical environment in terms of both a reduction in the density of water and its oxygen concentration, both of which vary inversely with temperature. A warmer environment also influences directly the growth dynamics of aquatic organisms, through its influence on rates of ingestion, assimilation, activity, and metabolism. As temperature increases, respiration and heart rate of fish will increase in order to obtain oxygen for an increased metabolic rate. Also, thermal pollution means an increased photosynthesis rate; so that more plants grow and die. These dead plants are consumed by bacteria and other decomposers, and along with the plants consume oxygen. Consequently, dissolved oxygen can be rapidly consumed to form an aquatic zone with the low levels of dissolved oxygen. In this situation, it is more difficult for fish and other aquatic organisms to obtain the necessary oxygen for cellular respiration and can result in high mortality[5-8]. Besides, the entrainment and impingement of small organisms and early life stages of larger organisms in intake structures can significantly reduce populations due to exposure to the high velocity and pressure in the cooling water pumps, as well as to the high temperature[9, 10]. In summation of the adverse effects, cooling water discharges are becoming more important in the environmental impact assessment of anthropogenic activities on surface water systems.

In addition, thermal plume trajectory and mixing behavior is a design concern because the thermal efficiency of power plants is reduced if the heated discharge plume contaminates the cooling water intake. Typical power plant cooling waters have discharge volumes of 10 to 200 m³/s and are heated to an average temperature increase above ambient of approximately $\Delta T = 10^\circ \text{C}$. Cooling waters may be discharged into estuaries, lakes, rivers or the coastal ocean. Because thermal discharges can have adverse environmental impacts they are often subject to regulation and monitoring.

1.2 Definition of Terms in this Study

The following terms are used throughout this study. In order to avoid confusion, the definitions for these terms are presented below.

Simulation: The exercise or use of a model. A process for exercising mathematical models through simulated time wherein one or more models can be run with varying values of input parameters to evaluate the effects of interaction among variables[11].

Prediction: The act of forecasting. A statement deduced from a theory or a model stating the value, or approximate value, of an quantity, and which can be checked by observation[11].

Validation: The process of determining the degree to which a model is an accurate representation of the real world from the perspective of the intended uses of the mode[11].

Calibration: The process of adjusting numerical or physical modeling parameters in the computational model for the purpose of improving agreement with experimental data[11].

1.3 Purpose

All aqueous discharges containing conventional, non-conventional, toxic, heat, or sediment pollutants in the United States are subject to federal, state, and local

regulation. An important aspect of regulation is the concept of a mixing zone. The mixing zone is defined as an “allocated impact zone” where numeric water quality criteria can be exceeded as long as acutely toxic conditions are prevented. A mixing zone can be thought of as a limited area or volume where the initial dilution of a discharge occurs. Water quality standards apply at the boundary of the mixing zone, not within the mixing zone itself [12].

Within the United States (US), Total Maximum Daily Load (TMDL) temperature criteria are increasingly important as part ambient water quality standards. In order to comply with National Pollution Discharge Elimination System (NPDES) permits, thermal impact assessment is therefore becoming routine as part of the Total Maximum Daily Load (TMDL) process in many regions of the country. The U.S Environmental Protection Agency (EPA) is leading in development of procedures and application of modeling tools for point source assessment of thermal discharges on ambient water quality. EPA sponsored this study to i) collect and analyze field data on surface thermal discharges from four large electric power plants ii) develop a validation data base for the CORMIX mixing zone simulation of these discharges, and iii) develop a guidance document for CORMIX application to mixing zone modeling of thermal discharges on large mid-western rivers. This study focuses on the thermal plumes in the Missouri River discharged from four electric generation stations; Fort Calhoun, Cooper, Nebraska City, and North Omaha, all located in the state of Nebraska within EPA Region VII (7).

The Cornell Mixing Zone Expert System (CORMIX), a USEPA-approved water quality modeling and decision support system for mixing zone analysis CORMIX is designed for environmental impact assessment of mixing zones resulting from wastewater discharge from point sources. Simulation the thermal plume behavior is conducted using CORMIX3, the subsystem for surface discharge simulation. This study will include the development of a series of the techniques for model parameterization to generate the realistic and reasonable model input. The model parameterization consists of three components, including ambient, discharge, and geometric conditions and those parameters are determined based on the detailed

field observations on four Missouri River sites and daily motoring records taken at the power plant facilities.

The model validation is also carried out to test the performance of the model in predicting plume trajectory and mixing behavior by comparison with the field data collected onsite.

In addition to the validation of CORMIX, this study also gives guidance the utilization of the model for NPDES permitting for future discharge and river scenarios. Nebraska regulations state that the “temperature of a receiving water shall not be increased by a total of more than 5 °F (3 °C) from natural outside the mixing zone . . . and for warm waters the maximum limit is 90 °F (32 °C)”, and that “. . . mixing zones . . . shall be designed to not exceed 5,000 feet (1524 m) in length.”[13]. Using the results of the validation studies for the four sites, CORMIX will be used to assist the regulatory management of the thermal discharges under annual low flow, summer low flow, and winter low flow critical conditions.

With significant recent progress in remote sensing, new technology with satellite sensor capabilities may offer an additional method for field data collection on thermal discharges. Increased efficiency is possible from utilizing remotely sensed satellite data as a mixing model validation tool. Satellite thermal imagery was obtained to evaluate the feasibility of using remote sensed technology in power plant thermal plume surveys on the Missouri river and to assess the use of remote sensed data for thermal mixing zone analysis and CORMIX model validation.

This study will also provide the recommendations on field data collection for riverine assessment of thermal mixing zones, suggest techniques for field data analysis, propose methods for proper CORMIX model application, and offer additional improvements to the CORMIX system for modeling thermal discharges in riverine systems.

Thermal Plume Field Data Acquisition and Data Quality

2.1 Field Data Collection

In 2001 USEPA led a project to collect thermal discharge plume measurements in the Missouri River at four power plants; Fort Calhoun, Cooper, Nebraska City, and North Omaha as shown in Figure 2.1. EPA obtained logistic assistance, monitoring equipment, survey boat, and crew from the US Geological Survey (USGS). Field data collections were on three consecutive days, September 11th, 12th, and 13th 2001. Data was collected at Fort Calhoun on September 11th, at Nebraska City and North Omaha on September 12th, and at Cooper on September 13th. Late fall dates were selected for the surveys in attempt to capture the period of low ambient flows in the river which correspond to conditions of particular interest in regulatory management.

Conditions during the survey dates were close to ideal with calm clear days, low winds, and ambient air temperature in the 30°C range with relative humidity of 60-70%. The numerical average value of river discharge measured at the 4 sites during the survey dates in the project area was 864.63 m³/s (30.5 10³ ft³/s). Whereas low flow 7Q10 (7-day average low flow with a 10-year return period) discharge is the project area are 721.00 m³/s (25.4 10³ ft³/s)

In the field, a 600-kHz-frequency Workhorse Horizontal Acoustic Doppler Current Profiler (H-ADCP) measured velocity direction, velocity magnitudes, river discharges and bottom bathymetry profiles of each river transect. However, the

ADCP raw data can only read by the manufacturer's proprietary WinRiver software. WinRiver reads the raw ADCP data, plots the velocity magnitudes, and then tabulates the associated river discharge, water depths along the sampling transect. Ship track

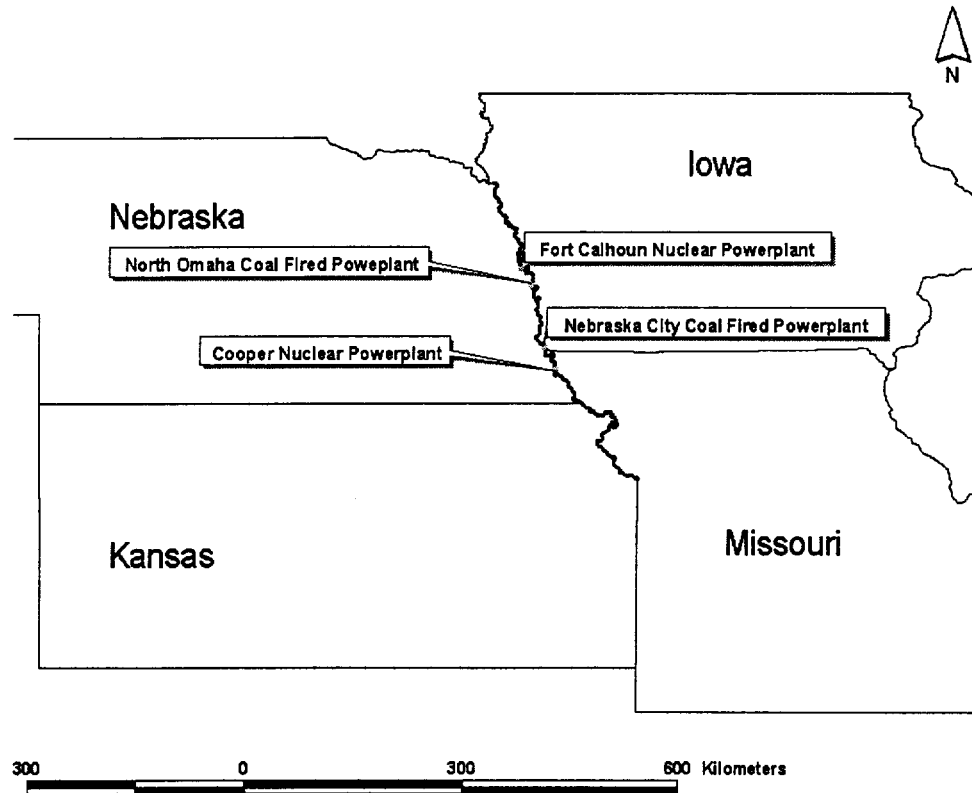


Figure 2.1 Thermal survey sites along the Missouri River

and navigation information are also included in the WinRiver output as shown in Figure 2.2. WinRiver Version 1.03 was used in this study for processing the profiling measurements and extracting the ambient input parameters for CORMIX simulations.

A thermistor string probe, Model 4159-1/8-TH55031-SL probe, was used to detect water temperatures. Readings were taken at surface level, 0.3-m, 0.9-m, 1.7-m, 2.1-m, 2.7-m, 3.7-m and 4.6-m depths. The time interval of the data collection was 5 seconds. The entire raw thermistor data set for the four survey sites was recorded in 57.3 Mbytes.

In addition to the thermistor string, the transducer on the ADCP also recorded the water temperature constantly at 0.21 m below water surface. This data was used to cross-check thermistor string data.

Both the ADCP and thermistor data are associated with time recorded by timer. The Geographical Positioning System (GPS) equipment, Model LGBX, manufactured by Communication System Internal, was mounted on the ADCP transducer and therefore, only the ADCP data is geo-location associated. Because the sampling time was recorded on both ADCP and thermistor data, it was straightforward to integrate thermistor string data with the ADCP data to present the temperature distribution geographically.

Nine (9) river transects were taken for each sites of interest. For each river transect, data collection started several meters away from the bank due to difficulties of placing the survey boat and sensitive equipment too close to the near-bank shallows. In fast flowing rivers like the Missouri, banks are often brush-filled overhangs with subsurface snags which present a hazard to the survey boat and crew. Estimated distances from the near bank to the point where data collection began were noted for each transect and recorded.

At each survey site, one bankfull transect was taken upstream of the location where the thermal discharge entered the river. The purpose of this was to provide detailed upstream ambient conditions such as temperature, velocity profile, cumulative discharge from the nearest bank, and river cross-section geometry. This data was necessary for ambient characterization and parameter input for CORMIX simulations. Random transects were also taken around the outfall in order to capture the plume properties at the discharge and plume development in the near-field.

Following the random transect, several incomplete river transects were taking along the Missouri river perpendicular to the shoreline. In each transect the data collection ended based on naked-eye judgment to estimate the lateral boundary of the thermal plume. The final complete transects were taken approximately 1500 meters downstream of the outfall. This transect was used to monitor overall changes in ambient environment within a plume survey.

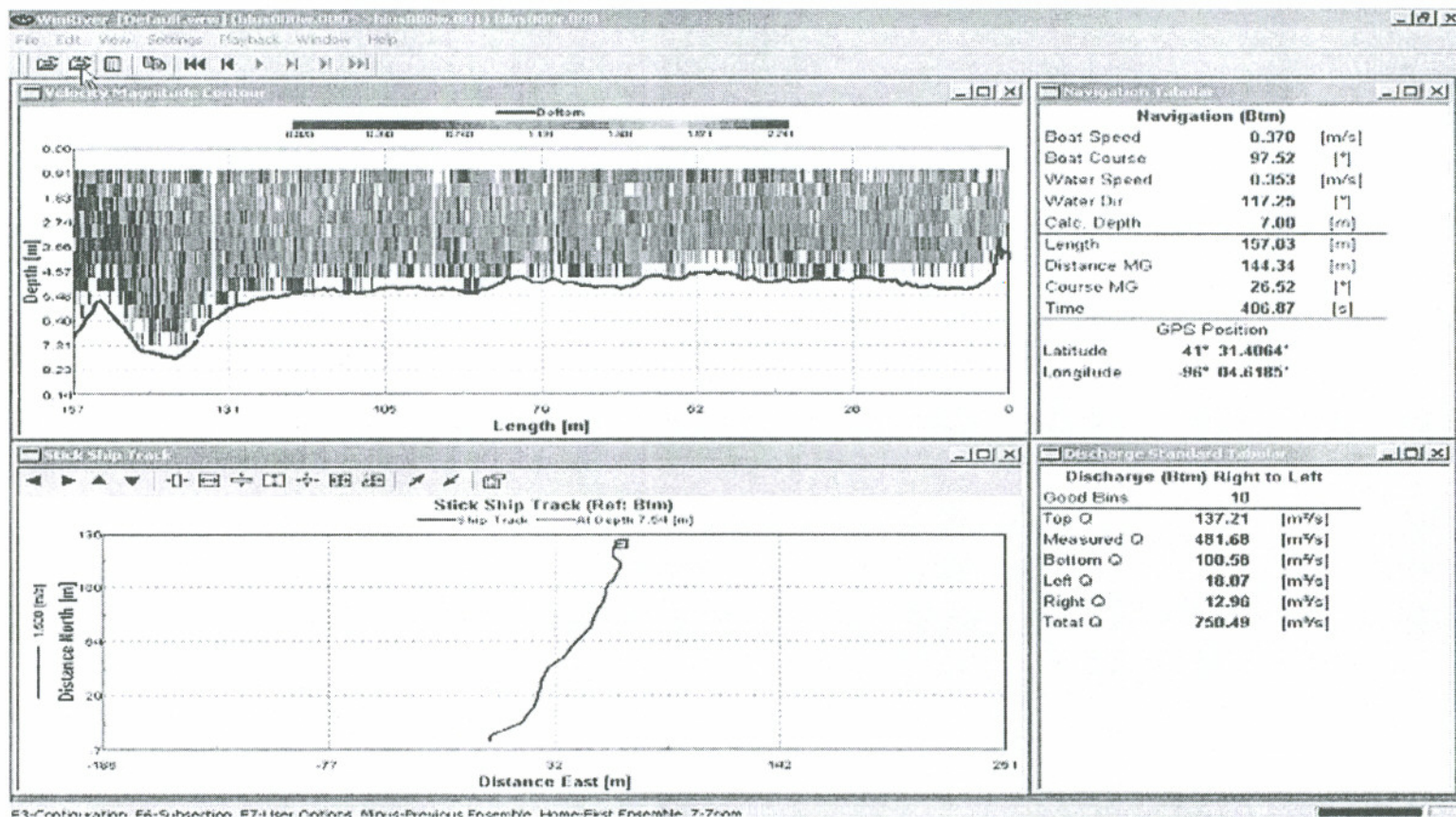


Figure 2.2 Screen Shot of WinRiver Program and ADCP data visualization

The upper left window shows in the velocity magnitude along the ship track. The lower right window lists the all the discharge variables. The lower window illustrates the ship track in the geographical coordinates and the navigation information is included in the table in the upper right window.

Thermal Plume Temperature Simulation

As noted previously, CORMIX was the mixing zone modeling tool used in this study. In this chapter the main features, hydrodynamic background, and associated simulation tools within the model are presented. The development of input parameters for ambient and discharge conditions is also covered. The schematization process for representing river channel and local discharge geometry at each study site is discussed case-by-case. In addition, the Far Field Locator (FFL) post-processor will be described for reconciling far-field plume width based on river cumulative discharge. These techniques are used in the model field data validation and optimization presented in Chapter 5.

3.1 Hydrodynamic Mixing Processes

The mixing behavior of any wastewater discharge is governed by an interplay of ambient conditions and discharge characteristics. The ambient conditions in the receiving water body, be it a stream, river, lake, reservoir, estuary or coastal waters, are described by the water body's geometric and dynamic characteristics. Important geometric parameters include plan shape, vertical cross-sections, and bathymetry, especially in the discharge vicinity. Dynamic characteristics are given by the velocity and density distribution in the water body, again primarily in the discharge vicinity

Discharge conditions relate to the geometric and flux characteristics of the submerged outfall installation. The flux characteristics are given by the effluent discharge flow rate, by its momentum flux and by its buoyancy flux. The buoyancy flux represents the effect of the relative density difference between the effluent and ambient and ambient condition which gives rise to a gravitational acceleration force.

The hydrodynamics of an effluent continuously discharging into a receiving water body can be conceptualized as a mixing process occurring in two separate regions. In the first region, the initial jet characteristics of momentum flux, buoyancy flux, and outfall geometry influence the jet trajectory and mixing. This region will be referred to as the "near-field", and encompasses the buoyant jet flow and any surface, bottom or terminal layer interaction. In this near-field region, outfall designers can usually affect the initial mixing characteristics through appropriate manipulation of design variables.

As the turbulent plume travels further away from the source, the source characteristics become less important. Conditions existing in the ambient environment will control trajectory and dilution of the turbulent plume through buoyant spreading motions and passive diffusion due to ambient turbulence. This region will be referred to here as the "far-field". It is stressed at this point that the distinction between near-field and far-field is made purely on hydrodynamic grounds. It is unrelated to any regulatory mixing zone definitions[14, 15].

For the typical thermal plume behaviors, the discharge often behaves as buoyant surface because not only the initial jet momentum but also the buoyancy influences the plume propagation in the near-field. In the far-field where the jet momentum becomes weaker, the buoyancy lifting is the predominant mechanism followed by a passive diffusion region, as buoyancy within the plume decreases and ambient turbulence dominates mixing.

3.2 Introduction of Cornell Mixing Zone Expert System (CORMIX)

Cornell Mixing Zone Expert System (CORMIX) consists of a series of software system for the analysis, prediction, and design of aqueous toxic or conventional pollutant discharges into diverse water bodies, with emphasis on the geometry and dilution characteristics of the initial mixing zone, including the evaluation of regulatory requirements. It specifies the plume trajectory and mixing behaviors into near-field and far-field simulations. The system emphasizes the role of boundary interaction to predict plume geometry and dilution in relation to regulatory mixing zone requirements. As an expert system, CORMIX is a user-friendly application which guides the water quality analysts in simulating a site-specific discharge configuration. To facilitate its use, ample instructions are provided, suggestions for improving dilution characteristics are included, and warning messages are displayed when undesirable or uncommon flow conditions occur. CORMIX contains three major subsystems. The first subsystem, CORMIX1, is used to predict and analyze environmental impacts of submerged single port discharges. The second subsystem, CORMIX2, may be used to predict plume characteristics of submerged multiport discharges. The third subsystem, CORMIX3, is used to analyze positively and neutrally buoyant surface discharges [16]. CORMIX3, the surface source discharge submodel, will be the focus of this study.

Mixing zone processes are controlled by the interplay of discharge and ambient conditions. The CORMIX methodology emphasizes the role of boundary interaction on mixing processes [17]. Boundary interaction occurs when the flow contacts either the water surface, channel bottom, or forms an internal terminal layer in a density-stratified ambient environment. Boundary interaction determines if mixing is controlled by stable or unstable discharge source conditions [18].

CORMIX employs rule-based expert systems to verify the input data consistency, calculate the basic length scales and flow parameters, and determine the flow classification needed for simulation and mixing zone analysis. The CORMIX flow classification identifies the important physical processes and which controls

initial mixing behavior and indicates what models should be executed for a complete mixing zone simulation. About 80 generic flow classes have been included in complete CORMIX flow classification system.

Boundary interaction also defines the transition from near-field to far-field mixing [19]. Near-field mixing processes are those for which the initial momentum, buoyancy, and geometric orientation of the discharge has the predominant effect on flow behavior. Far-field mixing processes are largely controlled by ambient conditions. CORMIX contains a rigorous flow classification developed to classify a given discharge/environment interaction into one of several flow classes with distinct hydrodynamic features [18-20]. The classification scheme places emphasis on the near-field boundary interaction behavior of the discharge. An example of the CORMIX3 classification scheme for surface buoyant discharges appears in Figure 3.1.

CORMIX3 classifications include the Free Jet (e.g. FJ1, FJ2, and FJ3) flow classes which are not attached to the near-shoreline, shoreline attached flow classes (e.g. SA1 and SA2) which have local near-shore recirculation regions immediately downstream from the discharge channel, wall jet flow classes (WJ1 and WJ2) in which discharges parallel to the shoreline have near-field Coanda attachment behavior, and plume flow classes (PL1 and PL2) where discharge buoyancy and near-shore attachments predominate the mixing process. The methodologies and criteria of surface discharge flow classification will be demonstrated in detail next section.

The latest research versions of CORMIX (v4.2 GT) provides access to advanced design tool for outfall visualization (CorSpy), mixing zone visualization (CorVue), access to legacy data (CorData) and sensitivity study analysis (CorSens). In the study, the CORMIX v4.2GT software package was the version of the model for the hydrodynamic simulations.

3.3 Surface Discharge Flow Classification

The *length scale* is used extensively in the CORMIX flow classification procedure. Length scales are measures of the physical mixing characteristics of a mixing process. Therefore brief descriptions of the physical meaning and formulation of length scales is presented below.

3.3.1 Length Scale

Length scales can describe and be measures of the relative importance of the initial volume flux, momentum flux, buoyancy flux, and crossflow velocity. Four scales have practical meaning for use in buoyant surface jets analysis; the discharge length scale, jet-to-plume length scale, jet-to-crossflow length scale, and plume-to-crossflow length scale. Two dimensional definitions of the first three length scales are also used for simulations where there is bottom interaction and the flow can be considered two dimensional.

The **Discharge length scale** measures the relative significance of the volume flux as compared to the momentum flux, and is defined as:

$$L_Q = \frac{Q_0}{M_0^{1/2}} \quad (3.1)$$

This length scale defines the region for which discharge channel geometry strongly influences the flow characteristics. This comprises the zone of flow establishment, and is generally insignificant in extent.

The **Jet-to-plume length scale** measure the relative importance of initial momentum and initial buoyancy, and it is defined as:

$$L_M = \frac{M_0^{3/4}}{J_0^{1/2}} \quad (3.2)$$

In the region where the offshore distance to the plume centerline $y \ll L_M$, momentum dominates the flow and therefore jet mixing prevails. On the other hand, where $y \gg$

L_M , buoyancy dominates and strong lateral spreading prevails. For this reason, the jet-to-plume length scale is an importance measure of where regimes characterized by jet mixing end and regimes characterized by buoyancy-induced lateral spreading begin.

The **Jet-to-crossflow length scale** measures the relative significance of the initial momentum and the ambient crossflow velocity and it is defined as:

$$L_m = \frac{M_0^{1/2}}{u_0} \quad (3.3)$$

This length scale is also used to determine where the flow changes from the weakly deflected regime to the strongly deflected regime.

The **Plume-to-crossflow length scale** measures the relative importance of the initial buoyancy flux to the ambient crossflow velocity. It is defined as:

$$L_b = \frac{J_0}{u_a^3} \quad (3.4)$$

This length scale has a significantly different meaning for surface plumes than for submerged buoyant jets. Since this length scale represents an interaction of the initial buoyancy of the effluent and the velocity of the crossflow, its most apparent measure is the extent of upstream spreading that a surface plume may exhibit. It also plays a role in the increased lateral progression of free jets caused by the thinning of the buoyant surface jet due to buoyancy.

3.3.2 Classification Criteria

Several basic classification criteria make up the CORMIX3 flow classification scheme (Figure 3.1). Each of these criteria and the rationale behind them are discussed below.

The first criteria in the classification scheme differentiates flows with jet-like behavior from those with more plume-like characteristics. A direct measure of the relation between initial buoyancy and the momentum is given by the channel densimetric Froude number:

$$Fr_{ch} = \frac{u_0}{\sqrt{g_0' h_0}} = \left(\frac{L_M}{L_Q} \right) \frac{1}{A^{1/4}} \quad (3.5)$$

Where u_0 is the discharge velocity, g_0' is the buoyant acceleration, and h_0 is discharge channel depth.

The aspect ratio factor $(1/A^{1/4})$, in which A = channel height h_0 / channel width b_0 , is a result of length scales L_M and L_Q being defined based on the discharge area a_0 instead of the discharge height h_0 . The critical value of $C1 = 1.5$ arises from the observed lack of a jet-like mixing behavior for lower values of discharge[20-22].

For jet-like flows, the discharge configuration is an important index to determine the existence of the ambient crossflow deflection. The criterion for this identifies the flows which are issued near parallel to the bank or at a discharge angle σ small enough to cause Coanda attachment to the downstream bank. If σ is less than the angle $C2$, the flow is classified as a wall jet, otherwise is classified either free jet or shoreline attached jet that is determined by relative magnitude of discharge momentum and strength of the ambient crossflow. A value of $C2 = 20^\circ$ is generally accepted as the limit for Conanda attachment.

The criterion combines several effects to distinguish free jets from shoreline attached jets and is given as follows:

$$(1 + \cos \sigma) \frac{L_Q}{L_m} \left(\frac{L_M}{H} \right)^{3/2} = C4 \quad (3.6)$$

The term $(1 + \cos \sigma)$ is a correction added to the criterion to account fro the directed momentum. $\frac{L_M}{H}$ is depth dependency variable. The ambient depth H is calculated according to the location of the maximum depth, $H = 3.89L_M$ and this results $\frac{L_M}{H}$ as a constant. Therefore, to determine the free jet or shoreline attached jet is basically dependant on the resulting criterion, ratio of L_Q to L_m . If L_m is small, i.e.: less than the discharge length scale L_Q , then the jet is very rapidly bent over an attachment to the downstream bank will result. On the other hand, if L_m is very large, it will take a

much greater distance for the jet to become bent over and it will remain free from shoreline attachment. The constant in the criterion has been determined empirically by Chu and Jirka, $C_4 = 0.25$, and contains some uncertainty[22].

Besides those major criteria, there are several subclasses under these four main flow classes. More detailed criteria, such as depth dependency and magnitude of buoyancy, are applied for these purposes and are depicted in detail in CORMIX3 technical report[20].

3.4 Parameterization for CORMIX Simulation

In order to develop accurate data input for the conditions at the discharge locations, detailed ambient and discharge information is essential for CORMIX mixing zone simulation[15]. Ambient environment parameters such as ambient density, temperature, velocity field, and river geometry were determined directly from field measurements. Discharge conditions such as discharge channel geometry, density, temperature, and flow rate were based on the discharge channel documentation and field survey data. In addition, the discharge flow rates and temperatures from the facilities discharge records on the specific sampling dates and times were used in input data specification.

In order to minimize variance between different sites resulting from different assumptions about ambient and discharge conditions, the same procedures were used to synthesize ambient and discharge information for CORMIX data input. Furthermore, validation data sets were classified by the CORMIX hydrodynamic flow classification. Flow classification may provide a consistent basis for improvement of mixing model hydrodynamics. The goal is to have comprehensive and consistent input data set to validate the simulation results with observational data.

FLOW CLASSIFICATION FOR BUOYANT SURFACE DISCHARGES

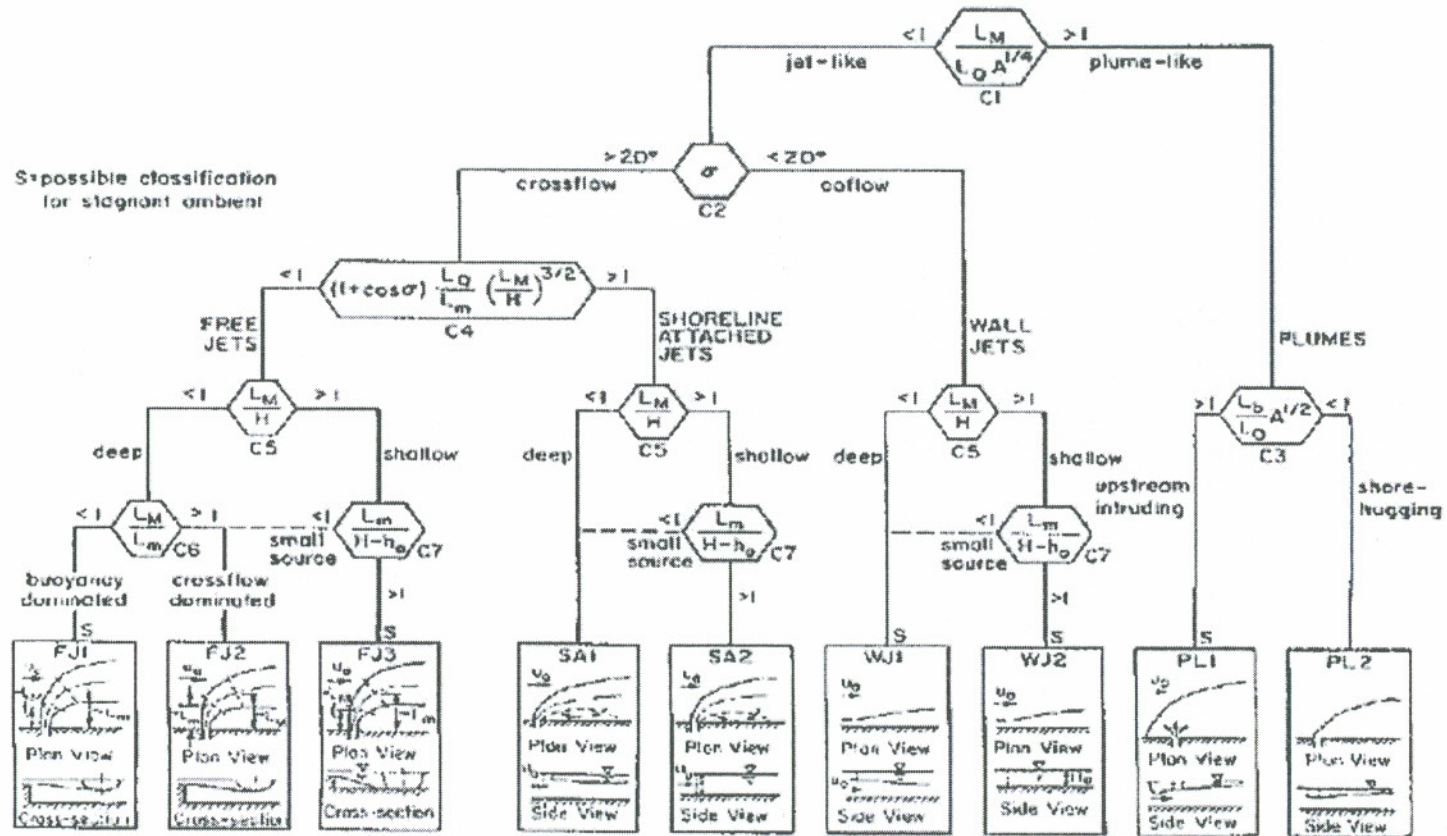


Figure 3.1 CORMIX3 Classification

Assessment of buoyant surface discharges as free jets, shoreline-attached jets, wall jets, or plumes[15]. The flow classes focused in this study are Shoreline Attached Jets in deep water (SA1), in deep water (SA2), and shore-hugging Plumes (PL2).

In a typical application, flows are specified at the upstream boundary and water surface elevations or a rating curve specified at the downstream boundary. Specification of flows for the downstream boundary is not good practice since errors in initial conditions (specified conditions at the start of the simulation) might not quickly propagate through the model domain[23].

3.4.1.1 Ambient Temperature and Density Profile Data

Ambient thermistor string data was collected approximately 200 m upstream from the discharge outlet at Cooper, Nebraska City and Fort Calhoun, and 1000 m upstream of North Omaha discharge. Water temperature was observed to be relatively constant at different depths along these upstream river transects. Figure 3.2 shows the thermistor string data collected at upstream at each survey site.

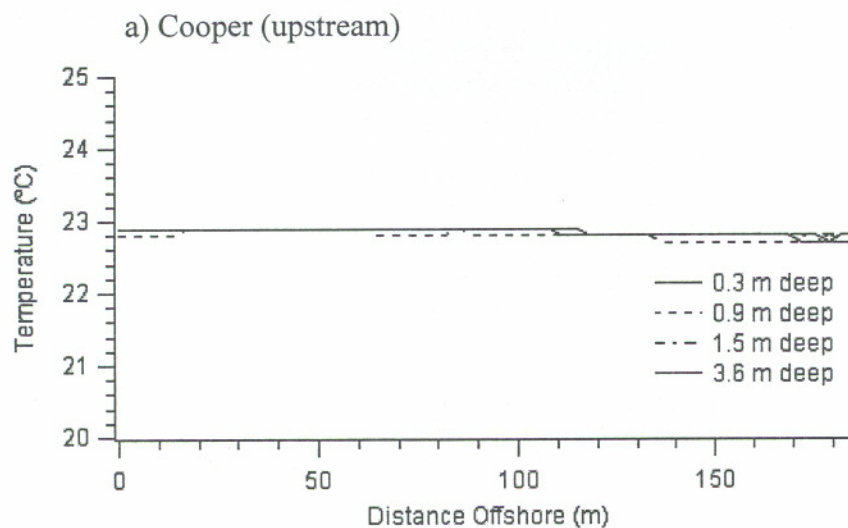
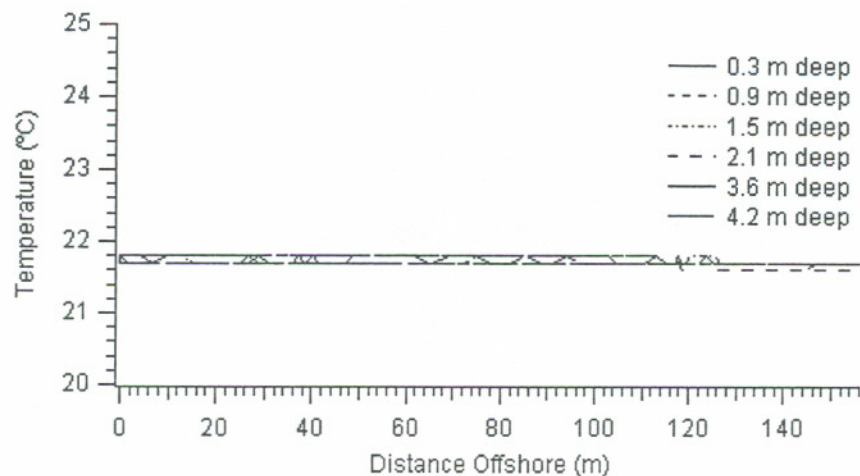
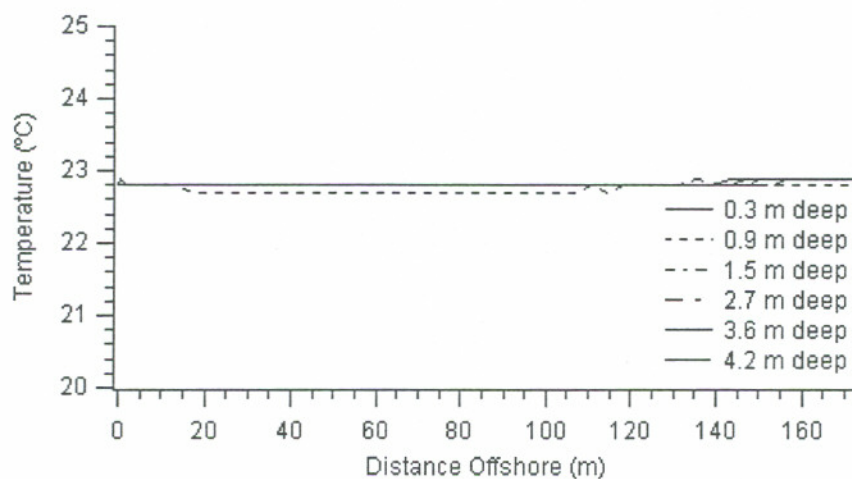


Figure 3.2 Upstream Thermistor String Data

b) Fort Calhoun (upstream)



c) Nebraska City (upstream)



d) North Omaha (upstream)

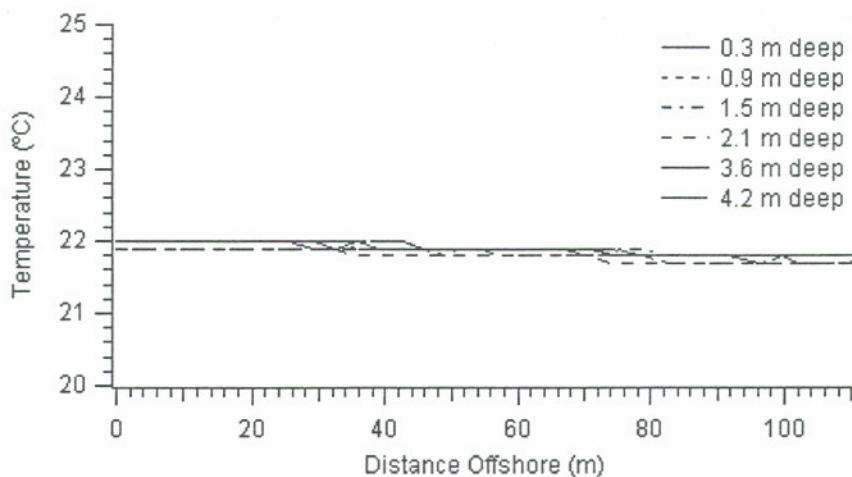


Figure 3.2 (cont'd)

The near-uniform temperature distribution of upstream transects supports the assumption of uniform ambient temperatures both vertically and laterally in the water body. Therefore, uniform ambient density is also indicated. This is because water density can be expressed with little error as a linear function of temperature in freshwater systems above 4°C. The unstratified environment eases the concerns regarding the internal boundary in the ambient.

In addition, in transects downstream of the discharge, within regions outside the lateral boundary of thermal plume signal, thermistor data indicates that temperature differences are within the range of 0.3 °C from profile to profile at most transects. This indicates the spatial variation in background temperature is small and therefore differences in background ambient temperature can be assumed negligible in simulation.

The ambient temperature field downstream of the discharge or upstream transects may not always be uniform as observed in the upstream thermistor data. Inputs such as upstream discharges, tributary inflows or groundwater discharges may result in spatial temperature variation both vertically and laterally. Evidence of these effects may have been observed from the upstream profile at the North Omaha site. The procedure for developing the input data in this case is described below.

At the North Omaha site, the downstream thermistor data taken outside the lateral plume boundary consistently indicate a 0.7 °C rise in the ambient temperature from the upstream profile. As previously noted, the North Omaha upstream profile was taken 1000 m upstream of the discharge location, not 200 m upstream as for the other sites. For this only, to optimize model input ΔT with observed ambient conditions, discharge ΔT is set to be equal to the difference between the discharge temperature and downstream ambient temperature taken outside the lateral plume signal, rather than upstream ambient temperature as in the other 3 sites in this study. The input ΔT for each site is included in Table 3.2.

3.4.1.2 River Geometry

CORMIX emphasizes the flow the effects of boundaries on the mixing process. CORMIX requires a “schematization” of the river cross-section as a first step in the ambient data specification. Schematization is a process where the boundaries, ambient velocity and density field simplified for representation within CORMIX. A river can be simply schematized as a bounded section with rectangular cross-section geometry and uniform velocity field. Determination of the cross-section width and average depth is therefore essential for schematization. The field ADCP measurements contain the river width and depth information used in the schematization process. Figure 3.2 demonstrates the CORMIX width and depth schematization and ADCP profile data.

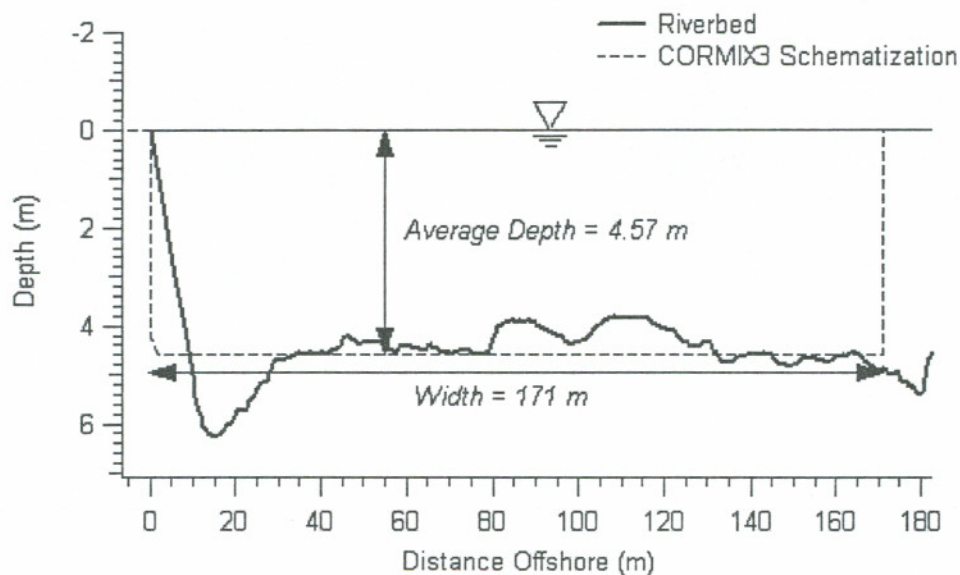


Figure 3.3 CORMIX Schematization Created by Field ADCP data

In CORMIX schematization, the rectangular cross section is assumed to simplify the river geometries in the modeling environment. In natural situations, uneven bottom bathymetry and sloping banks are often observed. The Missouri river is a typical flat-bed river and its river cross section to ideal environment for a simple schematization. Thus any error introduced by schematization of the uneven

bathymetry for the Missouri river will be minor. However, the sloping bank may cause instability of the plume near the shore region and the wider plume lateral extent may be also expected.

Due to the turbulence and strong currents at the sampling sites, survey boat tracks were not always perfectly straight and perpendicular to the shoreline in terms of the small scale. However, as a whole tracks were fairly straight and close to perpendicular to the shoreline. Thus, the summation of transect distance and distances from the right and left banks at the starting and ending points represents river width. Within each transect, the average river depth is reported by the ADCP and is representative of the average depth used for schematization.

In addition to the rectangular ambient schematization, for surface discharges CORMIX3 needs information about the local bottom slope near discharge channel entry to account for plume bottom attachment at the discharge outlet. The ADCP bottom profile data was used to estimate near-shore ambient slopes near the discharge outlet locations as shown in Figure 3.3, since there was no river profiling information available near the discharge outlet.

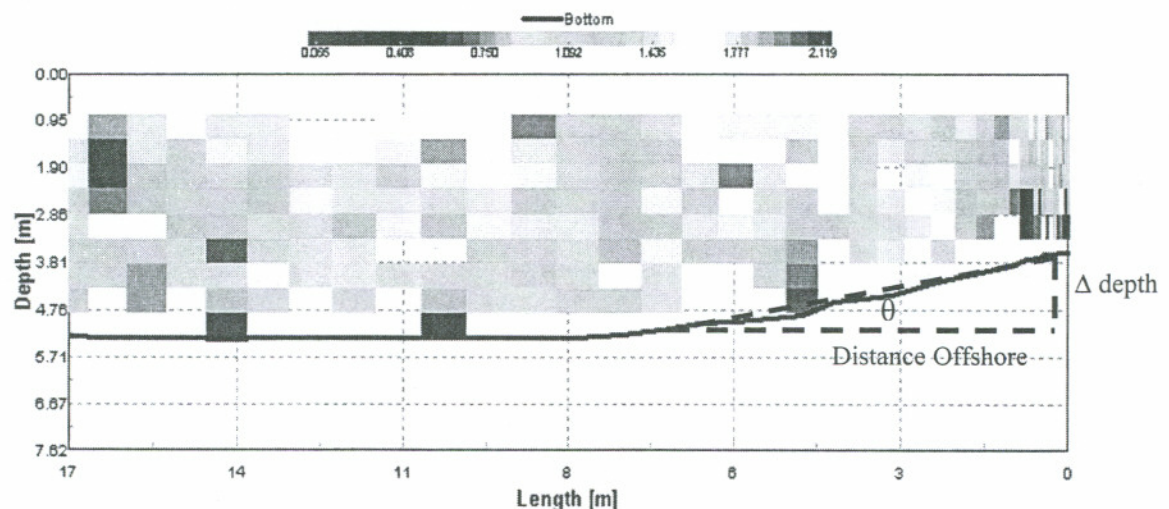


Figure 3.4 Channel entry bottom slope estimation from ADCP profile

To calculate bottom slope: Locate the deepest transect depth in the near-shore region and note Δ depth and distance offshore. Bottom slope θ can be described as $\tan(\theta) = \Delta \text{ depth} / \text{Distance offshore}$. The bottom slope is $\text{Arctan}(\theta)$.

Spatial variation in river cross-sections can affect mixing behavior and trajectory of plumes. The cross-section schematization is created based on the upstream cross section profiling measurements. The upstream cross-section was used because it was the most complete cross-section available measured near the discharge location. Because the same schematization is applied in the entire simulation, it might not be completely applicable when local changes in downstream cross-section occur. However, by looking up the downstream near-shore ADCP data, the near-shore water depth of most of the downstream transects is fairly equivalent to the schematized water depth and only slight shallowness or deepness was observed at 1500 m downstream. According to this observation, the lower boundary is considerably consistent from upstream to downstream.

3.4.1.3 Ambient Flow Rate and Velocity

If the ambient velocity U_a is determined from river discharge and cross-section area, the ambient is computed as a uniform velocity field. Commonly a stage-discharge relationship is used, where gauge ambient depth H is known and rating curves determine the corresponding ambient flow Q_a and cross-sectional area AS . This approach is similar in the case analysis presented here, where an average ambient velocity is computed from ADCP data. However local variation in velocity field can occur, especially near shorelines and other boundaries, due to friction drag induced by boundaries on the velocity field. The theoretical results are not often corresponded to the actual velocity field.

Water temperature, ambient velocity profile, bottom profile, and cumulative discharge and were measured by ADCP instruments in the field. This data was processed with the WinRiver software. In field data collection, due to the shallow water near the shoreline, it was not possible for the survey boat to position close to the bank and collect the profiling data, such as flowrate and velocity. For velocity and discharge measurements, ADCP instruments are capable of recording the water

velocity at different depths and interpolating the flowrate simultaneously based on the cross-sectional area along the survey boat tracks.

Regarding the near-bank discharge that was not directly recorded by ADCP instruments, WinRiver is capable of estimating the discharge near the banks by using an assumed geometry. Several shape coefficients, including rectangular, triangular, and irregular shape coefficients can be applied to demonstrate the bottom slope of the river geometries and introduced in the bank discharge estimations. The bank discharge is estimated through the simple discharge mathematical calculations with the known depth of the river and the distance at nearest point from the bank, the shape coefficient and mean water velocity in the first segment or last segment. Generally, nearly triangular bank geometries are almost always observed in natural environments and therefore in most cases the triangular coefficient is employed as the default setting for bank discharge estimation. In our case, the data were collected at only few meters away from the shoreline and bank discharge is relatively smaller with respect to the total discharge so that the effects of using different shape coefficients on estimated bank discharge are negligible. Thus, the default triangular shape coefficient was used to estimate the bank discharges. The total discharge can then be provided from WinRiver calculations. Table 3.1 lists the important settings used for extracting the river discharge information with the WinRiver software.

Table 3.1 Settings in WinRiver for Near-bank Discharge Estimates

Parameter	Value
Number of shore ensembles to average	7
Left bank edge type	Triangle (shape coeff. = 0.35)
Right bank edge type	Triangle (shape coeff. = 0.35)
Top Discharge Method	Power (default)
Bottom Discharge Method	Power (default)
Power Curve Coefficient.	0.1667

To compute ambient discharge flowrate Q_a , ambient velocity U_a can be determined at known points in a cross section and then integrated over area to get total discharge. Within transects, measurements of velocity may vary in direction and magnitude at any point. Variations might be due to turbulent fluctuations in the

ambient velocity vector or measurement tracks which are not always parallel to the shoreline or the river bottom. In WinRiver summary reports, velocity and direction are presented as mean values for the entire transect. The mean flow directions are perpendicular to the survey boat tracks. Since the survey boat track is assumed to be perpendicular to the shoreline, it follows that the mean flow direction is roughly parallel to the shoreline.

In CORMIX, the ambient velocity is the fundamental parameter used in flow classification and mixing zone analysis. For bounded sections, CORMIX accepts the ambient flow rate or velocity as ambient input data. If ambient flow rate is entered, the calculation of ambient velocity is based on an assumed rectangular river cross section by model. Thus, a calculated ambient velocity does not always reflect the actual ambient velocity conditions at the discharge channel entry into the cross-section.

If ambient flow rate is entered into CORMIX as data input, the width or depth must be must be adjusted in simulation to retain both ambient velocity and river discharge observed from the field survey. Since the depth is an important local parameter for initial mixing it should reflect the actual depths at the discharge location and should be preserved. For the large rivers like Missouri River, outfalls on the bank shoreline have initial discharge momentum that is not large enough to cause plume interaction with the opposite bank in the near-field. Thus, the width can be adjusted to preserve the observed ambient velocity as long as plume interaction with the far bank is outside the region of interest.

3.4.1.4 Wind Speed, Heat Loss, and Roughness

In CORMIX wind, heat loss, and roughness of the riverbed are the essential parameters to determine the intensity of the ambient turbulence, the predominant factor controlling the plume behaviors in the far field simulation. A flux Richard criteria, based on the ratio of plume buoyancy to the ambient mixing energy from shear stress, is used to determine the transition between buoyant spreading to passive

diffusion in most of the hydrodynamic models as well as in CORMIX[14, 24]. The wind speed, heat loss coefficient, and roughness coefficient are used to estimate the turbulent mixing energy.

Wind speeds were not measured while the field data collection occurred. It is known that the weather conditions on the sampling days were calm, so the wind speed U_w was assumed to be 2 m/s for the model input, the minimum value suggested for field conditions.

Heat loss, due to the surface heat exchange can be simulated in COMRIX. It is determined by the surface heat exchange coefficient K_s . The surface heat exchange coefficient is also related to the wind speed and ambient water temperature. Because the wind speed measurements were not taken in the field and the calm weather conditions are known on the sampling days, we assumed the surface heat exchange coefficient is $8 \text{ W/m}^2 \text{ }^\circ\text{C}$ by referencing the look-up table[25].

The Darcy's friction factor f or manning n is commonly used as the roughness coefficients for open channel hydrodynamics. Confirming the manning n calculated from Sayre's study in transverse mixing characteristics in Missouri River, 1973 with values referenced for the large rivers, the manning n , ranging from 0.030 to 0.032, is used as typical roughness coefficient for Missouri River[26-28].

3.4.2 Surface Discharge Source Conditions

Compared to specification of ambient parameters, determination of discharge parameters for CORMIX data input is fairly straightforward. Discharge data was primarily based on the daily reports issued from the power plant facilities, "as built" construction information, and observed discharge channel designs. In CORMIX discharge data input, discharge parameters refer to properties of the discharge at the entry point to the ambient channel.

3.4.2.1 Local Discharge Geometry

The surface discharge structures at the four sites were designed as flush discharges with the bank. The related input parameters of discharge geometry, such as the widths, depths, discharge angles, and depths at discharge were explicitly described by site descriptions and “as built” channel designs.

However, in CORMIX3, the bottom slope and local depth at discharge HD_0 are needed specifically to simulate the occurrence of the initial bottom attachment that forms the unstable and wider flow. As mentioned in the ambient parameterization section, the estimated bottom slope in the upstream river profiling measurement is used. By knowing the bottom slope, the local depth at discharge HD_0 , which was not measured in the field and unavailable from the discharge channel designs, can be interpolated from the known water depth and the distance offshore. It is important to note that the local depth HD_0 should not be less than the discharge depth H_0 and therefore, when the interpolated local depth is less than channel depth the local depth is equal to the discharge channel depth.

3.4.2.2 Discharge Flow Rate and Velocity

Since the dimensions of the discharge channels are known for the study sites, the discharge velocity U_0 can be computed by CORMIX from input of flowrate. For our cases, the discharge flowrates Q_0 are routinely measured and recorded at the power plant pumping station. This discharge flow data was used for CORMIX data input.

3.4.2.3 Discharge Temperature

In CORMIX data input, the density of the discharge ρ_0 and not temperature T_0 is the primary parameter controlling initial mixing. Similar to procedure used in

the ambient density specification, if the discharge is freshwater and above 4 °C then temperature of the discharge can be specified in data input. CORMIX then uses a linear equation of state to calculate discharge density ρ_0 .

For heated discharges, discharge concentration C_0 in CORMIX is typically specified as temperature excess ΔT above ambient. Thus if the ambient temperature $T_a = 10$ °C and the discharge temperature $T_0 = 20$ °C, then discharge concentration C_0 specified as temperature excess ΔT ambient would be $C_0 = 10$ °C. When interpreting CORMIX output, the background concentration (temperature) is then added to the predicted plume concentration (temperature) $C_{(x,y,z)}$ at any point to determine the actual concentration (temperature).

As previously noted discharge properties refer to conditions at the outfall entry into the ambient channel. However, the field temperature measurements were not always taken at the outfall entry or in the discharge channels themselves. It is important to note that the discharge is not direct from the pumping station into the ambient water body. At the study sites, discharges were pumped to outfall structures such as channels or canals before entry into the ambient. Heat loss may occur during transport from the pumping stations to the outfall. The magnitude of the heat loss may vary due to weather condition, outfall structure length, and other conditions.

If temperature values were available in the discharge channel and are significantly different from pumping station temperatures, then these values should be used for data input. Otherwise, the temperature values recorded at the power plant pumping station can be used to determine discharge properties for CORMIX simulation.

At three of our sites observations of the water temperature by thermistor strings in transects very near outfall observed temperatures were lower than temperatures measured in pumping stations of the cooling systems by less than less than 1 °C and therefore assumed to be insignificant for the purposes of this study. The exception to this procedure is outlined below.

The operating conditions of the power stations on the sampling days must be taken into consideration. Sometimes not all of the generators are in operation resulting in a lower

ΔT or lower discharge flowrates Q_0 . On the sampling date September 12th, the main generator was shut down during the field observation period at the North Omaha power station. As a result the ΔT measured in the cooling facilities was lower than that measured at full operation. Thus, for this case the highest temperature measured in the vicinity of the outfall is applied for source data input.

Although a number of assumptions and procedures have been reasonably applied to schematize the both the input ambient and discharge parameters listing in Table 3.2, sometimes additional optimization is needed to make the simulation results more representative of observational data. The procedure for optimization CORMIX predictions will be described in the following section in this chapter.

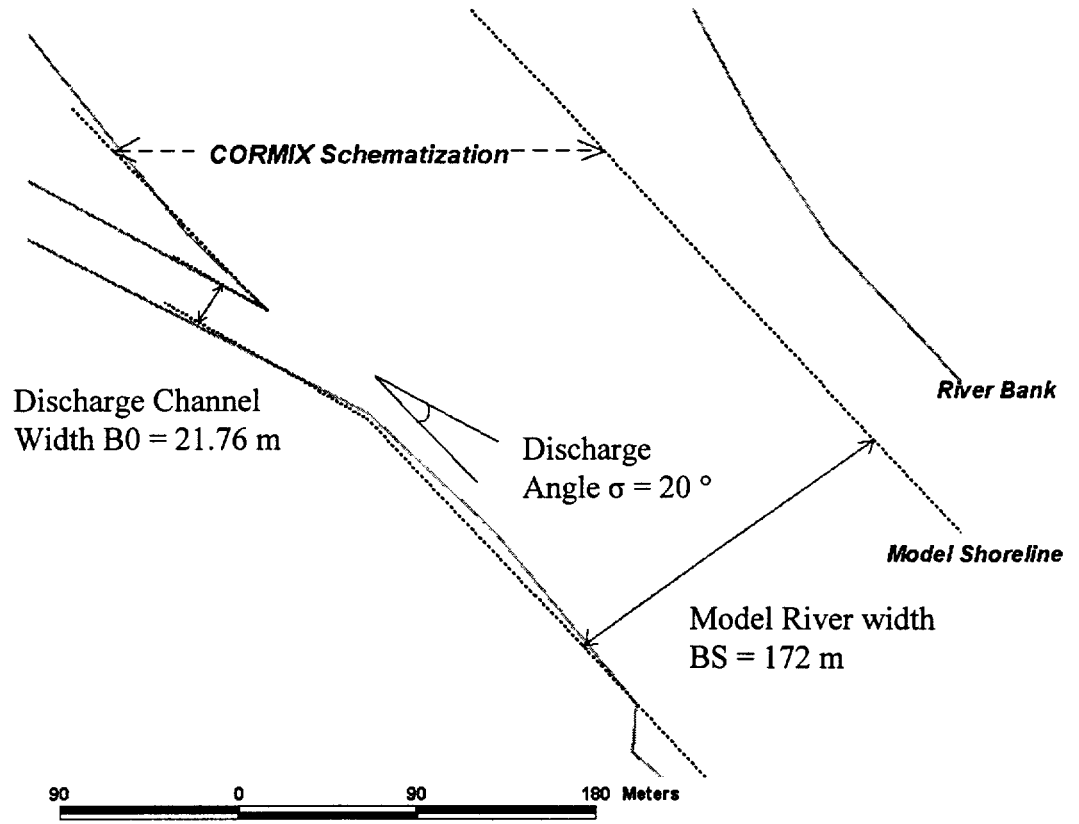
Table 3.2 Input Parameters for CORMIX Simulations

	Fort Calhoun Power Station		Cooper Nuclear Station	
Ambient	Observed	CORMIX Input Data	Observed	CORMIX Input Data
Width (m)	190.67	163	173.42	172
Ambient Flow Rate (m ³ /s)	801.14	801.14	900.94	900.94
Average Depth (m)	4.91	4.91	4.23	4.23
Ambient Velocity (m/s)	1	1	1.24	1.24
Manning's n	-	0.031	-	0.032
Ambient Temperature (°C)	21.76	21.76	22.7	22.7
Depth of Discharge (m)	-	4.32	-	3.48
Discharge				
Discharge Angle (°)	30	30	20	20
Bottom Slope at Discharge (°)	22.93	22.93	9.46	9.46
Discharge Flow Rate (m ³ /s)	22.71	22.71	41.58	41.58
Discharge Channel Width (m)	12.19	12.19	10.03	10.03
Discharge Channel Depth (m)	1.52	1.52	4.32	4.32
Discharge Temperature (°C)	34.1	34.1	33.97	33.97
Discharge Concentration (°C)	12.34	12.34	10.27	10.27
	Nebraska City Power Station		North Omaha Power Station	
Ambient	Observed	CORMIX Input Data	Observed	CORMIX Input Data
Width (m)	180.66	182	199.59	139
Ambient Flow Rate (m ³ /s)	1006.9	1006.9	749.54	749.54
Average Depth (m)	4.57	4.57	3.83	3.83
Ambient Velocity (m/s)	1.21	1.21	1.41	1.41
Manning's n	-	0.03	-	0.03
Ambient Temperature (°C)	22.28	22.28	21.8	21.8
Depth of Discharge (m)	-	3.05	-	2.13
Discharge				
Discharge Angle (°)	45	45	37	37
Bottom Slope at Discharge (°)	10.88	10.88	14.41	14.41
Discharge Flow Rate (m ³ /s)	22.08	22.08	22.78	22.78
Discharge Channel Width (m)	4.98	4.98	4.88	4.88
Discharge Channel Depth (m)	3.05	3.05	2.13	2.13
Discharge Temperature (°C)	32	32	27.4	27.4
Discharge Concentration (°C)	9.72	9.72	5.6	5.6

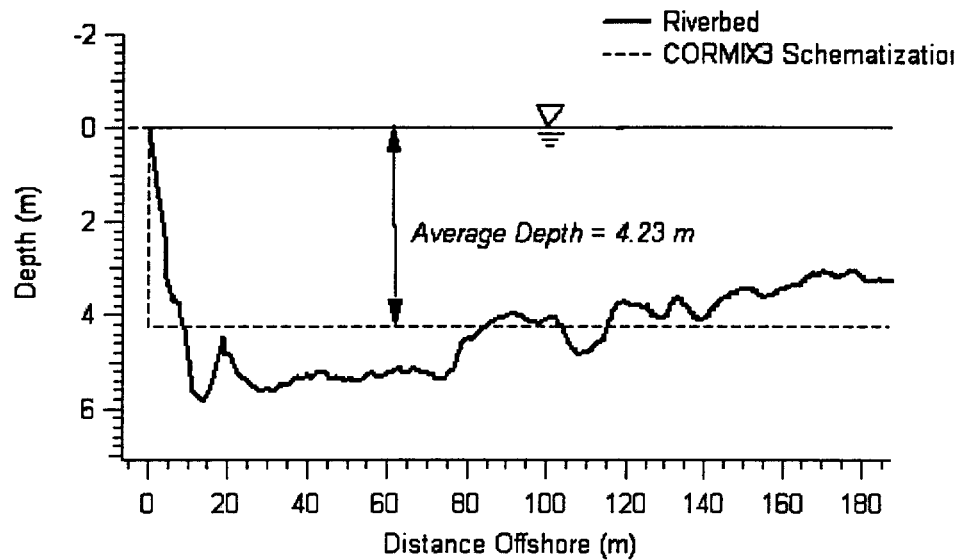
3.4.3 CORMIX Ambient and Local Discharge Schematization

To simulate the plume boundary interactions, schematization of river geometry and discharge structure is very important. The average depth H_A , depth at discharge H_D , river width B , discharge channel depth H_0 , local depth near discharge outlet H_{D0} , and near-shore ambient bottom slope are required. Figure 3.4 – 3.7 illustrate the schematization graphically in plan view, side view of the rectangular cross section, and the local discharge configuration for four case study sites.

a) Plan View (Cooper)

**Figure 3.5 Illustrations of CORMIX Schematization at Cooper Nuclear Station**

b) Cross-section (Cooper)



c) Local Discharge Cross-section (Cooper)

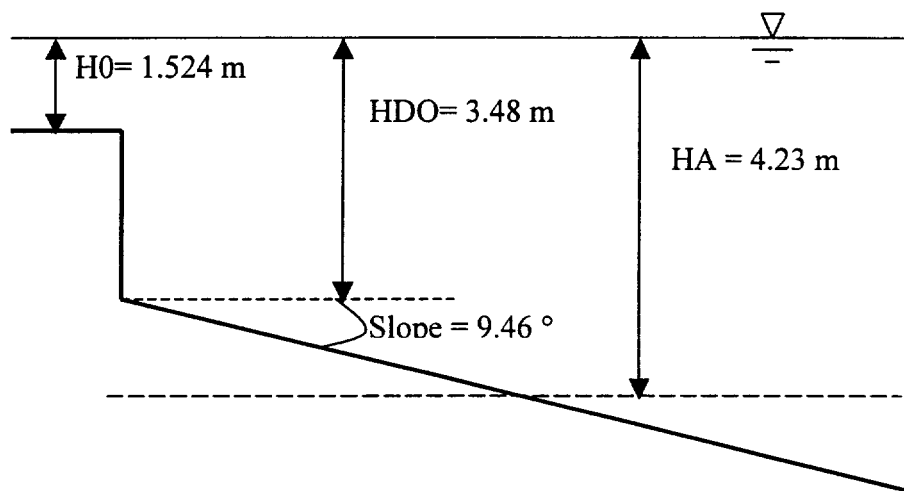


Figure 3.5 (cont'd)

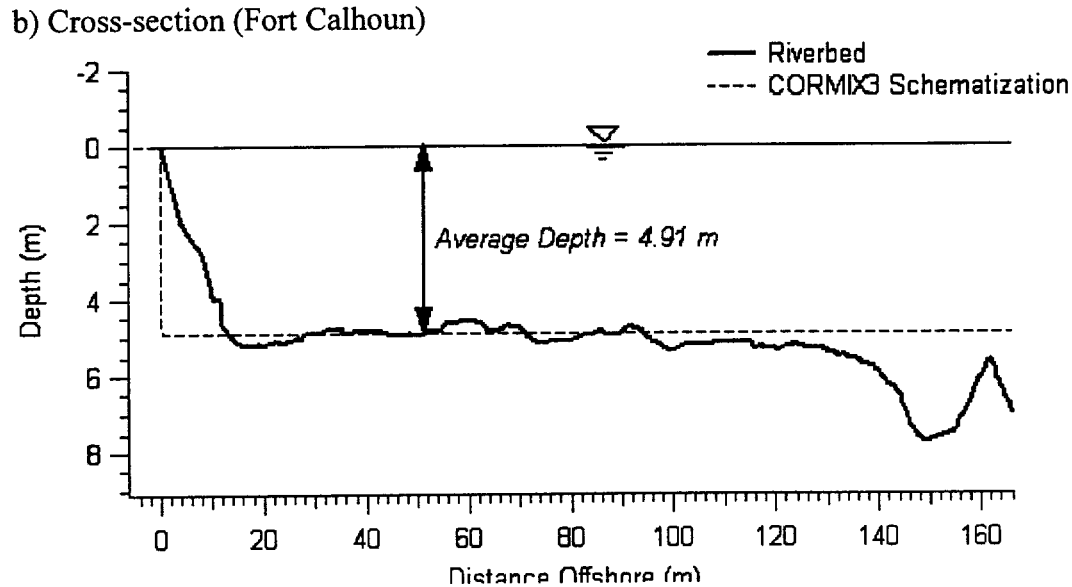
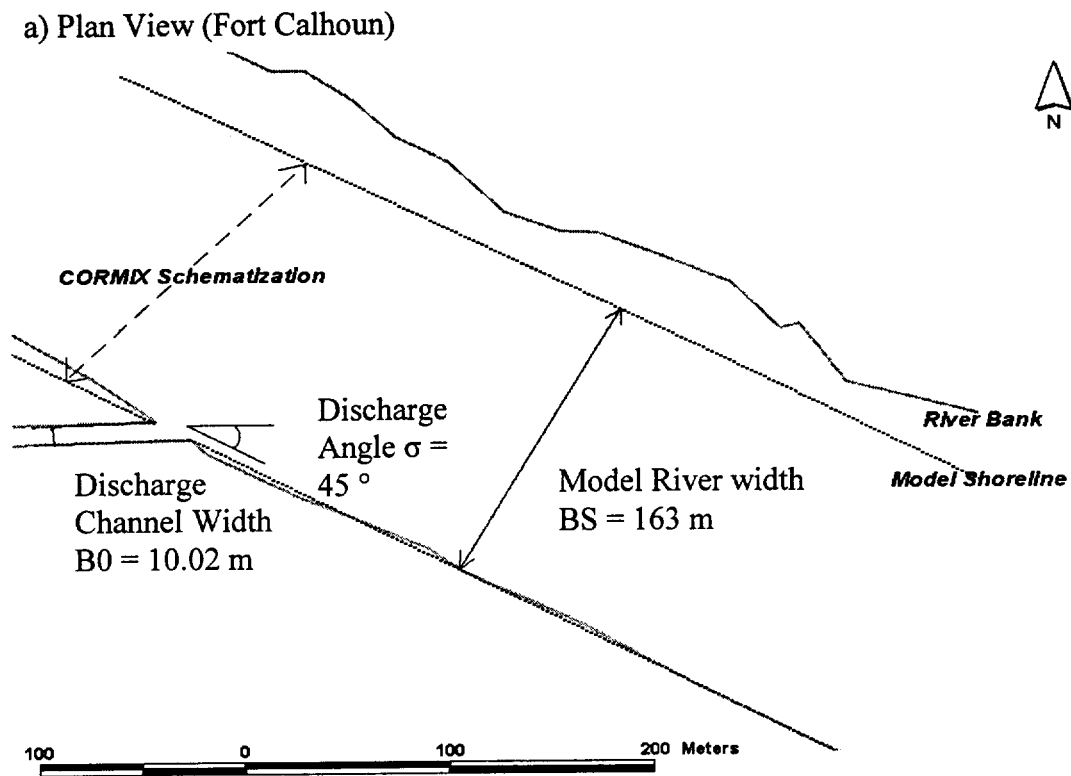


Figure 3.6 Illustrations of CORMIX Schematization at Fort Calhoun Nuclear Station

c) Local Discharge Cross-section (Fort Calhoun)

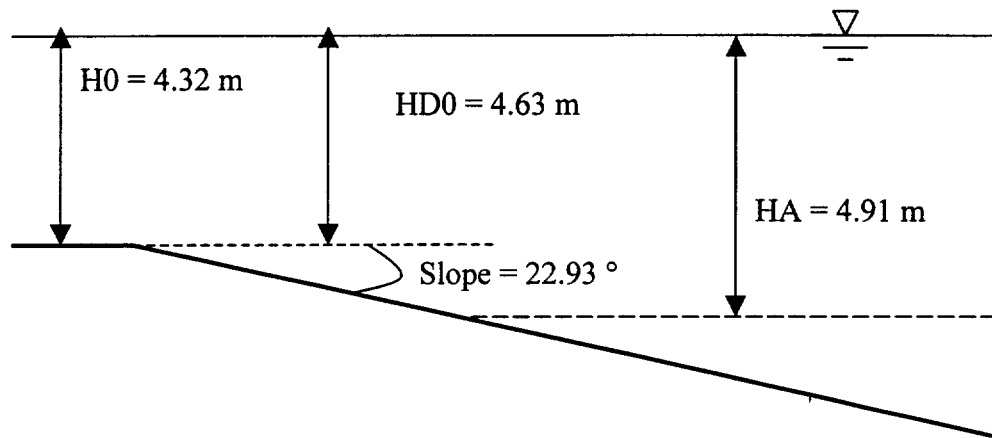


Figure 3.6 (cont'd)

a) Plan View (Nebraska City)

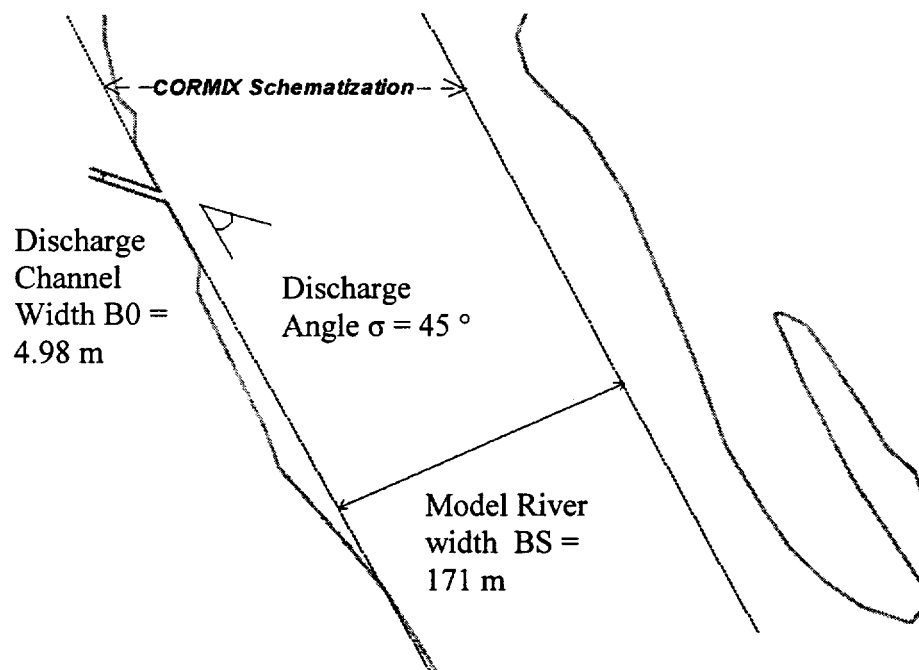
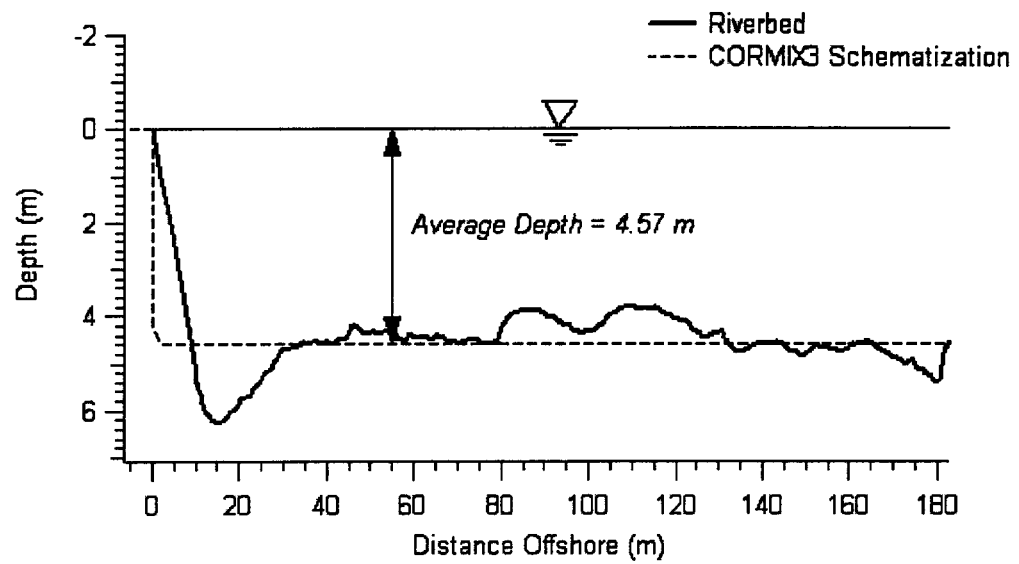


Figure 3.7 Illustrations of CORMIX Schematization at Nebraska City Power Station

b) Cross-section (Nebraska City)



c) Local Discharge Cross-section (Nebraska City)

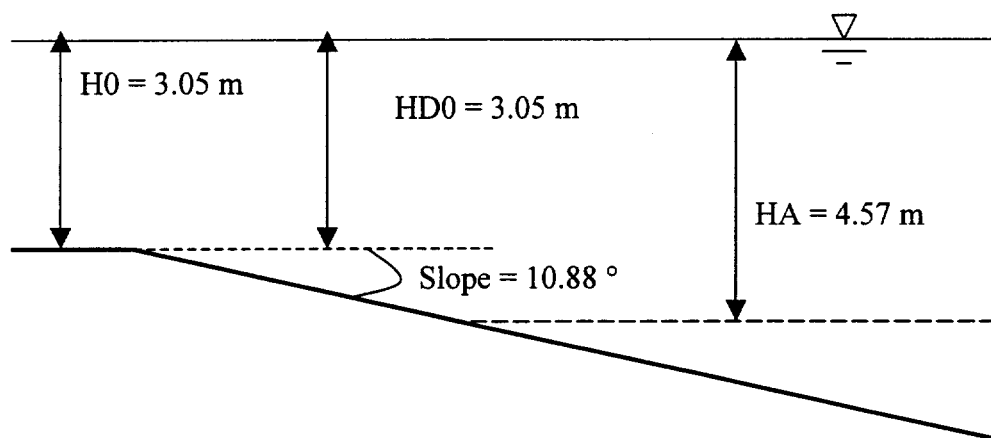
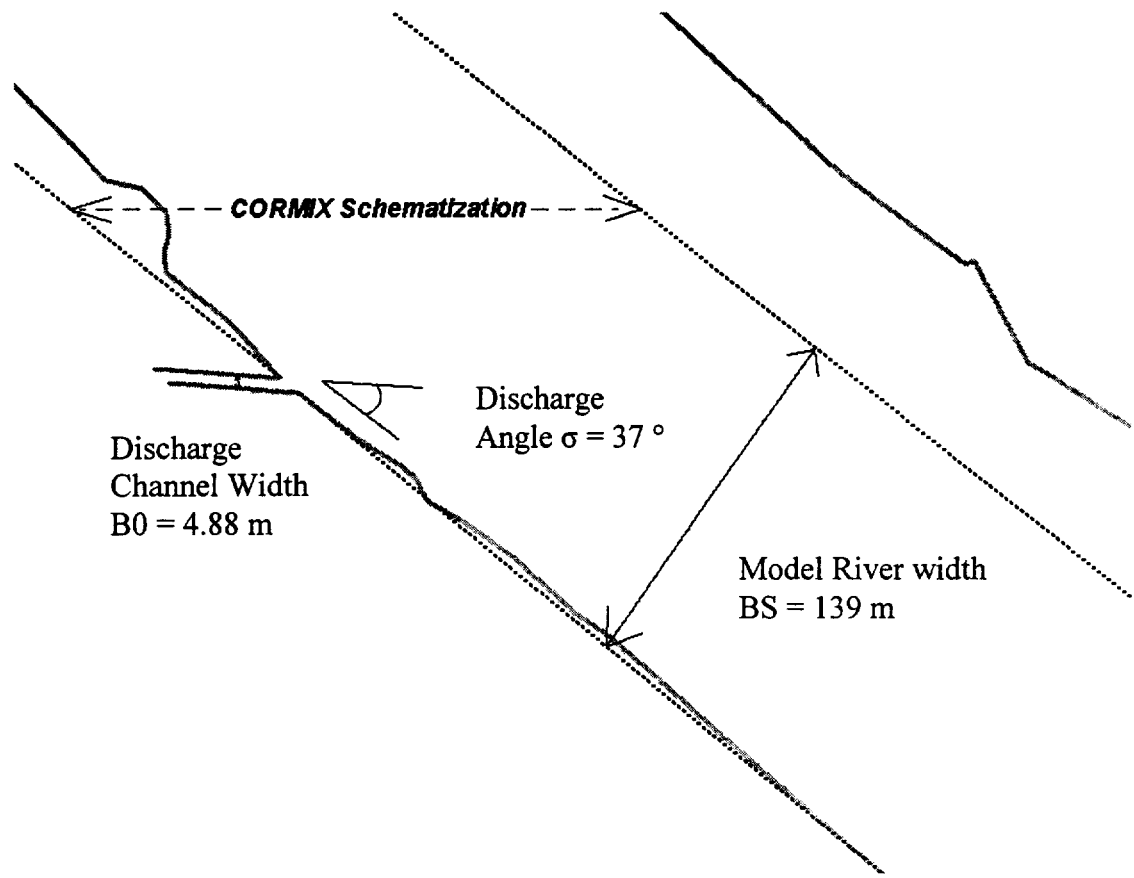


Figure 3.7 (cont'd)

a) Plan View (North Omaha)



b) Cross-section (North Omaha)

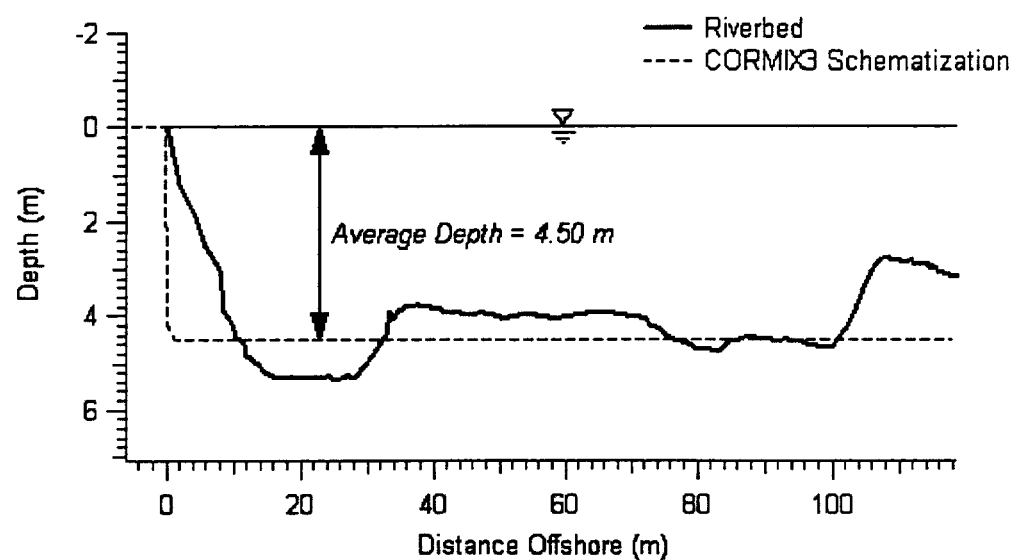


Figure 3.8 Illustrations of CORMIX Schematization at North Omaha Power Station

c) Local Discharge Cross-section (North Omaha)

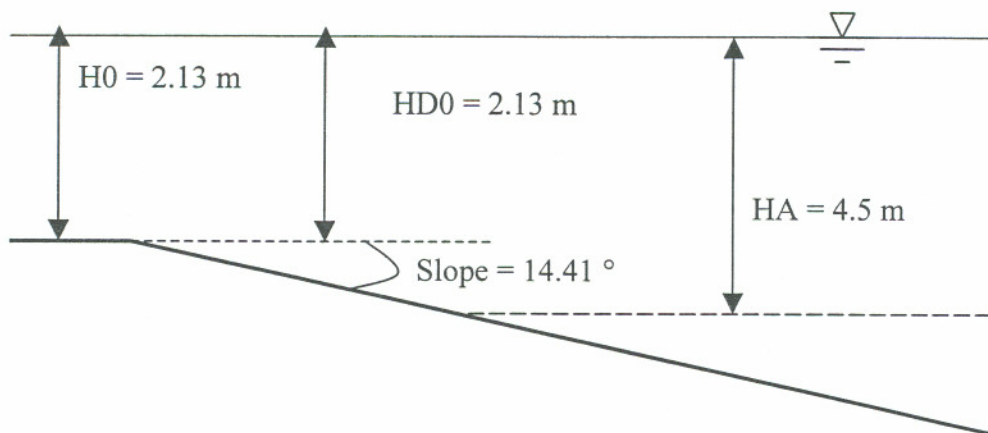


Figure 3.8 (cont'd)

3.5 Application of the Far Field Locator (FFL)

3.5.1 Introduction

Although the main emphasis of CORMIX is on the near-field mixing behavior of discharges it can also be used for providing plume predictions at larger distances in the far-field, provided the flow is not highly irregular with pronounced recirculating zones and eddies in the ambient flow. Due to the variations in the river geometry and bottom bathymetry, the ambient flow available for mixing is not constant when measured at a constant distance from the bank. To describe this downstream variation in ambient flow area available for mixing, the concept of cumulative discharge is introduced.

The CORMIX predicted far-field applies to a schematized rectangular cross-section, which represents a straight uniform channel. The Far-field Locator (FFL) is a simple method for interpreting the schematized CORMIX far-field plumes within the actual meandering flow patterns in natural rivers and estuaries. This procedure, based on the cumulative discharge method, is illustrated in Figure 3.13.

The **cumulative discharge method**, first proposed by Yotsukura and Sayre [29], is a convenient approach of dealing with lateral mixing in natural irregular (but not highly irregular with recirculating zones!) channels. In such channel geometry the passive far-field plume that is vertically mixed, or approaches vertical mixing, will be positioned around the "streamline", or more precisely the "cumulative discharge line", that passes through the plume.

Looking downstream at a particular cross-section (see Figure 3.13a) the cumulative discharge $q(y)$ is defined as:

$$q(y') = \int_0^{y'} \bar{u}_a(y') H(y') d'y' \quad (3.7)$$

in which y' is the lateral coordinate pointing from the right bank to the left across the flow (y' differs from y as defined in CORMIX whose origin is at the discharge location), H is the local depth, and \bar{u}_a is the depth-averaged local velocity. When the above equation is integrated across the full channel width B_s , then the total discharge will result $Q_a = q(B_s)$. Hence, if the local values $q(y')$ are divided by Q_a the results can be presented in normalized form as the cumulative discharge lines ranging from 0% at the right bank to 100% at the left bank. The full distribution of such cumulative discharge lines in a river or estuary gives an appearance of the overall flow pattern that is important for pollutant transport. Closely spaced discharge lines are mostly indicative of areas of large depth and higher velocities as they occur in the outside portion of river bends or meanders (as sketched in Figure 3.9 a).

The uniform CORMIX flow field with the constant depth laterally is indeed conforming to a cumulative discharge distribution with equally spaced discharge lines, as indicated in Figure 3.13b. It is then conceptually straightforward to translate the CORMIX plume prediction back to the actual flow distribution by calculating and plotting the plume boundaries within the given cumulative discharge lines as shown in Figure 3.13c. The actual plume pattern may then show some surprising features such as strong "shifting back and forth" between opposing banks and an apparent

"thinning" of the plume width. These realistic plume features are simply dictated by the non-uniform flow field.

3.5.2 River Discharge of ADCP measurement

As discussed in Chapter 2, cumulative river discharge is also contained in the ADCP data. However, complete bank-to-bank transects were taken only at the upstream and 1500 m downstream of the discharge. These transects contain the complete cumulative discharge (0 – 100%) for the entire cross-section. However, in most transects, only the region occupied by the thermal plume was measured. Therefore only an incomplete percentage of the cumulative discharge (e.g. 0- 40%) is known from ADCP data.

However, the Far Field Locator is still applicable with some assumptions. The complete ADCP transects reveal that the river discharge was consistent with no significant change in total discharge. Hence, it is reasonable to assume that the total discharge at each transect would be equal to upstream discharge. With this assumption, cumulative discharge can be normalized and the cumulative discharge line can be computed for the incomplete transects.

Since the complete transect cumulative discharge ADCP information is not available, the ADCP transects do provide cumulative discharge laterally from the bank well past the observed edge of the thermal plume. Therefore, for the regions of the transects no cumulative discharge data is available, reasonable estimates of cumulative discharge can be made and will not influence the analysis of the far-field locator program. Appendix B includes the detailed river discharge input for the use of far-field locator.

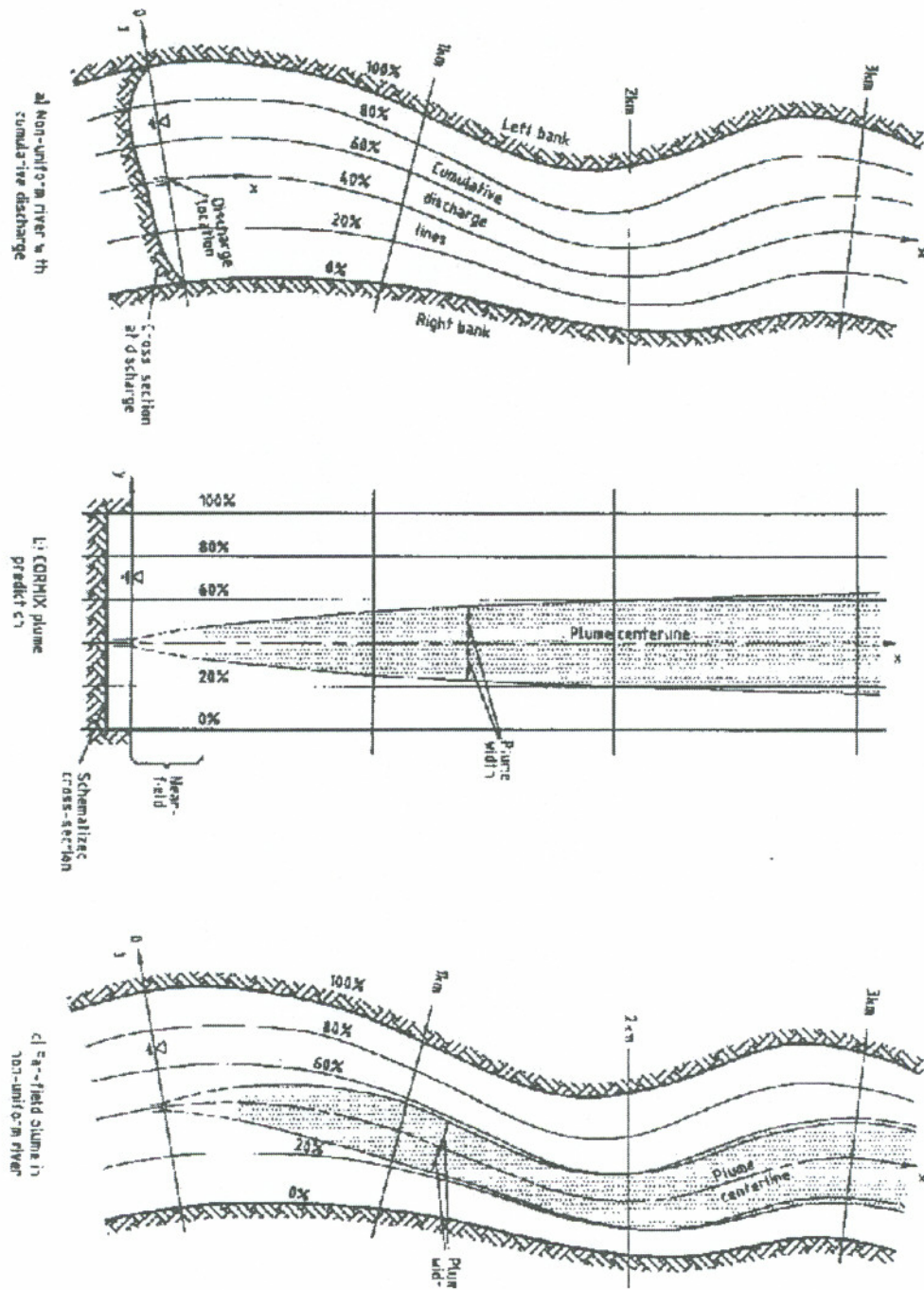


Figure 3.9 Illustration of the cumulative discharge method for translating the CORMIX predicted far-field plume to the actual flow characteristics in winding irregular rivers or estuaries [15]

Field Data Processing and Utility Development

Before utilizing field data to compare with the modeling results, processing the raw field data is an important step. Raw field data is not always representative of site conditions due to sampling errors, biases, and variation due the spatial and temporal properties of synoptic data. Therefore techniques for processing observational data are presented and then the processed data is illustrated case by case.

For geographical presentations, Geographic Information Systems (GIS) are widely used to comprehensively display and manipulate spatial data. ArcView is widely used GIS software with features that can display modeling results with geographic coordinates. In the second part of this chapter, details of development ArcView methodology that automates the processing of CORMIX prediction files for geo-referenced display and visualization will be introduced.

4.1 Field Data Pre-Processing

This section outlines the techniques developed to process and display the field data collected. The “Boxcar Window”, a generic signal processing in technique, was applied to spatially filter the synoptic measurements and irregular “spiky” thermistor string data taken along the river transects. By averaging data over space and time, this method smoothes the field temperature measurements to better represent the likely

“time-averaged” steady-state conditions. The technique processes the signal by averaging each data point with the surrounding data points to generate a series of the representative data sets.

4.1.1 Signal Processing Techniques for Thermistor String Data

Because of the time-varying nature mixing in turbulent thermal plumes, there is variation in a thermal signal measured over time at a given point in space. The time interval between two data points may also affect the quality of the field data. Due to turbulence, or subtle changes in ambient environment or discharge conditions and the instantaneous measurements at an individual point, significant discontinuities were found in the field data. These discontinuities become apparent when plotting the thermistor string temperature distribution. Discontinuities also make comparison of the simulation model results with the field data difficult.

These discontinuities, the so-called the “noise” in signal processing, can be removed through various signal processing procedures. For our case, the general spatial pattern in temperature is of interest and the time difference (due to turbulent eddies) is of secondary importance on discontinuities since i) the heated discharge volume flux and ambient velocity field was constant during the field data collection, and ii) time-averaged temperature data a given point is desired. Thus, the spatial filter can be simply applied to eliminate the spiked data points in the field data.

In filter processing, all filtering techniques can be simply formularized as following with different “window” definitions:

$$H = h \cdot w \quad (4.1)$$

Where, h is the impulse response, w is a finite-duration “window” and H is the product of these two elements. The Boxcar window, named rectangular window as well, is introduced to phase out some spatial “noise” in a pre-processing procedure. For the Boxcar window, w is defined by the following equation[30].

$$w = \begin{cases} 1, & \text{for all the data points within the length} \\ 0, & \text{otherwise} \end{cases} \quad (4.2)$$

Figure 4.1 depicts typical application of the Boxcar window and the resulting product. Thus, with the average effect from the Boxcar window, the spikes (e.g. due to turbulent fluctuations of the thermal plume signal) in the data sects can be removed. Thus the filtered temperature data from the river transects are representative of steady-state conditions.

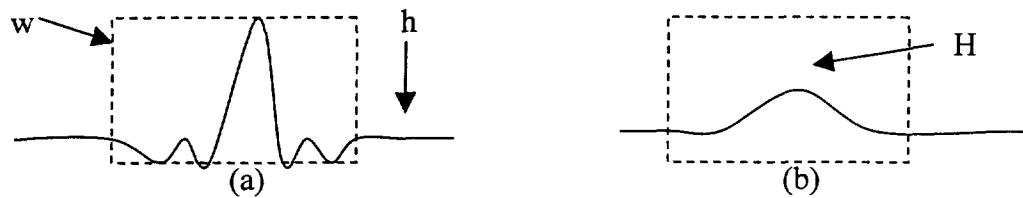


Figure 4.1 Illustration of the Boxcar Filtering technique on an input signal
 a) Shows illustration of the unfiltered (ideal) signal and the box window applied. (b) Typical output (filtered signal) approximation resulting from windowing the ideal impulse response.

Figure 4.2 shows an example of both processed and unprocessed data. This plot shows temperature excess ΔT versus lateral distance from the bank. Temperature excess ΔT is the increase above background temperature T_a observed at a location. Thus, if the ambient background temperature is 20 °C, and the actual plume temperature reading is 24 °C, then the temperature excess $\Delta T = 4$ °C would be indicated in Figure 4.2. For brevity, temperature excess in the discussion of plume transects for the sites in this study will simply be called “temperature”.

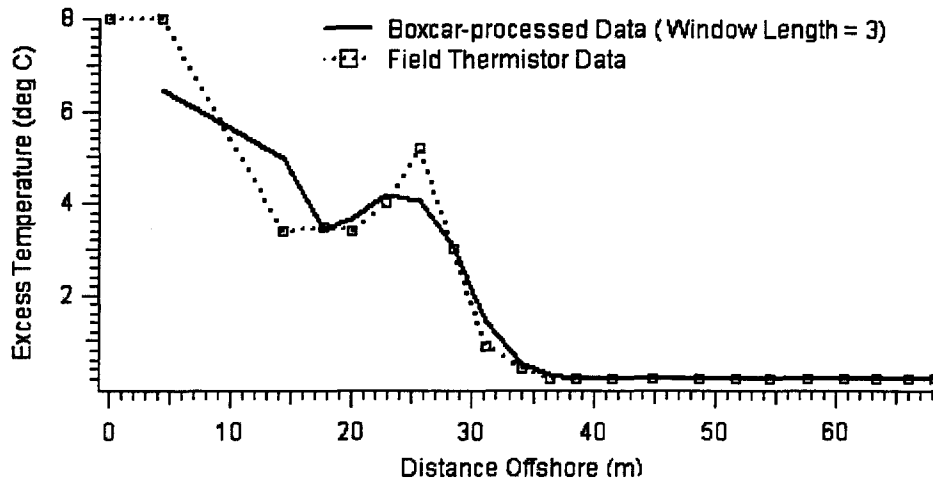


Figure 4.2 Trends of Unprocessed and Boxcar-processed Data

The length of the rectangle in Boxcar window represents the number of data points used to calculate the average value as the representative value. The representative value is then assigned to the middle point of these data points. The larger the length of rectangle is the more significant the averaging effects will be on the whole data set, and the variation between data points will be removed. However, the disadvantage of this method is that the first and the last few data points are removed, and more data points are removed after applying the larger length in the boxcar method. In addition, the averaging effect on the data decreases the maximum value and increase the minimum value. More importantly, the fuzzy signature of the signal response will appear with applying the longer length and as a result, for our case, the plume edge and lateral profile may not be revealed in detail in the processed data. Hence, the magnitude of these effects can be determined explicitly by the length of the rectangle applied and the data itself. Figure 4.3 shows the effects of one of the field data by using Boxcar window with different rectangle lengths.

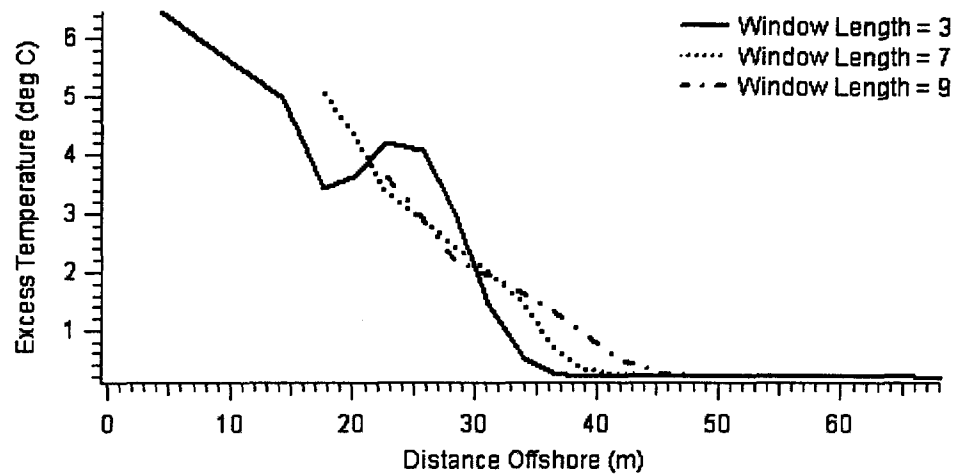


Figure 4.3 The processed data by applying Boxcar window with different rectangle lengths

For purposes of this study, it is unnecessary to average over large portion of whole data set which results in the significant decrease in higher temperatures, increase in lower temperatures, and the unrepresentative lateral profiles. Therefore, in order to keep the general pattern of the raw data, a window rectangle length, or boxcar length, equal to three (3) data points was adopted for the analysis presented below. It is noted that this signal processing method is only applied to the thermistor data and thus the associated sampling times and geo-coordinates are needed to be altered after the method is applied.

However, this signal-processing technique was not applied for the vertical thermistor data because of the less data points over depth and less spatial variation from the observation. Commonly, in our thermistor data, five (5) to eight (8) data point were collected in the vertical direction. With the understanding of the boxcar windowing, the averaging effect could be remarkable due to the less data points and the resulting data becomes unrepresentative as well. Furthermore, the true vertical profile may be an important indication of the relation between the magnitude of the vertical mixing and boundary interaction. Thus, the vertical thermistor data was truly preserved without being pre-processed.

4.1.2 Processed Field Thermistor String Data

After removing the “signal noise”, the processed thermistor string data becomes more representative of likely steady-state site conditions. In this section, the physical characteristics and possible mixing scenarios of the thermal plumes indicated by the processed thermistor data for each site is discussed.

Thermistor transects for each site presented in the following section have similar general characteristics. As expected in a mixing zone, transects show decreasing temperatures with increasing downstream distance from the discharge. Within each transect, temperatures decrease laterally from near-bank to mid-channel, where they approach background level at the lateral plume margin. At a given lateral distance from the bank, plume temperature generally decreases vertically from top to bottom when there exists a vertical profile. The largest vertical temperature differences occur closest to the bank, and vertical temperature differences decrease to zero at the lateral plume offshore edge. Vertical variation in temperature profile decreases downstream from transect to transect. Surface temperature in most transects is slightly lower than the 0.2 m (below surface) subsurface reading, perhaps evidence of surface heat transfer and cooling.

4.1.2.1 Cooper Nuclear Station

The processed field temperature data for the Cooper site is shown in Figure 4.4, plotted as temperature excess ΔT above background ambient T_a . At this site, the background ambient temperature was $T_a = 22.70$ °C and the discharge temperature $T_0 = 33.97$ °C, giving a temperature excess $\Delta T = 10.27$ °C at the discharge. The near-bottom (4.2 m depth) temperature excess ΔT measured is not zero, this indicates that the plume is interaction bottom, since the ambient depth at discharge $H_D = 4.75$ m and average cross-section depth $H_a = 4.23$ m.

From the observations shown in Figure 4.4, the plume can also be qualitatively separated into two general regions, before and after the 180 m transect. Within 180 m downstream of discharge (Figure 4.4 a, b, c, d) the vertical temperature profile varies considerably within the plume. In contrast, uniform temperature profiles over depth is observed in the following transects after 180 m (Figure 4.4 e, f). The start of the uniform temperature profile at 180 m downstream may be the indication of the transition between the buoyancy driven current and the ambient turbulence driven current.

The arbitrary temperature distribution observed within the region of the first 60 m might indicate the near-field boundary interaction with the bank to form a recirculation zone. At 30 m downstream, higher temperatures detected in the near-bank region reveals bank-attachment of the plume. From 60 m to 180 m downstream, the nearly uniform lateral temperature distribution in the near-bank region may simply imply the appearance of a recirculation zone where more lateral motions with the bank are arisen.

Generally, after 180 m downstream, the temperature continues to diminish and the plume width becomes wider gradually. According to the fluid dynamic characteristics of the density current, due to the mixing between the surface stratified layer and subsurface layers the vertical temperature profile becomes unobvious or tends to be nearly uniform when the plume layer thickens. Thus, the dominant mechanism controlling the dilution cannot be determined based on the vertical uniformity in temperature. However, in the region between 760 m and 1500 m downstream, because of the observation of the extremely slow temperature diminishing and lateral spreading, the plume propagation and dilution characteristics are thought to be entirely controlled by the ambient turbulence rather than buoyancy force.

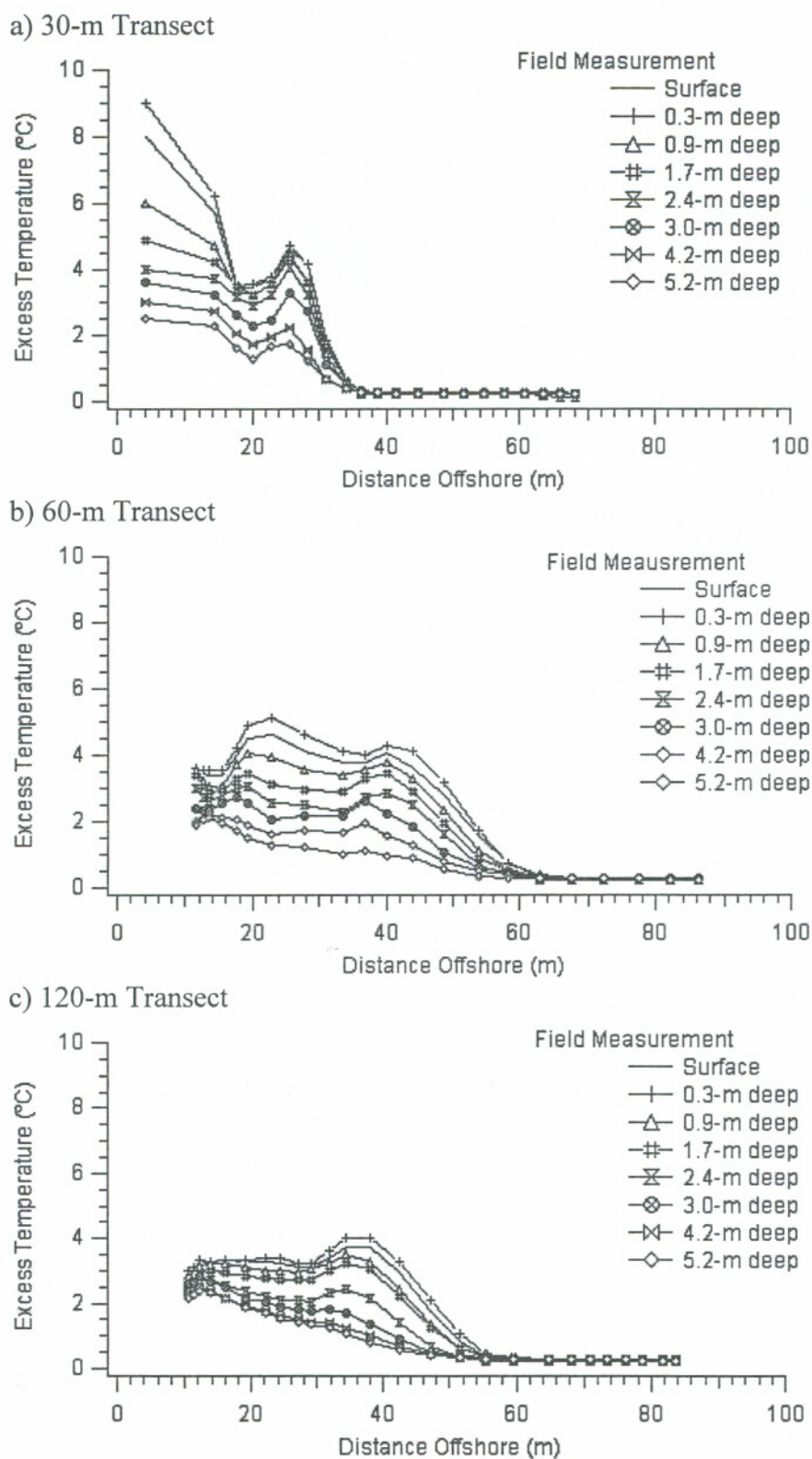
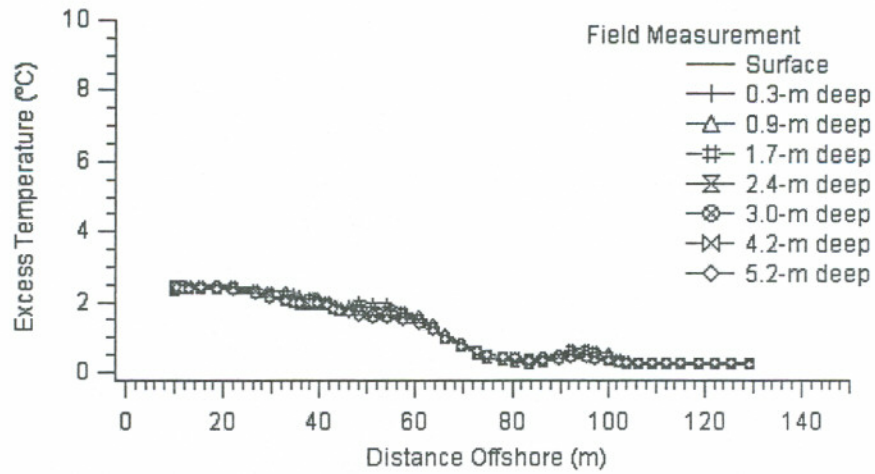
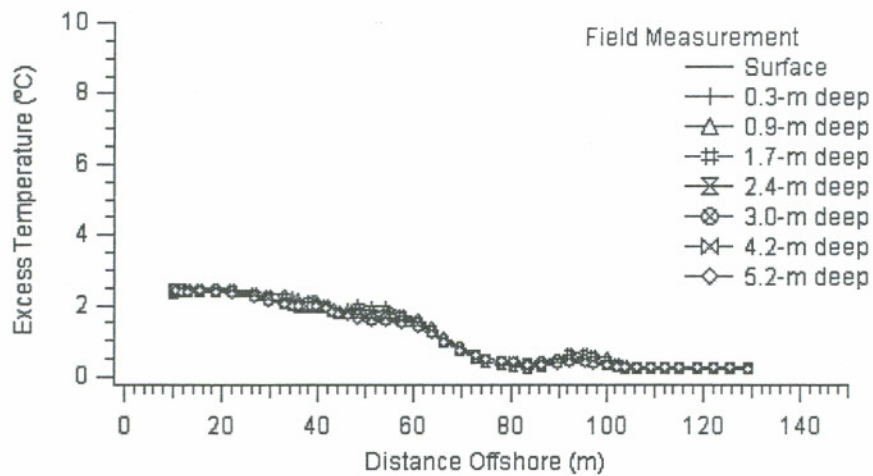


Figure 4.4 Transversal Excess Temperature Profiles at Cooper Nuclear Station

d) 180-m Transect



e) 380-m Transect



f) 762-m Transect

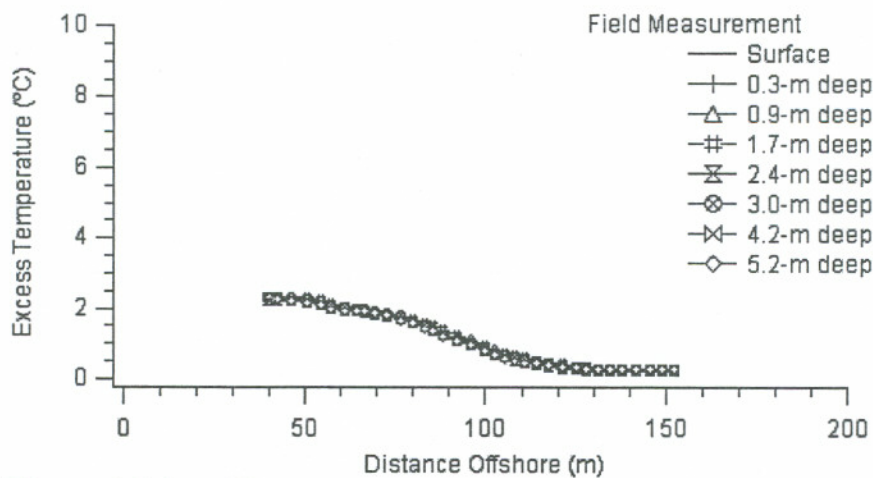


Figure 4.4 (cont'd)

g) 1524-m Transect

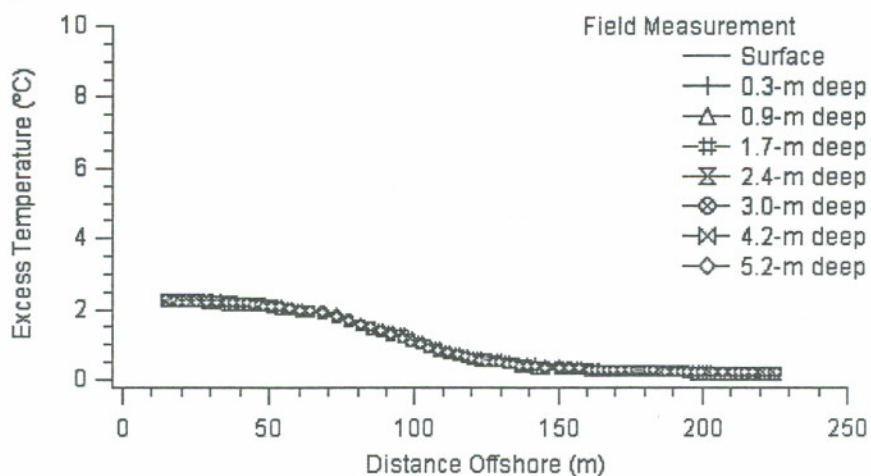


Figure 4.4 (cont'd)

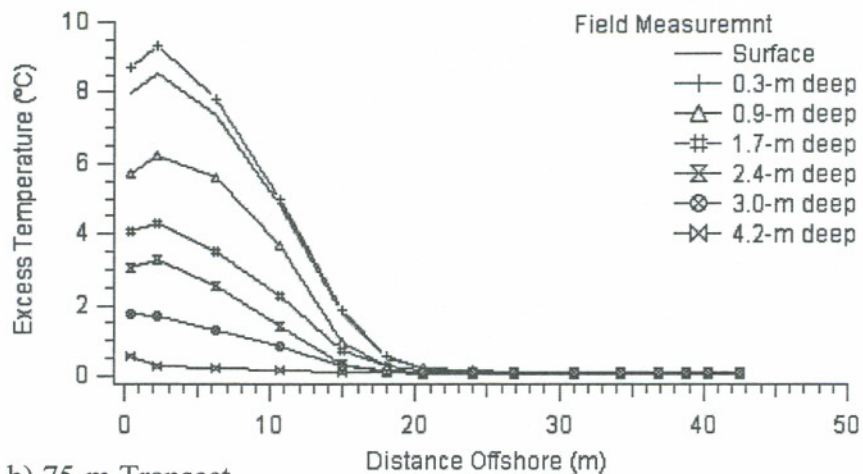
4.1.2.2 Fort Calhoun Power Station

The processed field temperature data for the Fort Calhoun site is shown in Figure 4.5, plotted as temperature excess ΔT above background ambient T_a . At this site, the background ambient temperature was $T_a = 21.76$ °C and the discharge temperature $T_0 = 34.10$, giving a temperature excess $\Delta T = 12.34$ °C at the discharge. Since the near-bottom (4.2 m depth) temperature excess ΔT measured is not zero, this indicates that the plume is interaction bottom, since the ambient depth at discharge $H_D = 4.63$ m and average cross-section depth $H_a = 4.91$ m.

A near 0 °C temperature is observed near the bottom of the water column within the first 90 m downstream of the discharge and significant vertical temperature differences are observed up to the 380 m transect. This indicates a plume with limited vertical thickness, occupying the upper surface layer interaction with the limited bottom interaction. Following 380 m transect, temperature at the upper level remains stratified and relatively high, a uniform temperature zone tends to form at the lower level. This reveals that the buoyancy force cannot lift up the plume anymore and as a result, the plume starts to collapse and transits into the passive diffusion where the

ambient turbulence is predominant.

a) 45-m Transect



b) 75-m Transect

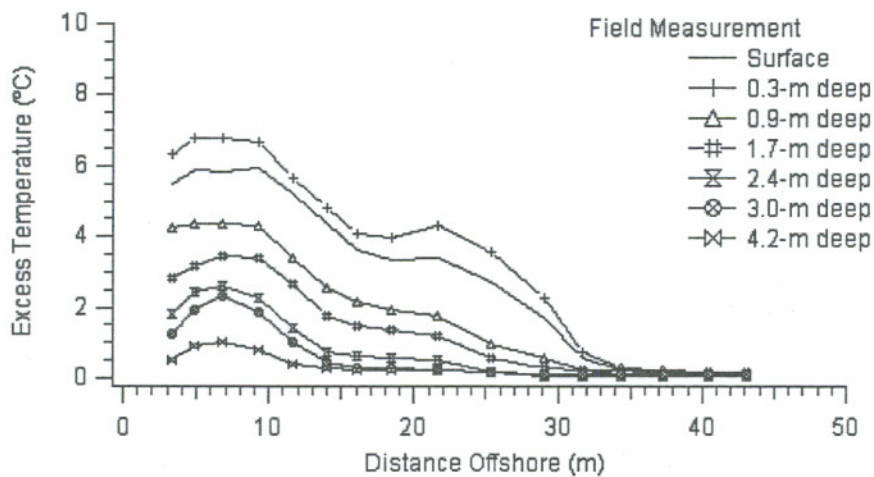
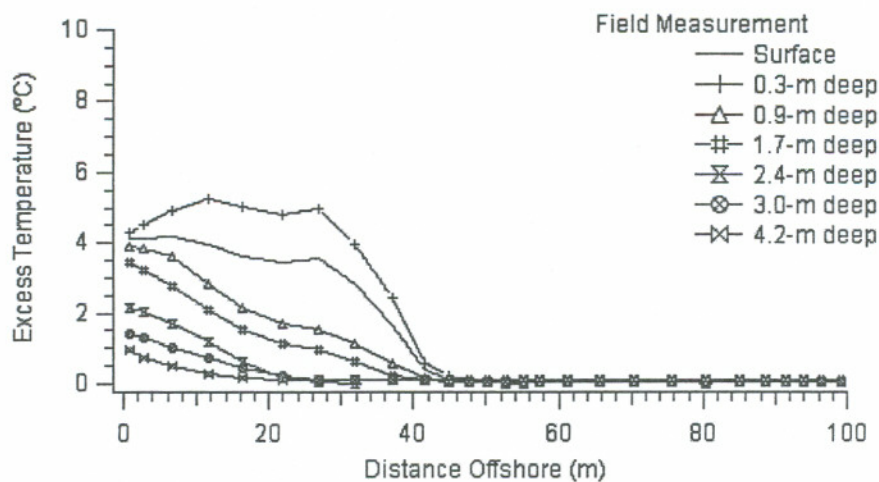
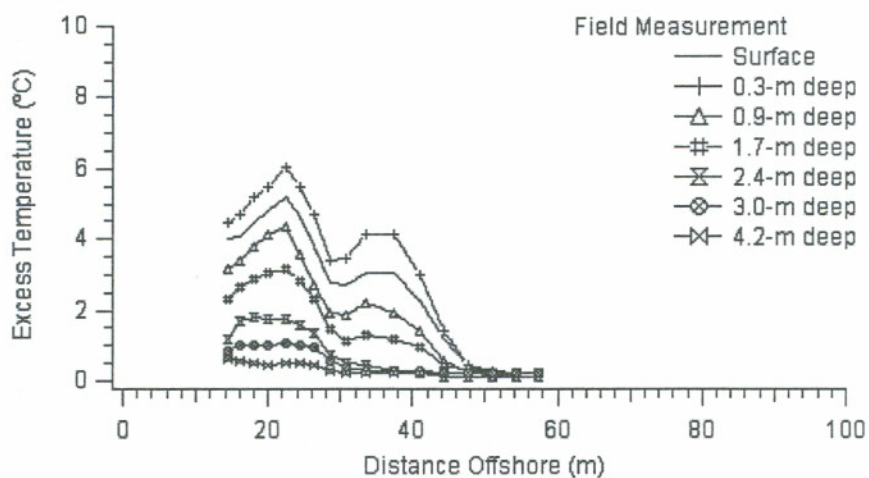


Figure 4.5 The Transversal Excess Temperature Profiles at Fort Calhoun

c) 90-m Transect



d) 120-m Transect



e) 180-m Transect

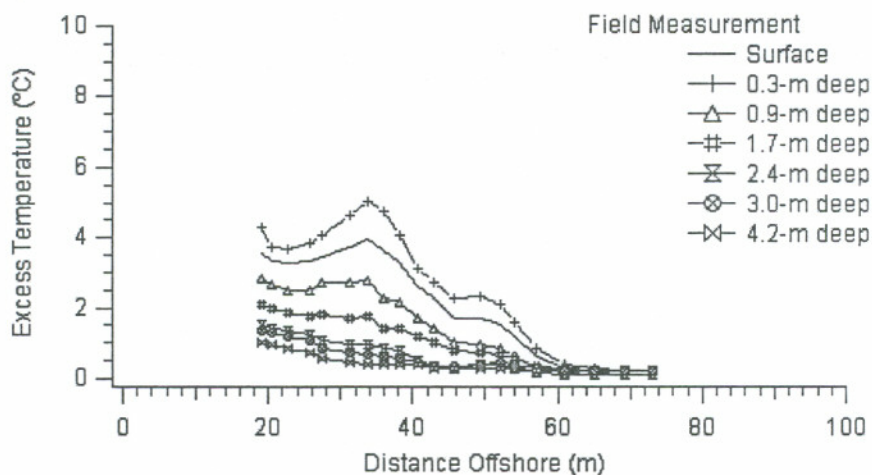
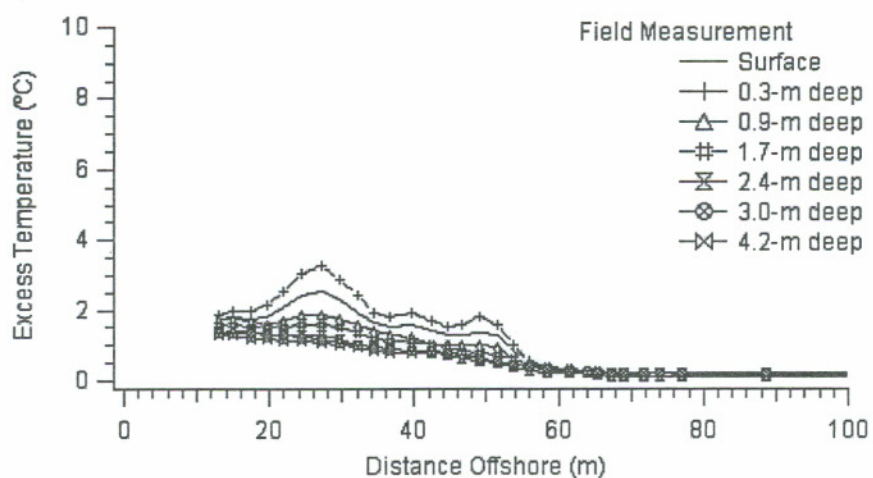
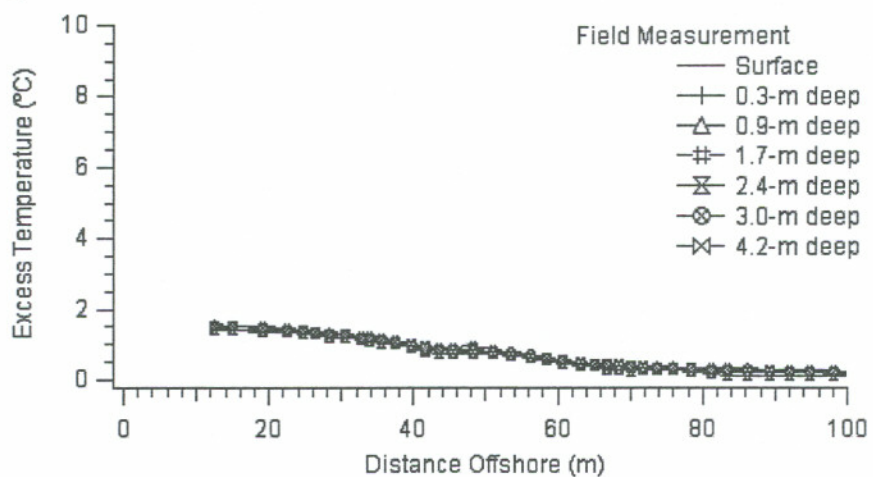


Figure 4.5 (cont'd)

f) 381-m Transect



g) 762-m Transect



h) 1524-m Transect

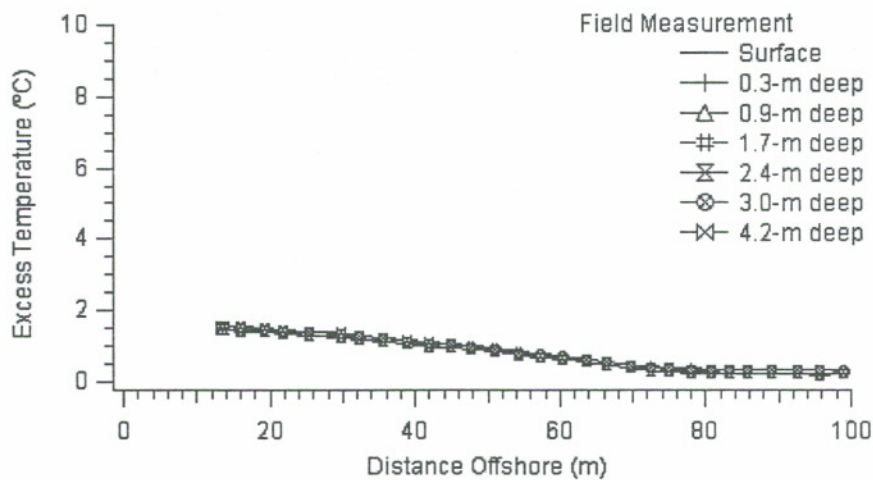


Figure 4.5 (cont'd)

4.1.2.3 Nebraska City Power Station

The processed field temperature data for the Nebraska City site is shown in Figure 4.6, plotted as temperature excess ΔT above background ambient T_a . At this site, the background ambient temperature was $T_a = 22.28^\circ\text{C}$ and the discharge temperature $T_0 = 32.00^\circ\text{C}$, giving a temperature excess $\Delta T = 9.27^\circ\text{C}$ at the discharge. Since the near-bottom (4.2 m depth) temperature excess ΔT measured is not zero, this indicates that the plume is interaction bottom, since the ambient depth at discharge $HD = 4.21\text{ m}$ and average cross-section depth $H_a = 4.57\text{ m}$.

As shown in Figure 4.6 a limited vertical the temperature variation is minimal, indicating the plume may be fully vertically mixed because of the shallower local depth at discharge. Partially due to the initial vertical mixing, the plume spreads much slower and the lateral extent remains approximately 40 m in the sampling area. Similarly, the transition between density current and the passive diffusion can also be allocated at approximately somewhere between 381 m and 760 m by the same indications mention previously.

a) 30-m Transect

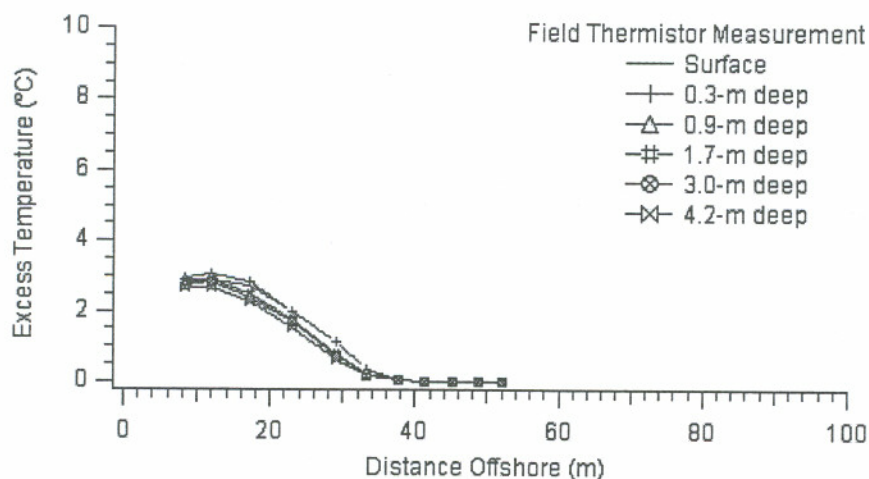
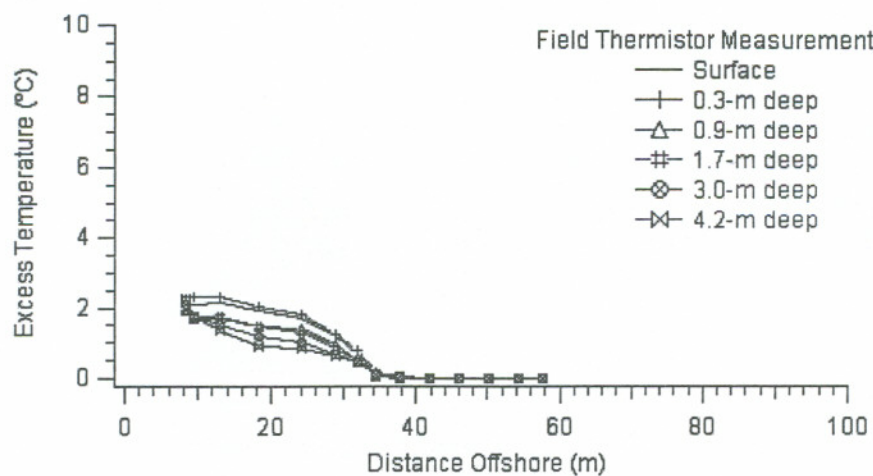
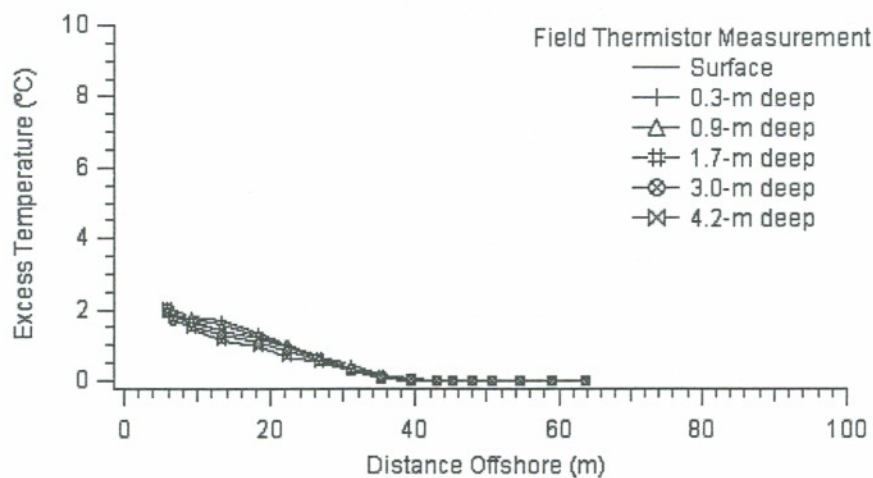


Figure 4.6 Transversal Excess Temperature Profiles at Nebraska City Power Station

b) 60-m Transect



c) 120-m Transect



d) 180-m Transect

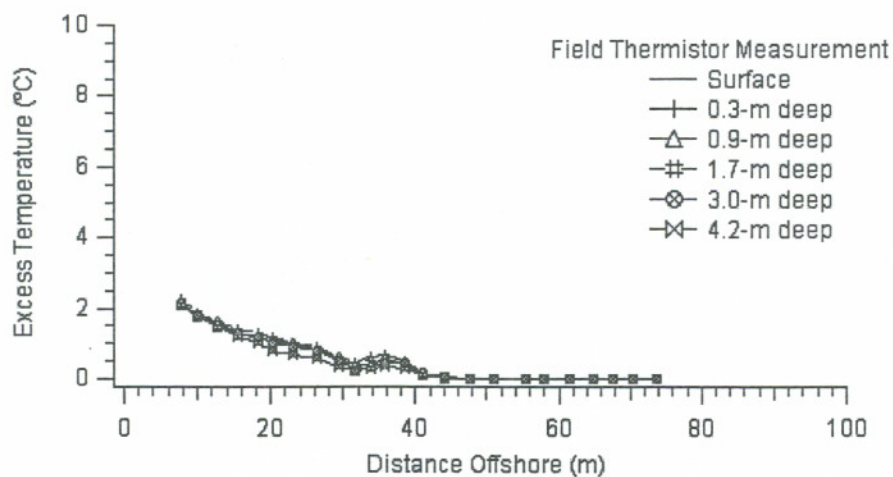
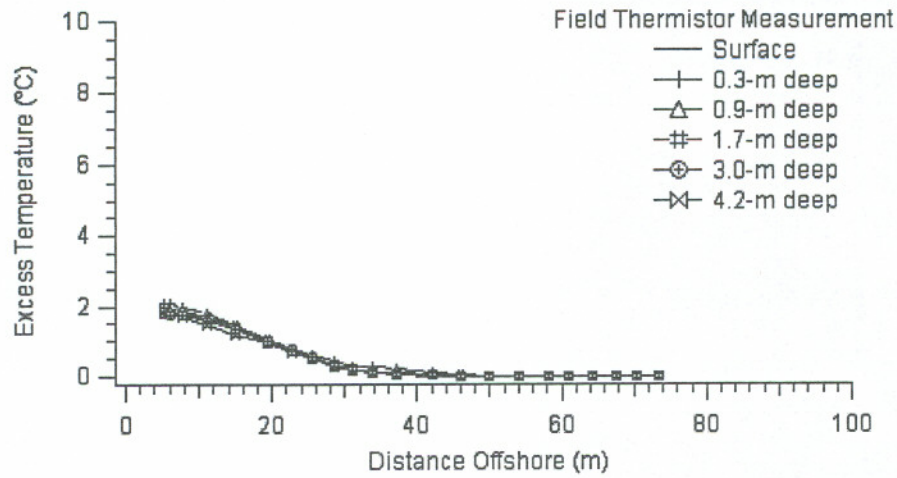
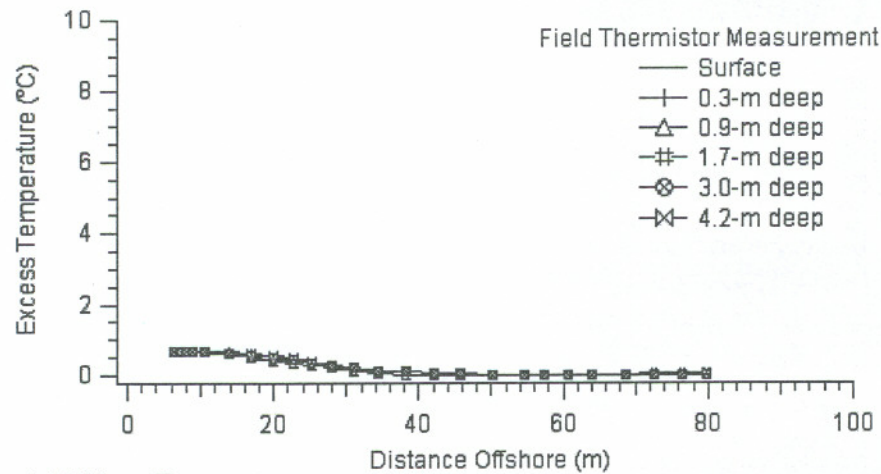


Figure 4.6(cont'd)

e) 381-m Transect



f) 762-m Transect



g) 1524-m Transect

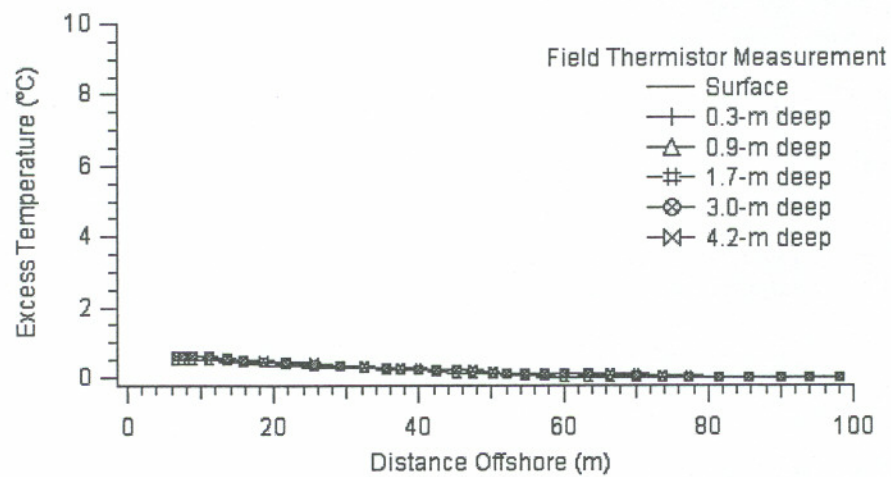


Figure 4.6 (cont'd)

4.1.2.4 North Omaha Station

The processed field temperature data for the North Omaha site is shown in Figure 4.7, plotted as temperature excess ΔT above background ambient T_a . At this site, the background ambient temperature was $T_a = 21.80$ °C and the discharge temperature $T_0 = 27.40$ °C, giving a temperature excess $\Delta T = 5.60$ °C at the discharge. Since the near-bottom (4.2 m depth) temperature excess ΔT measured is not zero, this indicates that the plume is interaction bottom, since the ambient depth at discharge $H_D = 4.15$ m and average cross-section depth $H_a = 3.83$ m.

Similar pattern as the observations in the Nebraska power station, a weaker magnitude of the vertical mixing occurs near the discharge entry because of the shallower depth at the discharge relative to the average depth. The transition between buoyant spreading and passive diffusion is approximately located between 381 m and 760 m downstream.

a) 30-m Transect

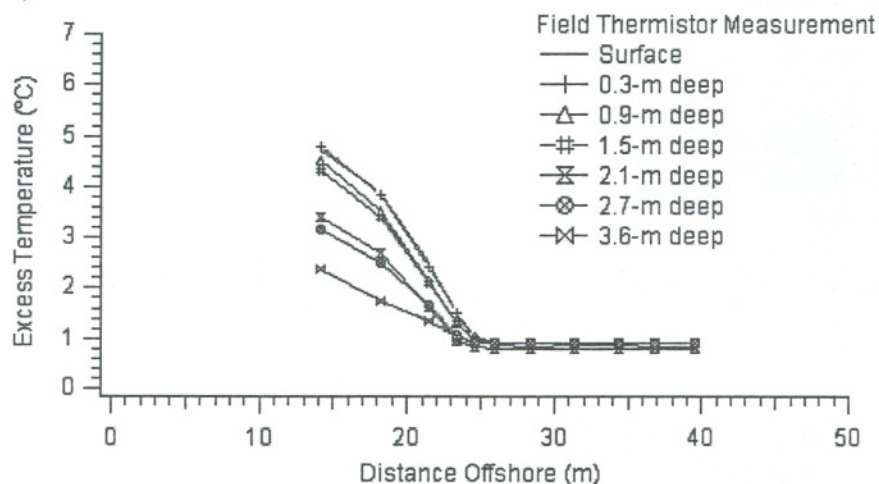
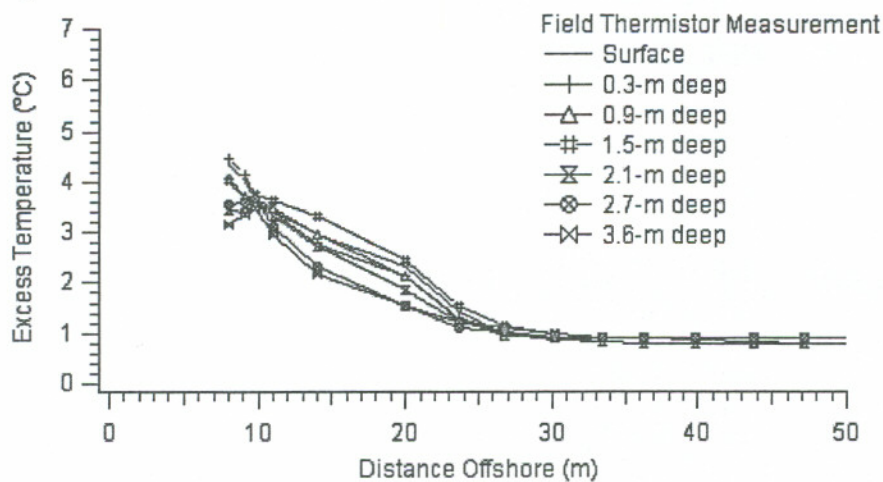
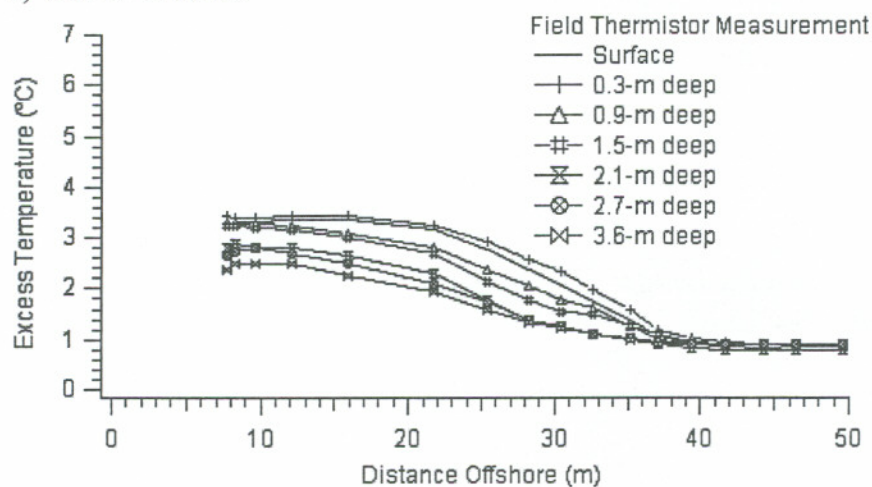


Figure 4.7 The Transversal Excess Temperature Profiles in North Omaha Power Station

b) 60-m Transect



c) 120-m Transect



d) 180-m Transect

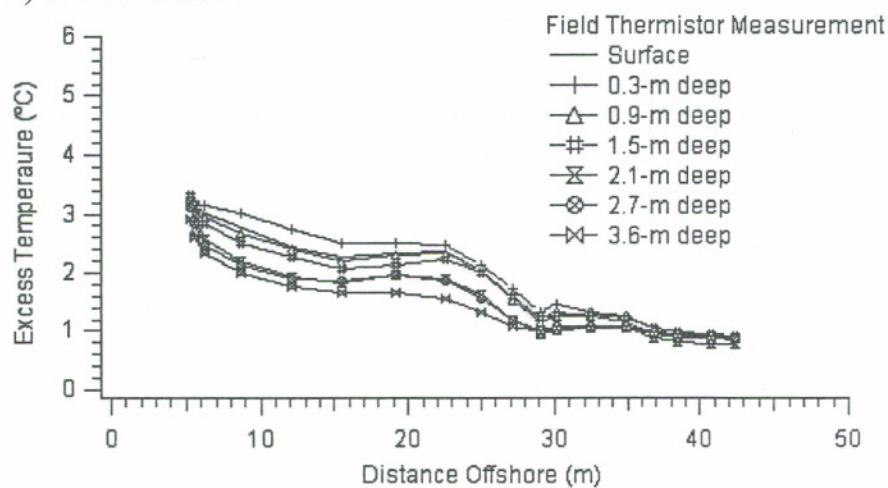
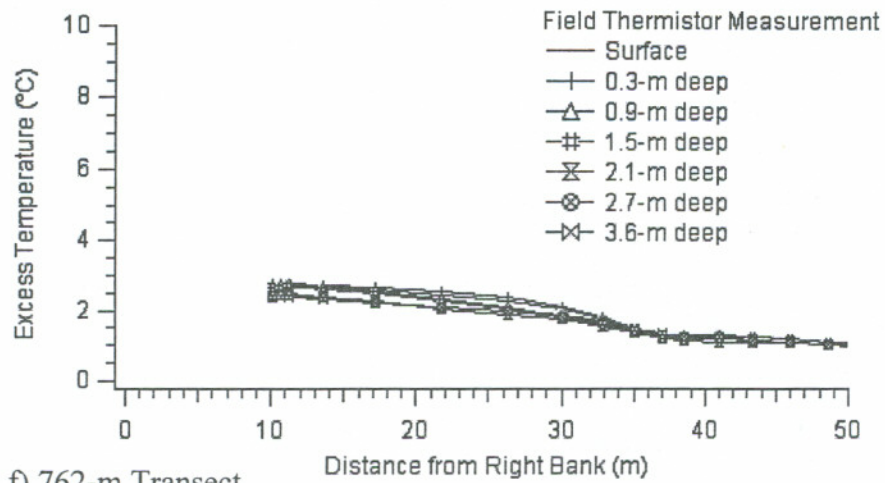
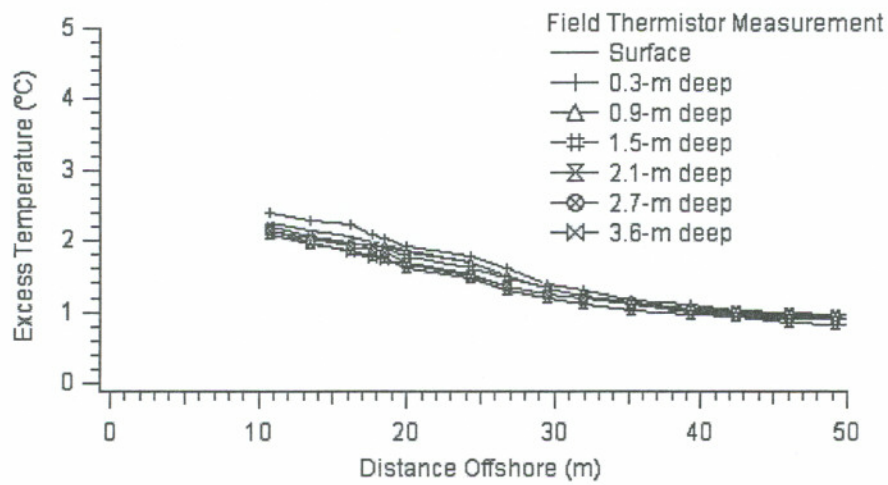


Figure 4.7 (cont'd)

e) 381-m Transect



f) 762-m Transect



g) 1524-m Transect

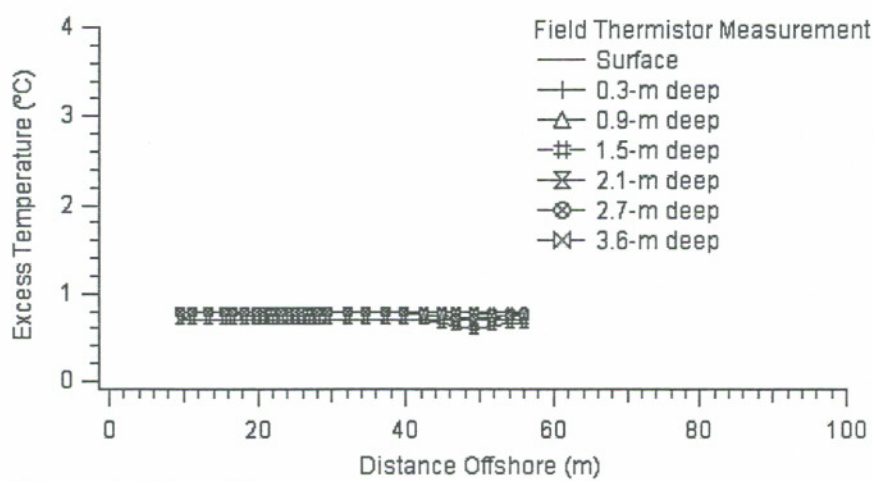


Figure 4.7 (cont'd)

4.2 ArcView Mapping Methodology Development

Spatial data is most often managed with Geographic Information Systems (GIS). GIS computer programs have special features that make manipulation spatial data efficient for visualization display. Therefore, development of automated GIS mapping techniques for display of processed thermistor string field data and model predictions may provide better understanding of the spatial properties of the thermal plume data sets. ArcView, a widely-used GIS computer program with functions for digital mapping and spatial data numerical interpolation, was the primary tool selected to generate spatial data comparisons and visualizations within this study.

For ArcView plume mapping methodology development, several assumptions were made to allocate the data points on the shoreline bank based on the field notes and the general principle of selecting representative data points to create plume plume visualizations through ArcView interpolation. In addition to the field data processing, geo-coding, the process of assigning geo-coordinates to the CORMIX prediction data sets, was another technique developed in this study to display CORMIX predictions and to assist in the reconciliation of simulation results with field measurements. The details of the geo-coding will be introduced in next section.

The interpolation of existing CORMIX modeling results and field data within ArcView can be accomplished by a number of different techniques. Grid interpolation is the most common method used in most cases. In this method, a simple x-y grid with uniform rectangular elements is set up for interpolation of the data set. Another interpolation method uses a Triangulated Irregular Network (TIN) where the grid elements are triangular and not of uniform size.

Several characteristics of grid approach might result in some practical limitations. The details of the grid interpolation are primarily determined by the grid size; and selection of the grid size can also be affected by the distribution of the data points. For the cases under consideration, the field data are arranged in terms of river transect and the transect intervals are much larger than the intervals between data

points. By applying small grid sizes, although the resolution is high, the appropriate interpolations only can be observed in the individual transect sections and thus discontinuities appear between transects. Inversely, by using the larger grid sizes, the resulting interpolations can better reflect the field thermistor data in the general plume presentation; however the resolution is much lower and the details cannot be distinguished in each individual transect. Therefore, in this study, the grid interpolation is adopted for creating plume patterns in ArcView.

The main feature of a TIN is using 3 points to form a triangle whose size can be varied based on the distribution of data points and thus, the resulting interpolations can be in irregular shapes corresponded to the distribution of data. Thus, both modeling results and the field data are presented through TIN interpolation. It is also important to note that in order to obtain the representative map on field data, less than 3 data points of each transect are selected and in general, the data points containing highest and lowest temperature are taken into considerations except some random transects, which need to be carefully filtered out some “noise” in the data sets.

4.3 CORMIX-Related Software Developments

Although several visualization tools have been included in the CORMIX-GI v4.2GT including 2-dimension and 3-dimension plume visualizations, the incapability of illustrating the plume dimensions in geographical scale causes some inconvenience with the conversion between two coordinate systems. One of the goals of this study is to develop the methods to process CORMIX prediction files with geo-codes and then process the plume prediction into ArcView-readable delimited text files. Because ArcView has a powerful geospatial graphic toolset and desired the interpolation features, it can illustrate the plume dimensions graphically by using Triangulated Irregular Network (TIN). ArcView includes internal scripting language called Avenue which can automate the procedures to create the desired plume visualizations.

4.3.1 Filter Program Design

The filter algorithm, CorGC, is written in C++ programming language and compiled in Microsoft Visual Studio v.5.0. The first step of CorGC is to strip out the numerical predictions in CORMIX prediction files and to compute the physical dilution factors and diluted concentrations on the edges of the plume based on the profile definitions in each module. The tasks of arranging and organizing the output delimited text files are also included in the first stage. Geo-Coding is the main portion in the second algorithm step. Related information, such as outfall locations and desired ending locations, is required to match the latitudes and longitudes with the predicted data points.

4.3.1.1 CORMIX Prediction Extraction and Dilution Calculations on Plume Edge

CORMIX predicts the plume centerline trajectory and dilution within a series of regional flow models. Thus, the near-field, boundary interaction, and far-field mixing is simulated with a sequence of regional flow models, call modules (MODS) within CORMIX. Each MOD contains one of four possible cross-sectional profile definitions for lateral distributions of concentration for plume vertical and horizontal width dimensions (Figure 4.8).

To visualize the plume in 2-dimensions, the lateral profile is of primary concern in filter algorithm program development for computing the diluted concentration on the edge of the plume. A Gaussian $1/e$ (37%) profile is adopted for describing the submerged round and submerged plane jet/plume laterally though different vertical profiles are used individually. For buoyant spreading regime, top-hat profile presents the uniformity in concentration vertically and laterally. On the other hand, in ambient diffusion process, a Gaussian distribution with the plume width defined as $\sigma^*(\pi/2)^{**1/2}$ (46%) is applied for vertical and lateral profiles.

Plume profile definitions vary from module to module. Each profile definition is recognized by an *if* statement in the algorithm, with by character string matches in

C++ language to identify the profile definitions. Then the algorithm computes the associated concentration C and dilution S on the edge of the plume (based on the lateral plume profile definition) and creates data points with the associated x and y coordinates. The algorithm also preserves the original trajectory and concentration information as well as the plume vertical thickness (BV), upper plume boundary (ZU), lower plume boundary (ZL). Although these parameters are not used in the methods developed here for calculating the plume horizontal edge data points, the information will still be helpful for understanding the plume dimension in 2D plume patterns.

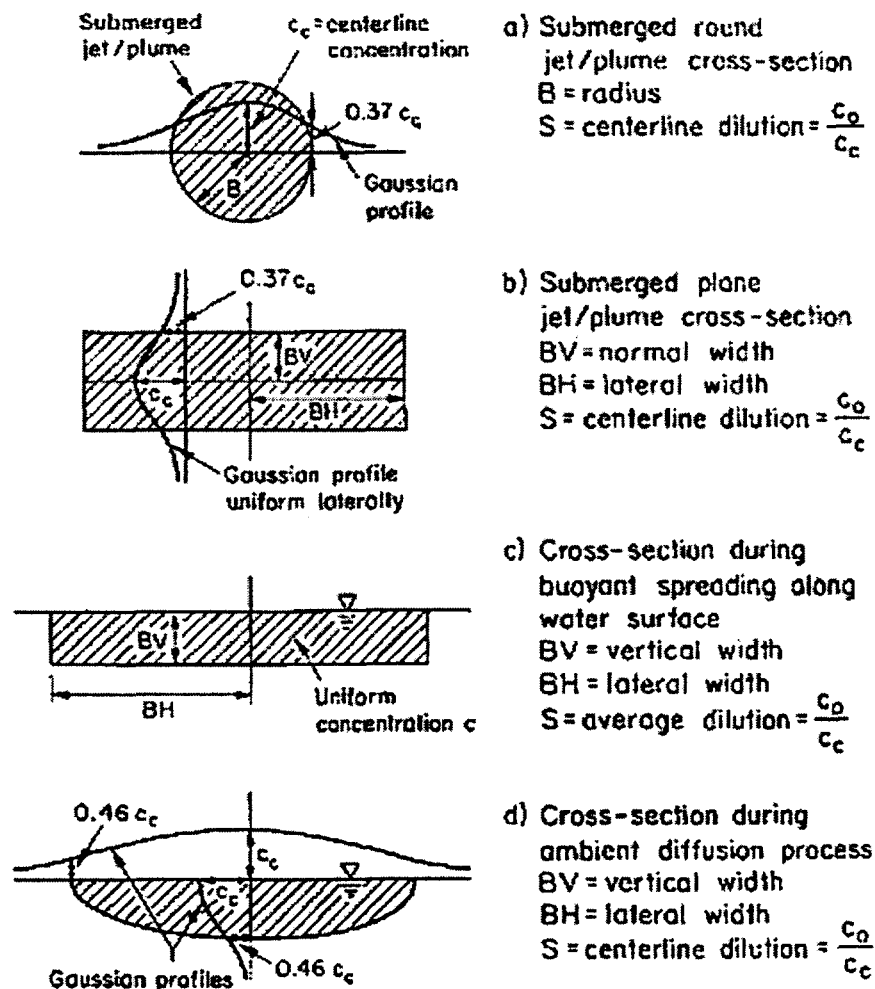


Figure 4.8 Cross-sectional distributions of CORMIX predicted jet/plume sections[15]

It is important to note that in CORMIX predictions, overall concentration C is determined not only from physical dilution, but also includes any reaction effects, such chemical decays or heat transfer. The dilution S , simply the reciprocal of the concentration at a point and the initial concentration, only represents the physical dilution property rather than the overall dilution. To avoid data points with different concentration values, physical diluted and overall concentration, instead of calculating the precise concentration and dilution on the plume edge individually, CorCG only allocates edge points based on the lateral profile definition and simply assigns the edge data point's concentration C to be zero as a boundary.

After these steps, the prediction extraction for each module occurs with the text manipulations to convert the space-delimited format of CORMIX predictions into tab-delimited format accepted in ArcView.

4.3.1.2 Geo-Coding CORMIX Predictions

In geo-coding, the locations of starting and ending points are required as input parameters. The starting point always refers to the outfall location and the ending points can be varied depending on the users preference. The methodology used to convert the CORMIX coordinate system to geo-coordinate system is based on the theory of triangle geometry. Since the outfall location is always referred to $(x=0,y=0,z=0)$ in CORMIX coordinates, the CORMIX prediction can be propagated from the starting point in geographical scale (x,y) as the outfall location.

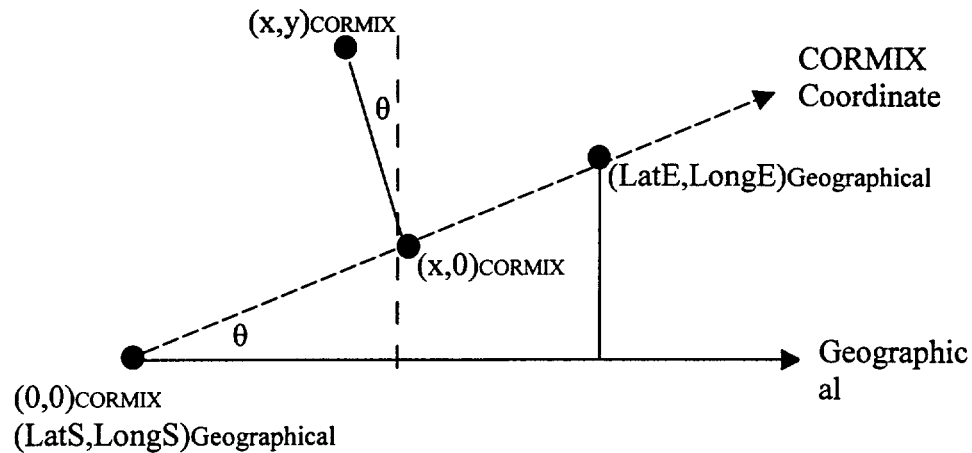


Figure 4.9 Scheme of the Conversion between CORMIX and Geographical Coordinates

To transform the CORMIX predictions into the geographical coordinate is to simply rotate CORMIX internal coordinate axis by an angle, θ , based on the river direction in geographical coordinate. The transformation of CORIMX prediction can be easily accomplished through trigonometric functions. The unit conversion is also involved in the filter algorithm to convert the SI unit used in CORMIX into the common geographical coordinates unit, decimal degrees. Figure 4.1 shows the scheme of this methodology.

First step is unit conversion. The starting and ending points are used to calculate the ratios between degree and distance in longitude and latitude individually, and ratios can be illustrated as following:

$$\text{Unit Conversion}_{\text{longitude}} = (\text{LongE} - \text{LongS}) / \text{Dist.} (\text{LongE} - \text{LongS}) \quad (4.3)$$

$$\text{Unit Conversion}_{\text{latitude}} = (\text{LatE} - \text{LatS}) / \text{Dist.} (\text{LatE} - \text{LatS}) \quad (4.4)$$

It is important to note that 1-degree interval in longitude is approximately equal to 85,277 m and 1-degree interval in latitude is approximately equal to 111,182 m. Since the distances between two points in latitude and longitude are derived from differences between two points in degrees and 1-degree unit conversions, the two equations can be simplified as:

$$\text{Unit Conversion}_{\text{longitude}} = 1 / 85277 = 0.00001173 \quad (4.5)$$

$$\text{Unit Conversion}_{\text{latitude}} = 1 / 111182 = 0.00000899 \quad (4.6)$$

Since the two coordinates, geographical and CORMIX coordinates, are neither parallel nor perpendicular to each other, both X and Y coordinates in CORMIX predictions are needed coordinate conversions. This is accomplished with trigonometric functions as following. With the known starting and ending points, the angle between two coordinates can be determined by the simple triangular functions within the triangle created by the starting and ending points. To tile CORMIX coordinates, only $\cos(\theta)$ and $\sin(\theta)$ are used in the computation and the ratios can be derived from distances between two points in longitude and latitude over the distance between two points, respectively.

CORMIX predictions can be geo-coded from the outfall location as the starting point coordinating with all the required parameters and the mathematical equations can be presented as following:

$$\text{Long}_{\text{CORMIX}} = \text{Long}_{\text{outfall}} + (X_{\text{CORMIX}} \cos(\theta) - Y_{\text{CORMIX}} \sin(\theta)) / 85,277 \quad (4.7)$$

$$\text{Lat}_{\text{CORMIX}} = \text{Lat}_{\text{outfall}} + (X_{\text{CORMIX}} \sin(\theta) + Y_{\text{CORMIX}} \cos(\theta)) / 111,182 \quad (4.8)$$

Following these two simple conversion equations, each of the trajectory data points in CORMIX predictions can be presented in geographical coordinates. Similarly, when more detailed geological information on the river curvature is available, CORMIX predictions presented in the geographical coordinates could nearly follow the nature river curvature by rotating the CORMIX axis sequentially by inputting multiple ending points and executing this algorithms repetitively. Due to assumptions in CORMIX, the centerline locations are always relative to the cumulative discharge from the bank and thus some adjustments can be made to shift the CORMIX predictions when the geological information is available.

However, CORMIX does not predict the complicated recirculation flows (eddies) which sometimes occur in streams bends. Additionally, if the larger plume

widths are predicted at the river bends there is a tendency for occurrence of the overlapping modeling results by executing the geo-coding algorithms repetitively with the multiple inputs of ending points. Sequentially, incorrect graphical interpolations may be produced by Triangulated Irregular Network (TIN) in ArcView. To avoid the occurrences of possibly incorrect results in visualizations, the geo-coding process is only executed once in the filter program as a default setting and only present the plume mapping in the assumed straight channel in ArcView. Figure 4.8 demonstrate the control flow of the filter program and Table 4.1 lists all the names, outputs, inputs, and functions of the algorithms in the program.

4.3.1.3 Filter Program Execution

After debugging and compiling the C++ codes in Microsoft Visual Studio, an executable command-line program (.exe), CorGC.exe, is created. The CORMIX prediction file name without the extension, *filename.prd*, is required to input manually and for geo-coding, the locations of outfall and desired ending point, in longitudes and latitudes, are also the input parameters. After all the executions are completed, the output text file is created as the same input name with “.prd.txt” extension and can be directly loaded in ArcView for plume visualizations.

4.3.2 ArcView Avenue Script Composition

The purpose of writing the ArcView scripts is to automate the procedures of creating the plume visualizations while a filter-program-processed file has been loaded. Although the plume visualizations can also be created manually it can be a tedious process. Among the several interpolation approaches provided in ArcView, Triangulated irregular network (TIN) is the most suitable method for demonstrating the irregular plume dimensions graphically.

Regarding the graphical performance, the COMRIX graphical tools, CorVue,

can only illustrate the centerline concentration distribution in terms of bulk concentration by far. However, on the other hand, with the advanced calculations in filter program, the centerline- and bulk- concentration distributions of the CORMIX modeling results can be both presented by TIN in ArcView.

To create the plume visualizations through ArcView Avenue scripts, several steps are needed. First, the data sets should be loaded in Arc View and presented in a "Table". Then a "Theme" can be created from "Table" as the data source and added into a "View" by setting the X- and Y- fields from the data source. Following the theme creation, Triangulated Irregular Network (TIN) is implemented to interpolate the CORMIX predictions and create the color plots, which is desired as the final product.

The composition of the ArcView scripts basically follows the procedures mentioned above. Because ArcView is also compatible of different types of text or table files, to clearly list the filter-program-processed files, the file type is specified as "*filename.prd.txt*" in the file loading menu. The associated table is created after the processed file has been loaded. In our case, longitudes and latitudes are set as X field and Y field, respectively, to create the theme presented as "points" in the view.

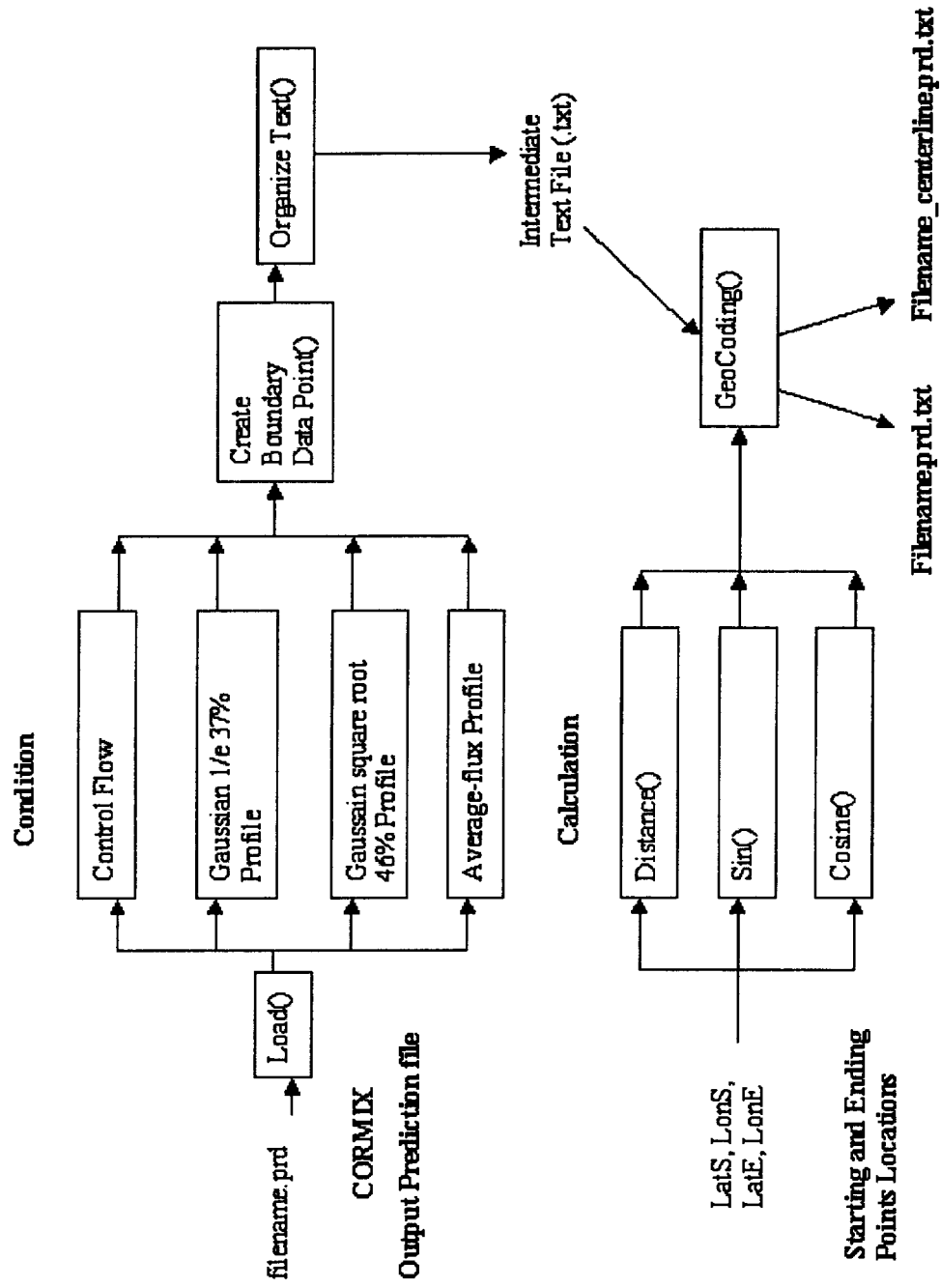


Figure 4.10 Control Flow of CorGC

Table 4.1 List of Algorithms

Algorithm	Input	Output	Purpose
Load()	CORMIX output	mid.txt, out.txt	1. Identify plume profile
			2. copy the into both mid.txt and out.txt
Create Boundary()	mid.txt	out.txt	Generate plume boundary
Organize Text()	out.txt	out.txt	out.txt
Distance()	LatS, LonS	integer distance	Calculate the distance, Δ Lat, and Δ Lon
	LatE, LonE	integer Δ Lat	
		integer Δ Lon	
Sin()	integer Δ Lat	integer sin	Calculate the sin() value
	integer distance		
Cos()	integer Δ Lon	integer cos	Calculate the cos() value
	integer distance		
GeoCoding()	LatS, LonS	filename.prd.txt	Geocode each data point
	integer sin		
	integer cos	filename_centerline.prd.txt	
	out.txt		

The default interfaces of creating TIN are employed to create the plume visualizations from the “points in the view”. The Z factor should be specified as concentration while presenting the concentration distribution within ArcView. Figure 4.9 illustrates the scheme of the avenue script.

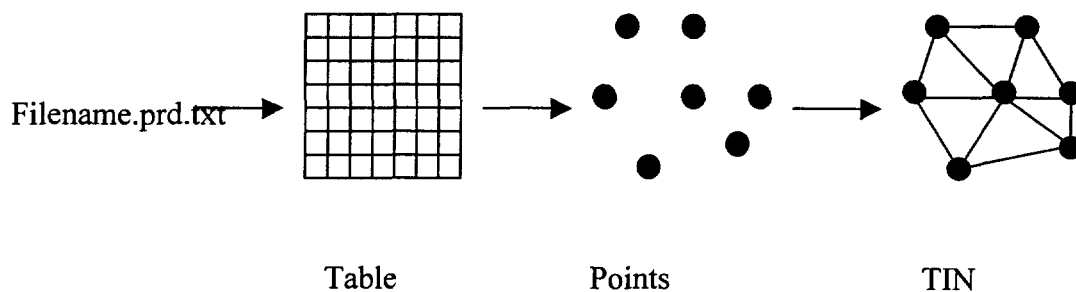


Figure 4.11 Scheme of Avenue Script in ArcView

Several customized features have also available within ArcView. For the convenience when working with multiple cases, one view and one table are created for each case and are then named after the input file names. Thus, each case can be manipulated individually without interference to or from other cases. A customized menu is also applied specifically for CORMIX and the scripts can be executed by a click on the CORMIX button in the tool bar.

5

Model Validation

This chapter presents CORMIX model predictions compared with the processed field survey data. The model input and field data was collected and processed for presentation with the tools and techniques described in Chapters 2 through 4 for the four field survey sites on the Missouri River; Cooper Nuclear Station, Fort Calhoun Power Station, Nebraska City Power Station, and the North Omaha Power Station. The CORMIX simulations are included in Appendix A.

The far-field locator is the primary tool used to reconcile the plume width in the far-field and the outputs can be found in Appendix B along with the detailed river discharge.

5.1 Cooper Nuclear Station

5.1.1 General Features of the CORMIX Flow Classification and Simulation

CORMIX predicts this thermal plume as flow class SA1 which describes a shoreline attached jet in “deep” water. The SA1 flow class description advises that this flow is dynamically attached to the downstream bank, however as a “deep” water condition it does not interact with bottom in the near field. Along the bank a zone of re-circulating effluent occurs which will reduce the dilution. The penetration into the

crossflow is reduced due to this dynamic near-shore attachment.

The prediction indicates that the plume behaves as buoyant surface jet in near-field and in the far-field transitions to buoyant ambient (density current) spreading and passive ambient mixing. Figure 5.1 illustrates the CorVue visualizations in 3D, plan view, and side view.

The prediction file shows the following details. Within the first 10 m after discharge (MOD302) in the buoyant surface jet region, the plume is fully vertically mixed with bottom interaction. Thereafter the plume lifts off from the bottom and forms a stratified surface layer in a buoyant surface jet region (MOD310) which lasts from $x = 11$ m to $x = 291$ m downstream of the outfall. In this region, the flow decreases in depth with increasing downstream distance and uniform vertical concentration profile (flux-averaged) is used, while a Gaussian profile is used to describe the lateral temperature profile. The plume extends laterally into the crossflow within a recirculation bubble that reaches its maximum lateral extent at $x = 14$ m downstream of outfall, with the maximum distance from centerline of the jet to the bank of $y = 6$ m. The recirculation bubble ends at 26 m downstream and continues as wall jet until 291 m downstream, with the maximum plume width of 41 m.

In the far-field, the buoyant ambient (density current) spreading occurs from $x = 291$ m until $x = 1614$ m downstream. The plume is laterally fully mixed at the end of the density current region. The plume is attached to the near-bank in far field. Uniform (top hat) profiles are used to describe temperature profiles in the density current region. The transition for passive diffusion occurs at 1614 m downstream and the flow start to interact with the riverbed and cause the vertically fully mixed. Thereafter, with no additional mixing available, only heat loss effects plume temperature.

5.1.2 Comparison Thermistor String Data with CORMIX Average Velocity Predictions

In the section, the comparison of predicted plume behavior and observed in field data will be discussed. The lateral and vertical temperatures profiles predicted by CORMIX will be examined in relation to profiles observed in field observation.

5.1.2.1 Vertical Temperature Profiles at Cooper Station

As noted in chapter 4, thermistor temperature shows a distinct vertical temperature variation within the first 200 m and is vertically uniform thereafter. In the near-field, in the first 11 m after discharge CORMIX shows a vertically fully mixed discharge that then stratifies vertically. After stratification the vertical profile can be represented as a Gaussian profile (1/e) profile in the near-field region of CORMIX MOD 310 predictions.

In the stratified buoyant surface jet regime of MOD310, a 1/e (37%) Gaussian vertical profile is adopted to describe the vertical temperature distribution and can be presented in a mathematical equation:

$$c(n) = c_c e^{-\left(\frac{n}{b}\right)^2} \quad (5.1)$$

where $c(n)$ is the lateral concentration, n is the coordinate position measured normally away from the centerline, c_c is the centerline concentration, e is the natural logarithm base, and b is the local plume vertical width (b_v , given in the prediction file).

Figure 5.2 shows the vertical temperature distribution of thermistor data and the CORMIX vertical profiles using the above Gaussian 1/e (37%) profile. In this region, the measured and predicted temperatures at the 0.3 m are generally in good agreement in term of the temperature. Within the profile, the predicted temperatures to the 1.7 m depth are generally corresponded to the thermistor data. Below the 1.7 m level, there is a tendency that temperature is under predicted.

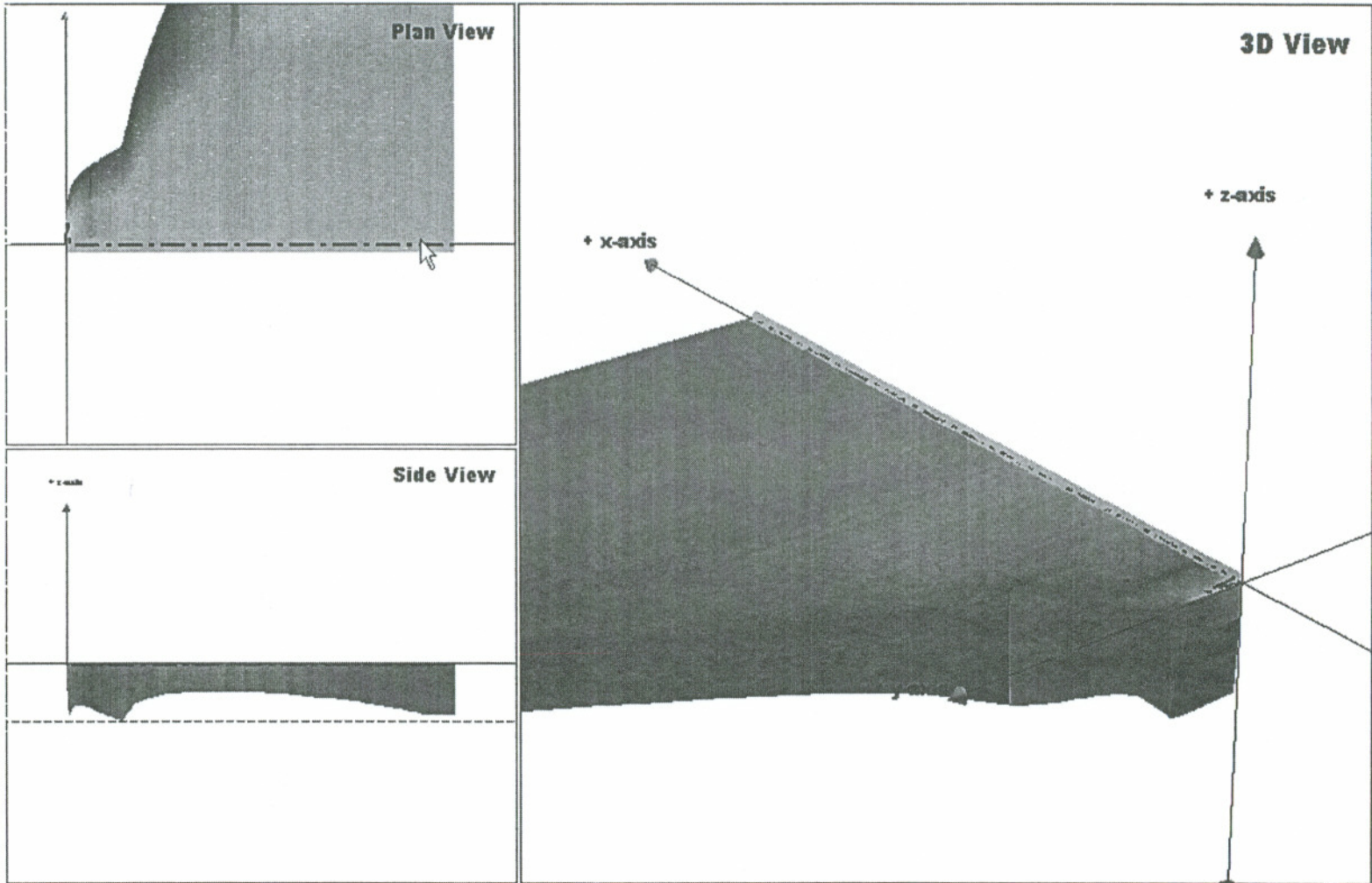


Figure 5.1 CorVue Plume Visualization for Flow Class SA1 at Cooper Nuclear Station

In general, modeling results indicate the stratification in the near-field region and have good overall agreement with the field observation in terms of the maximum temperature at various depths.

In the ambient spreading from $x=291$ m to $x=1670$ m, the thermal plume is predicted in a surface layer with uniform vertical and lateral temperature profile. Predicted plume thickness b_v decreases initially and then increases with downstream depth. The vertical thickness b_v varies from 2 to 4 m in this region. The plume is back attached to the near-shore and expanded in horizontal width b_h with downstream distance. However, observed thermistor data shows a uniform vertical temperature profile in this region. The difference could imply the buoyancy diminishes faster than simulated by CORMIX and the force the flow into the passive ambient diffusion where the ambient turbulent takes over in the mixing mechanism.

In the passive ambient mixing region after $x=1670$ m, the predicted plume grows vertically and become fully vertically mixed at 1736 m. Observed thermistor data shows a uniform vertical temperature profile in this region as well.

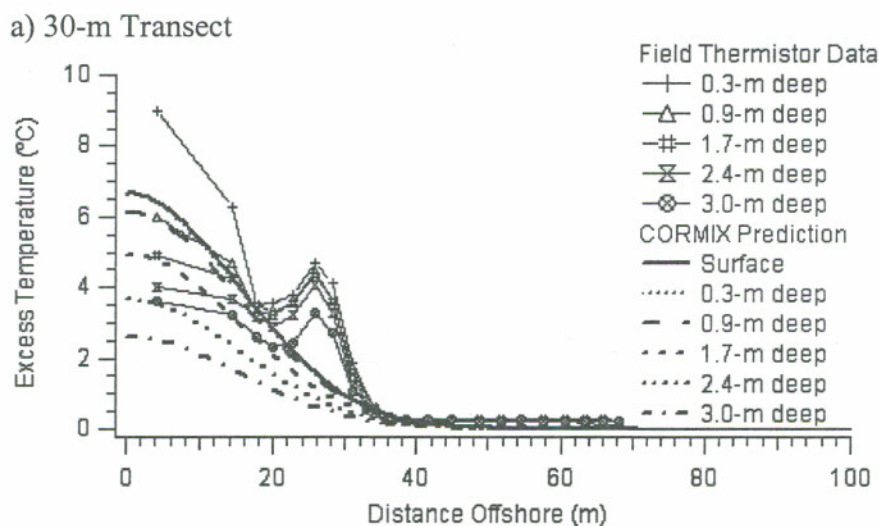
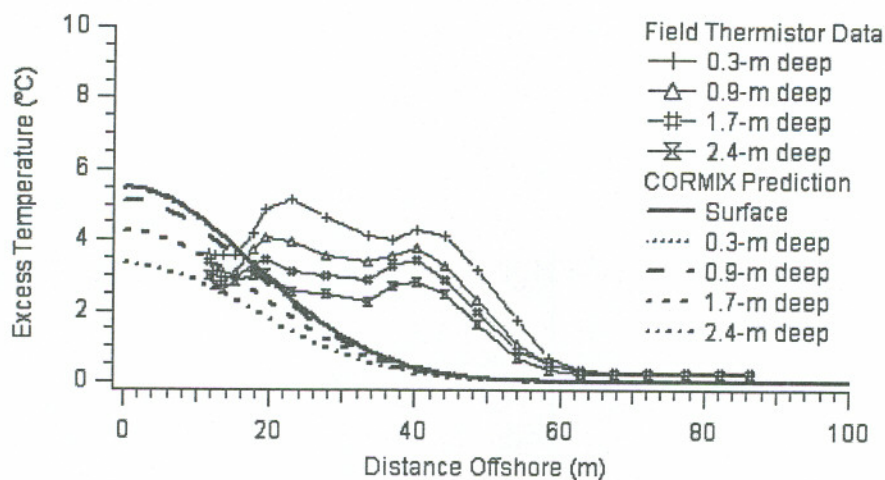
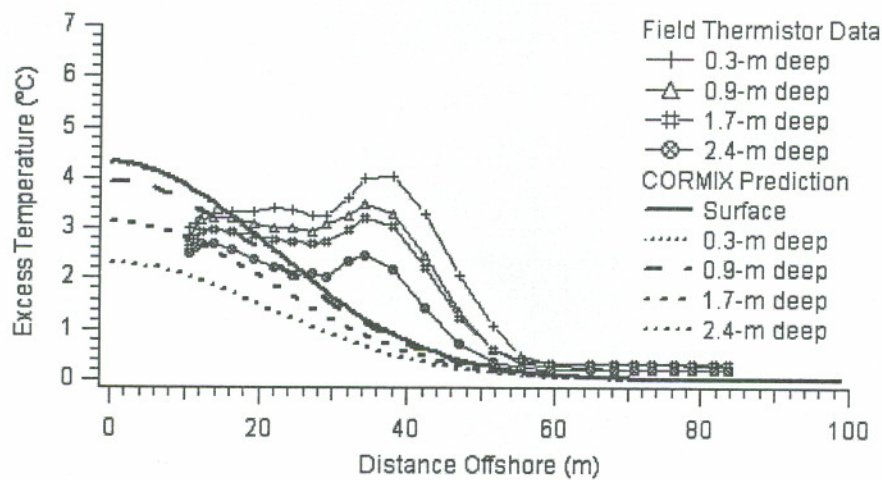


Figure 5.2 Vertical Temperature Profiles of Thermal Surveys and CORMIX Predictions (Cooper Nuclear Station)

b) 60-m Transect



c) 120-m Transect



d) 180-m Transect

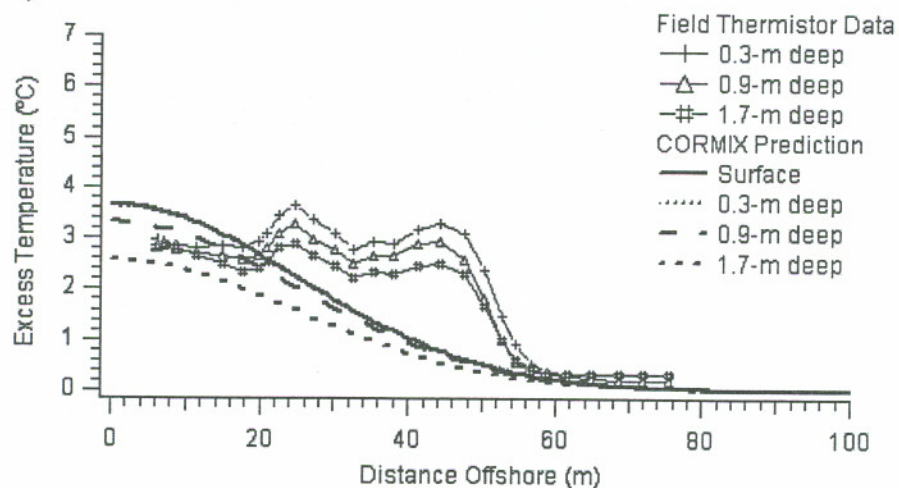


Figure 5.2 (cont'd)

5.1.2.2 Lateral Temperature Profiles at Cooper Station

In this section, thermistor data and predictions will be presented at the 0.3 m depth in the near-field regime where a vertical and lateral Gaussian $1/e$ (37%) distribution is employed for the predicted temperature profile. Before the bank attachment occurs, CORMIX predicts the plume development in the term of horizontal half-width b_h . After bank attachment, the full-width is reported in prediction files and the centerline shifts to the bank. It is important to note that the predicted horizontal width b_h is the distance offshore where the temperature is 37% of the maximum centerline temperature. The plume lateral temperature distribution can be calculated through equation 5.1.

In the near-field, by applying mean ambient velocity for the cross-section, predictions and thermistor data are shown in Figure 5.3(a)–(d). The thermistor data show near-uniform lateral temperature distribution in the near-bank region, and then a sharp decrease in the profile as it approaches background levels offshore when the plume partially recirculates as shown in the thermistor string data in Chapter 4. This similar laterally uniform averaged temperature profile may maintain for a distance until the most heat is dissipated at the plume edge. From observation of general trends in the thermistor data, the plume width is well-predicted but the overall plume lateral profile because of the appearance of recirculation zone near the discharge entry.

In the far-field buoyant spreading processes, lateral spreading due to the buoyancy results in formation of a laterally uniform temperature profiles within the plume, so top-hat profile is used for predictions and the thermistor data is averaged over the actual plume vertical thickness to compare with modeling results. From Figure 5.3(e)–(g), although plume horizontal width b_h is underestimated, the difference between field measurement and predictions tends to be relatively small as downstream distance increases.

5.1.2.3 Maximum Temperatures within Lateral Profiles at Cooper Station

In terms of the maximum temperatures, except for 1°C under prediction at 30 m transect and nearly 2 °C over prediction at 1500 m, all the modeling results are nearly equal to the field observations in the near-field within 0.5 °C.

The transition between buoyant spreading and passive ambient diffusion regions might not be correctly simulated from the mismatches in temperature vertical distribution. However, it is still unrealistic that there was nearly no temperature dissipation observed in the field data from 762 m to 1500 m downstream of the discharge outlet. Thought the dilution characteristics are different in these two regions, unlike stagnant reservoirs, the velocity fluctuation in the moving flow of the large rivers generates the turbulent energy that mainly increases the mixing. Thus, some other unknown factors, such as additional ground water discharge, other heated discharge downstream, or other branches discharging in to the main channel, affect the plume behaviors in the far-field and cause extremely slow dilution.

a) 30-m Transect (Buoyant Surface Jet)

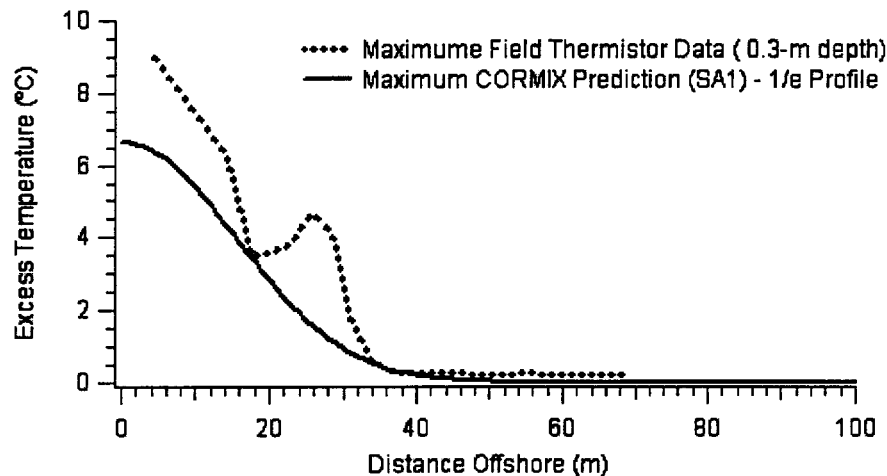
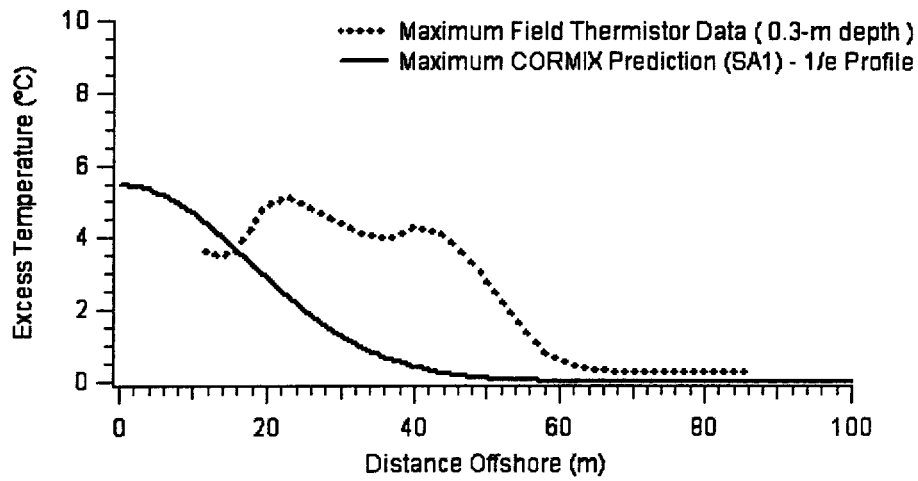
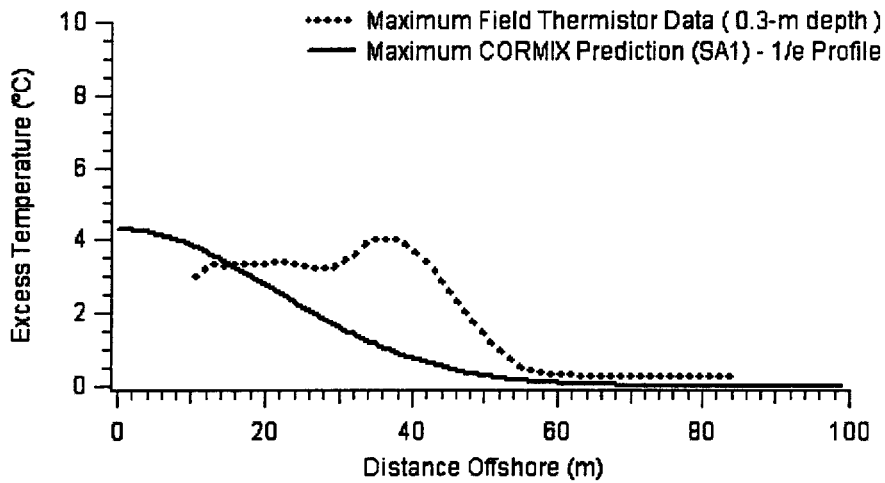


Figure 5.3 Excess Temperature Lateral Profiles of Field Surveys and CORMIX Predictions (Cooper Nuclear Station)

b) 60-m Transect (Buoyant Surface Jet)



c) 120-m Transect (Buoyant Surface Jet)



d) 180-m Transect (Ambient Buoyant Spreading)

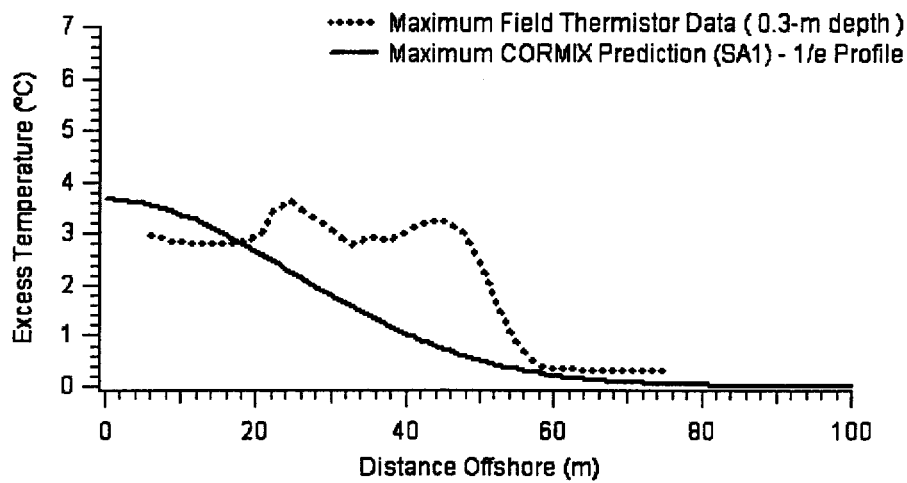
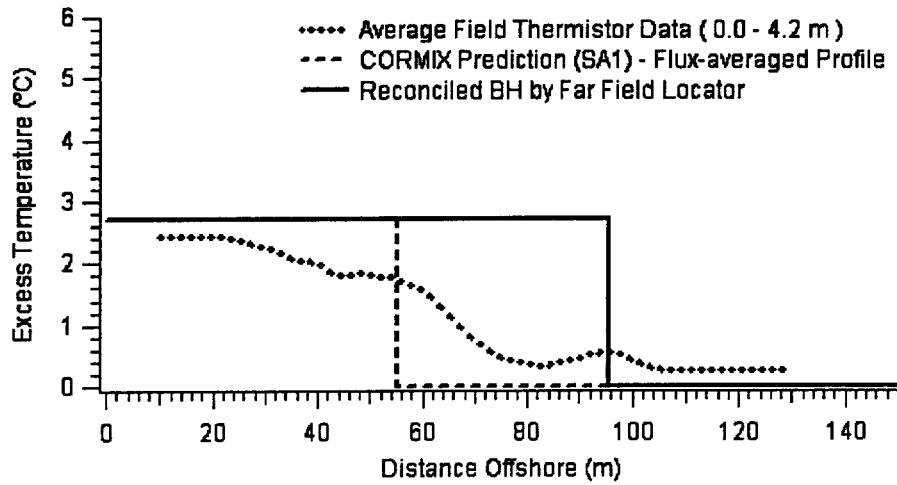
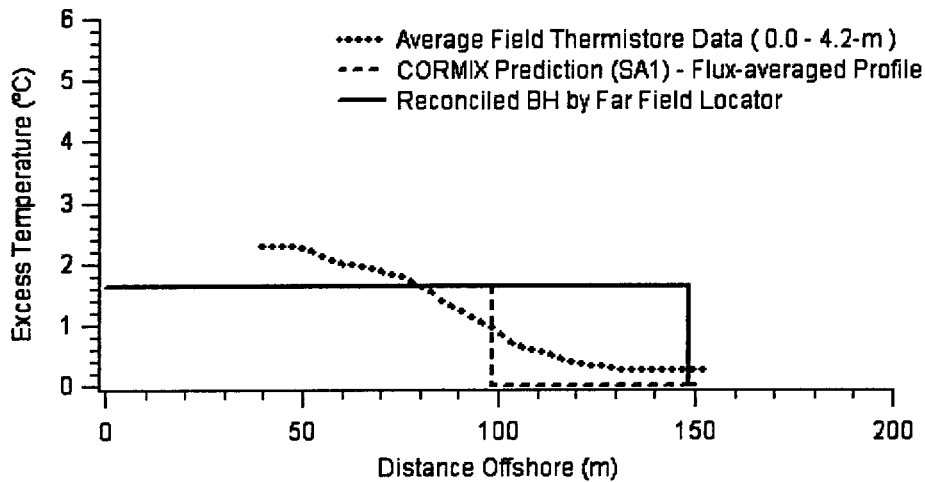


Figure 5.3 (cont'd)

e) 381-m Transect (Buoyant Surface Jet)



f) 762-m Transect (Ambient Buoyant Spreading)



g) 1524-m Transect (Ambient Buoyant Spreading)

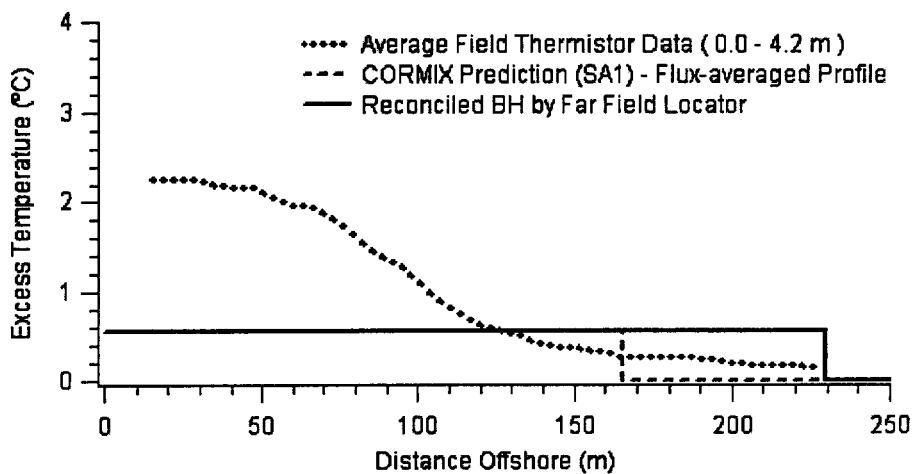


Figure 5.3 (cont'd)

5.1.3 Optimized Far-Field Simulations for Cooper Station

In far-field optimization, the velocity field is adjusted to better reflect the ambient conditions the plume encounters in the far-field. In addition to optimizing the velocity field, the post-processing tool Far Field Locator is also applied to reconcile the plume lateral dimensions extent based on the cumulative discharge method. The details of the cumulative discharge method and the procedures of using ADCP data to extract the cumulative discharge are discussed in Chapter 3.

With the application of Far Field Locator based on the actual site cumulative discharge data, the plume width is significantly wider and very close to the observed width (Figure 5.3). At $x = 381$ m, the unadjusted plume with $b_v = 50$ m and after being adjusted, b_v is approximately equal to 95 m and closer to the actual width $b_v = 105$ m. Similarly, $x = 762$ m, the unadjusted plume with $b_v = 95$ m and after being adjusted, b_v is approximately equal to 145 m and closer to the actual width $b_v = 130$ m. However, at $x = 1524$ m, the plume edge is not easy to judge from the thermistor data and all predicted widths fall in acceptable range.

5.2 Fort Calhoun Generating Station

5.2.1 General Features of the CORMIX Flow Classification and Simulation

The flow in this case is identified as flow class PL2 in CORMIX. In the PL2 flow class, the strong buoyancy force, partially caused by higher ΔT and a relatively weak crossflow, makes effluent to intrude upstream near the outlet location. An unstable recirculation occurs in the vicinity of the outfall followed by a stable restratification in the far field. A CorVue visualization for the simulation appears in Figure 5.4.

CORMIX predicts the near-field region (MOD302) is confined within 5 m downstream of the outfall in an unstable region with fully vertical mixing. Within this region, the relatively small discharge momentum results in little mixing with the

ambient. Consequently, plume temperature does not decrease much within the near-field.

Following the plume development stage in the near field, the buoyant ambient (density current) spreading (MOD341) occurs from $x = 5$ m to $x = 1250$ m downstream. In this region, the plume is bank-attached to the right shoreline. The initial plume width $b_h = 5$ m and reaches its maximum extent $b_h = 108$ m at $x = 1250$ m. The vertical plume thickness b_v decreases from $b_v = 4.46$ m (equal to the depth at discharge $HD = 4.63$ m) to a minimum value of $b_v = 1.3$ m at $x = 254$ m as the flow is stratifying and then increases to $b_v = 4.9$ m (equal to the average depth $HA = 4.9$ m) at the end of the region at $x = 1250$ m.

After transition from the ambient spreading, passive ambient mixing (MOD361) in uniform ambient is predicted in the far-field region after $x = 1328$ m downstream. The flow still remains bank-attached. Due to bottom interaction, the plume is fully vertically mixed at $x = 1250$ with a uniform flux-averaged (top-hat) vertical temperature profile. The lateral temperature is Gaussian square root (46%) definition of lateral plume width b_h .

5.2.2 Comparison Thermistor Data with CORMIX Predictions at Ft. Calhoun

The plume dimensions will be discussed in terms of vertical profile and lateral profile. Later on, the evaluation of the predicted temperature will be depicted as well.

5.2.2.1 Vertical Temperature Profiles at Ft. Calhoun

As noted in the previous section, due to the buoyant lifting, the plume forms a stratified flow in the buoyant spreading region (MOD341) and the temperature distribution is presented by top-hat (flux-averaged) profile. Correspondingly, in Chapter 4, the stratification in temperature is also observed from $x = 0$ m to 381 m in the thermistor data. Thereafter, the temperature is observed uniform vertically, whereas the predicted flow still remains stratified in the buoyant spreading region

until the end of the region at $x = 1250$ m where the vertical temperature distribution becomes uniform. The early appearance of the vertically uniform temperature distribution in the field data might indicate the actually shorter period of the buoyant spreading and the earlier start of the passive ambient diffusion region than predicted. This remarkable mismatch could affect the dilution characteristics and plume geometry in the passive diffusion region in the model.

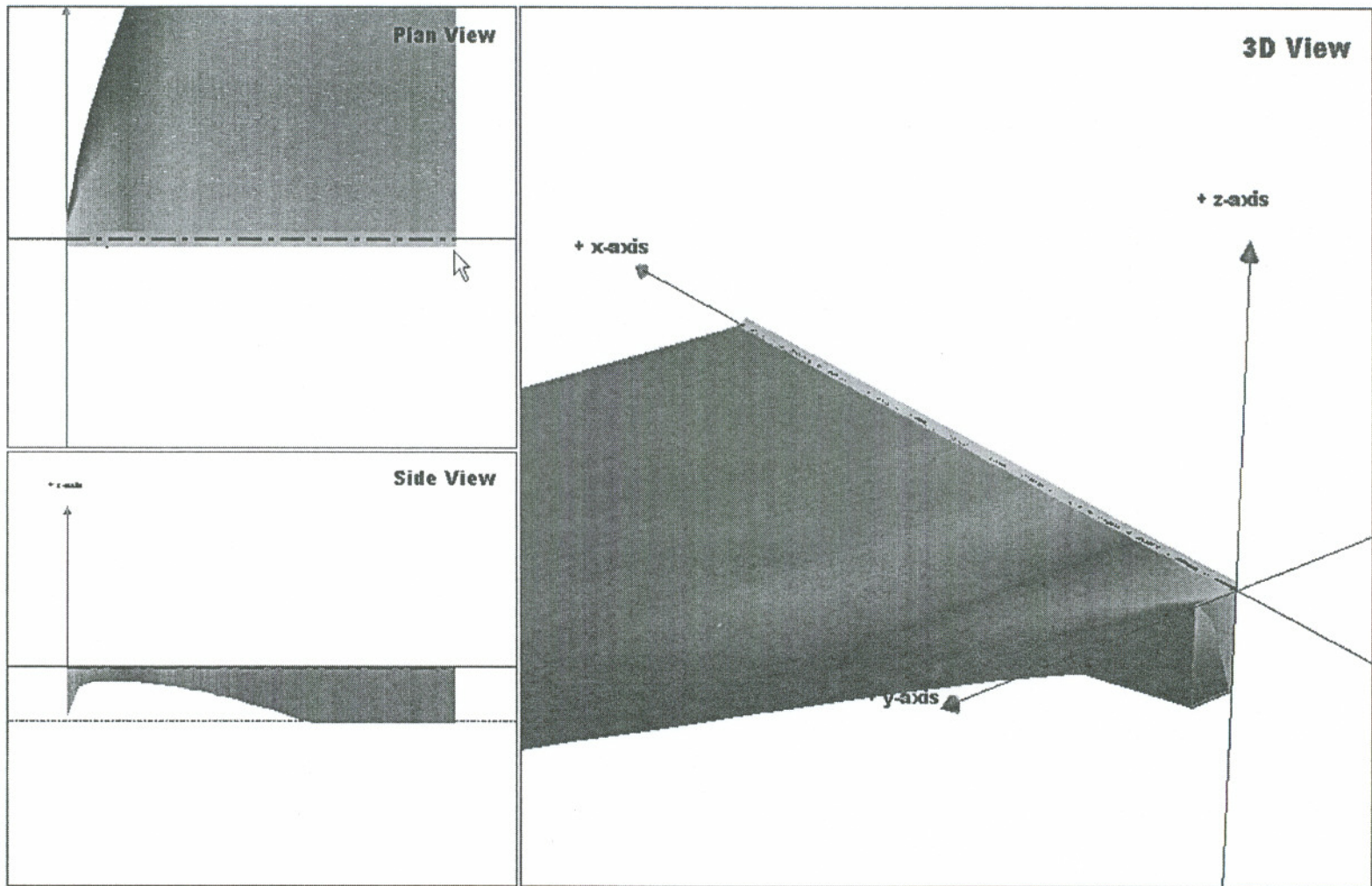


Figure 5.4 CorVue Plume Visualization for Flow Class PL2 at Fort Calhoun Nuclear Station

5.2.2.2 Lateral Temperature Profiles at Ft. Calhoun

Due to the weak initial momentum of the discharge, a main characteristic of flow class PL plumes is the early appearance of the lateral spreading primarily driven by the buoyancy. From Figure 5.5, except for the relevant agreement in plume width at $x = 45$ downstream, the modeling results reveal the consistent 25-m under prediction of plume widths in the region between $x = 45$ m to 762 m. The wider observed plume widths indicate that the actual magnitude of transverse spreading is greater than expected. Since the flow is in far-field and controlled by the ambient, this could be due to the changes in the river discharge conditions since and can be improved by using the Far Field Locator.

In the passive mixing regime (MOD361), the actual plume width is about 80 m at $x = 1524$ m and CORMIX over predicts the horizontal width b_h by 30 m. However, by comparing the actual lateral extent observed at $x = 762$ m, the horizontal width b_h is about 80 m as observed at $x = 1524$ m, possibly implying that this flow has reached the passive diffusion region at $x = 762$ m or before and results the dramatic slow-down in dilution and spreading even with long traveling distance.

a) 45-m Transect (Buoyant Ambient Spreading)

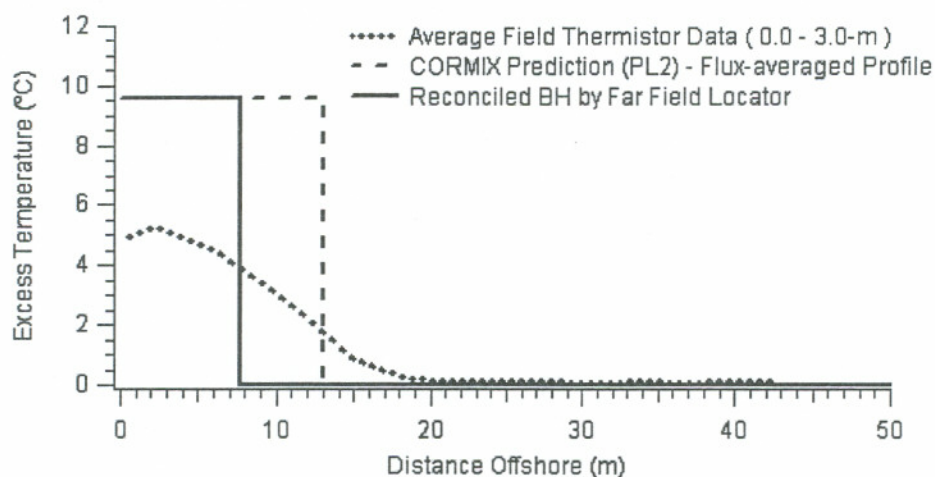
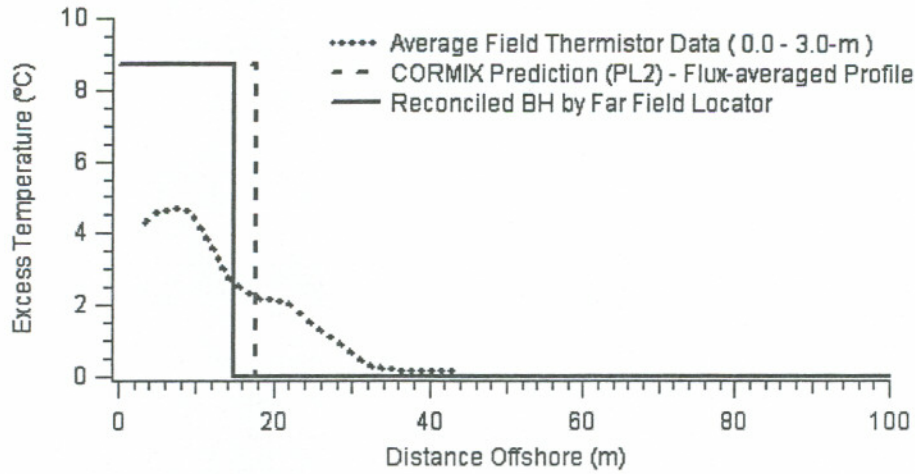
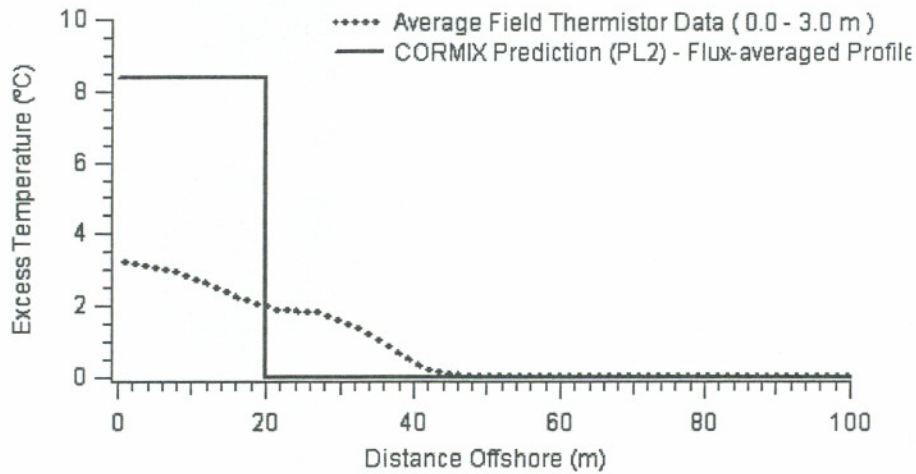


Figure 5.5 Averaged Excess Temperature Profiles in of Averaged Field Surveys and CORMIX Predictions (Fort Calhoun Power Station)

b) 75-m Transect (Buoyant Ambient Spreading)



c) 90-m Transect (Buoyant Ambient Spreading)



d) 120-m Transect (Buoyant Ambient Spreading)

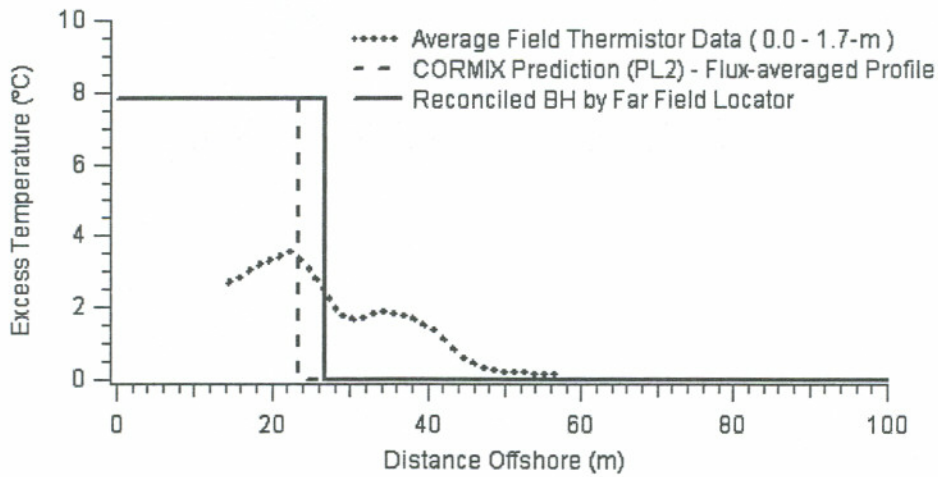
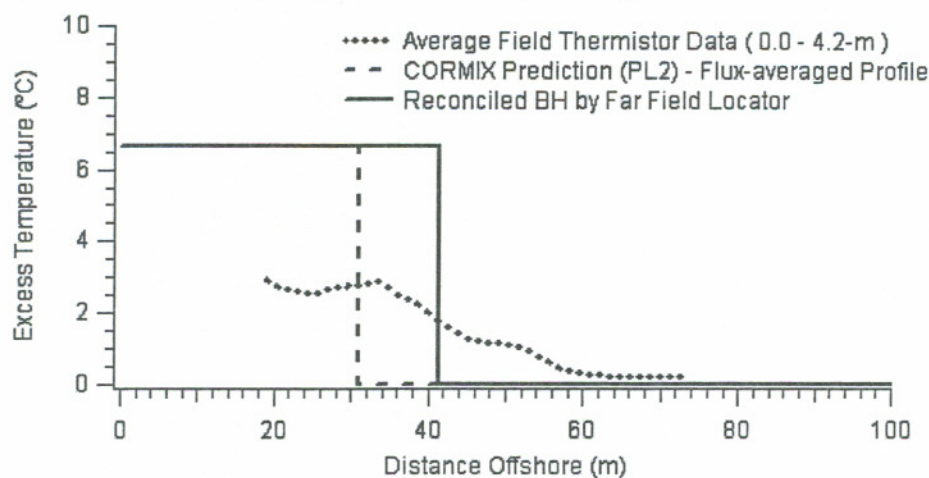
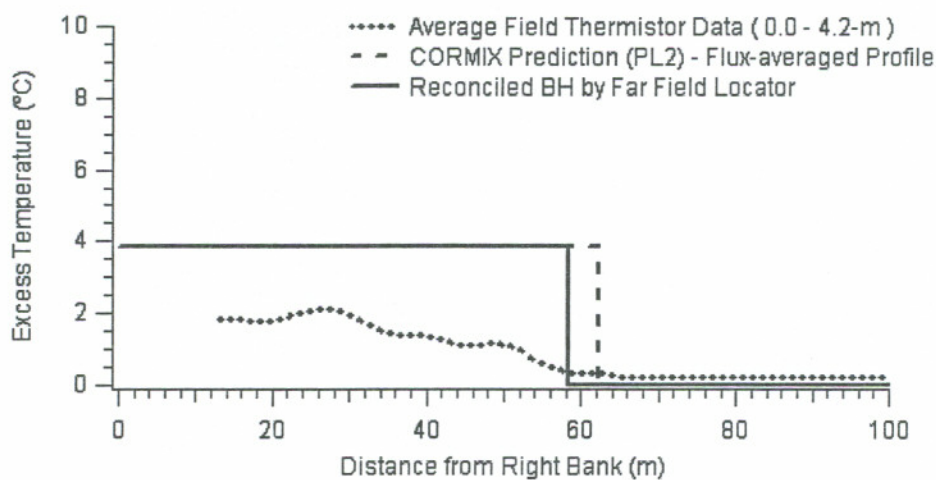


Figure 5.5 (cont'd)

e) 180-m Transect (Buoyant Ambient Spreading)



f) 381-m Transect (Buoyant Ambient Spreading)



g) 762-m Transect (Buoyant Ambient Spreading)

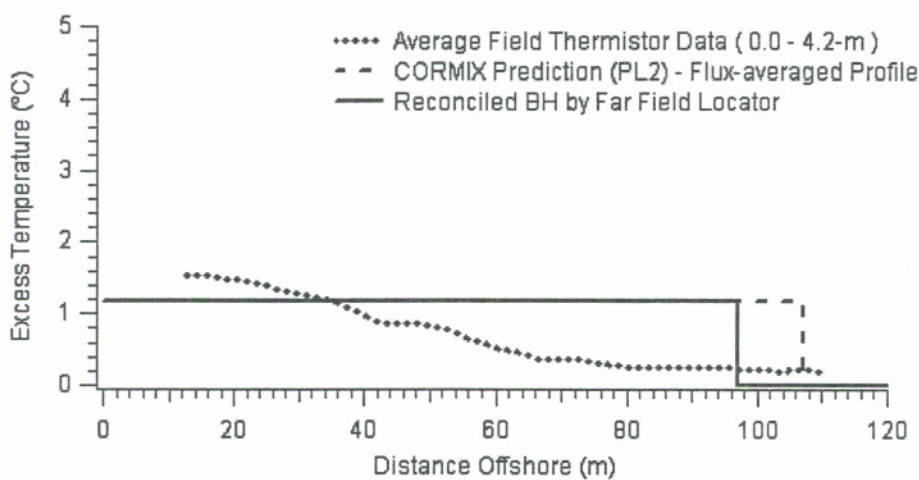


Figure 5.5 (cont'd)

h) 1524-m Transect (Passive Ambient Mixing)

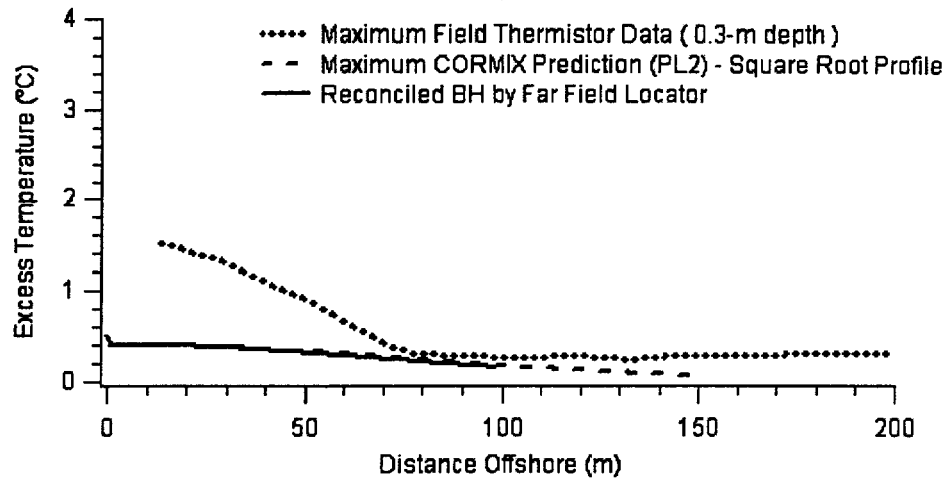


Figure 5.5 (cont'd)

5.2.2.3 Maximum Temperatures within Lateral Profiles at Ft. Calhoun

In the general aspect, the remarkable excess in maximum temperature, approximately 3°C, is observed in the buoyant spreading process. The temperature difference between thermistor data and prediction remains the same consistently in the first 200 m region and after 200 m downstream begin to diminish. At $x = 762$ m, predicted temperature is corresponded well to the maximum observed temperature.

In the passive ambient mixing region, CORMIX under-predicts the temperature by about 2 °C. From the observations on both 1560-m and 760-m transects in the thermistor data, the fairly similar temperature profile is observed, implying the presence of the extremely slow mixing process. The indication of the mismatched transition between passive diffusion and buoyant spreading region can be the explanation for the over predicted results in the passive mixing region.

5.2.3 Optimization of Temperature Simulation for Ft. Calhoun

To optimize the Ft. Calhoun simulation, the velocity field is adjusted to better reflect the ambient conditions the plume encounters in the far-field. Optimizations of the plume width b_h are also carried out through the post-processing tool, Far Field Locator.

With the application of Far Field Locator based on the actual site cumulative discharge data, the remarkable improvement in plume width is observed (Figure 5.5). The plume horizontal width is significantly wider and very close to the observed horizontal width. Particularly in the last three transects, the adjusted plume horizontal widths b_h are highly corresponded to the actual plume horizontal width b_h . However, in general, there is a 10-m deficit in plume width between the modeling results and the field data. This could be mainly due to the initial source conditions specified within CORMIX mentioned in the previous section.

5.3 Nebraska City Power Station

5.3.1 General Features of the CORMIX Flow Classification and Simulation

This thermal plume is classified in the flow class SA1, shoreline attached in “deep” water, in CORMIX 3 and the general plume pattern is similar as shown previously. According to the SA1 flow class description, the flow is dynamically attached to the downstream bank and a zone of recirculating effluent develops near outfall, having a tendency to reduce the dilution. The flow tends to attach the bottom since the depth of the receiving water is nearly equal to the depth of discharge channel. And because of the bottom attachment, ambient currents can be blocked off, causing the shoreline attachment in downstream.

As the common sequence of hydrodynamic motions in CORMIX3, the buoyant surface jet is predicted in the near-field and ambient spreading and passive mixing are in the far-field.

When this flow acts as the buoyant surface jet in the near field, the discharge is fully vertically mixed for the first 3 m and then re-stratified. A recirculation zone is form from $x = 2$ m to 37 m downstream of outlet. Within the recirculating zone, because of the abundance of the bank interaction with the discharge, the near bank temperature predicted is uniform and the corresponding temperature is 5° C. Later on,

the flow continues as wall jet, where the plume starts bank attaching on the right bank until $x = 221$ m downstream.

In the far field, buoyant ambient spreading happens from $x = 221$ m to 1390 m. This discharge remains bank-attached and stratified. The lateral spreading and dilution slow take place in this region. Following the buoyant spreading, the passive ambient mixing becomes the dominant hydrodynamic motion. The temperature stratification is vanished due to the fully vertical mixing and the vertical temperature is uniform.

5.3.2 Comparison Thermistor String Data with CORMIX Predictions

5.3.2.1 Vertical Temperature Profile at Nebraska City

According to the observations of the field thermistor data in Chapter 4, the vertical temperature distribution in each transect is fairly uniform over the depth (water surface to 4.2-m deep) from 0 m to 1524 m downstream of the discharge entry. And this indication reveals the strongly and fully vertical mixing is dominant in this flow. In contrast, this phenomenon is not simulated in CORMIX. The simulation indicates the flow is stratified until 1390 m downstream.

5.3.2.2 Lateral Temperature Profile at Nebraska City

From Figure 5.7, compare the modeling result with the actual plume width observed, in the near-field, generally the lateral extent is precisely predicted and has excellent agreement with the actual plume widths except for 10 m under-predicted at 30 m. Because of the appearance of the recirculation zone, the lateral temperature profile does not have good agreement with observation in the first two transects.

The model over predicts the plume width b_h by 10 m at $x = 380$ m and by 30 m at $x = 762$ m. Farther downstream, due to the low excess temperature, it is hard to allocate the actual plume edge.

5.3.2.3 Maximum Temperatures within Lateral Profiles at Nebraska City

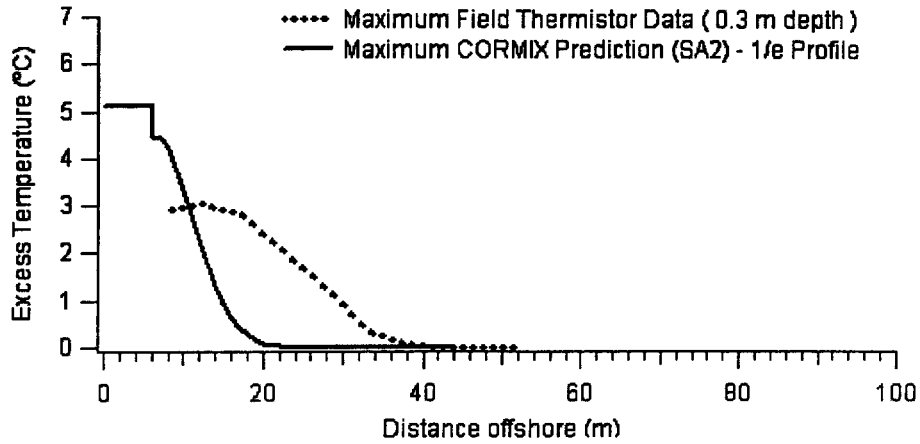
In first 60 m region, the approximate 2.0°C differential in highest temperature is observed (Figure 5.10 a), b)). The over predicting results can be the lack of the vertical mixing in the vicinity of the outlet, resulting in less dilution in the simulation. Farther downstream, the modeling results are well corresponded to field observation, indicating the similar rate of temperature dissipation.

In far-field, the highest temperature predicted is close to the highest temperature measured in the field and the difference is less than 0.5 °C.

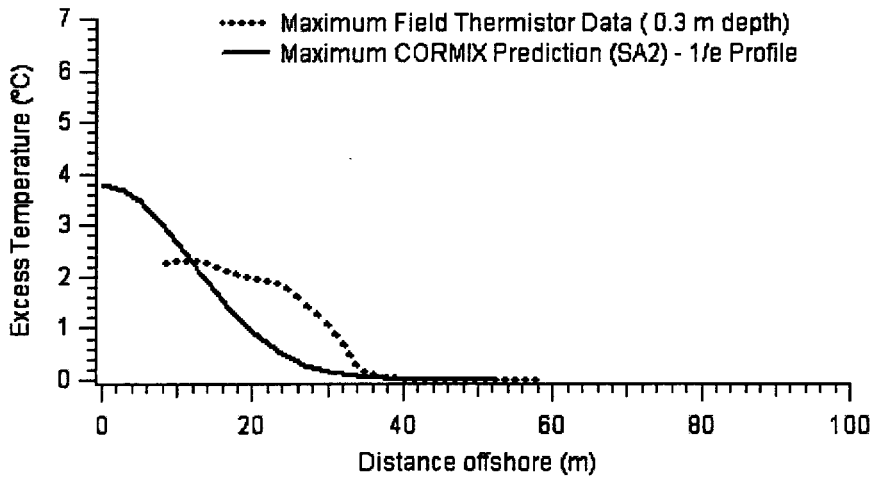
5.3.3 Optimized Far-Field Simulations for Nebraska City Station

Except for 381-m transect, whose predicted width is nearly equal to the width measure, the reconciled plume width is still over predicted by approximately 20 m (Figure 5.6). According to the indication of fully vertical mixing in the field data, the density difference between plume and ambient becomes less and as a results, magnitude of buoyancy is not sufficiently strong to lift up the plume and cause to plume lateral spreading.

a) 30-m Transect (Buoyant Surface Jet)



b) 60-m Transect (Buoyant Surface Jet)



c) 120-m Transect (Buoyant Surface Jet)

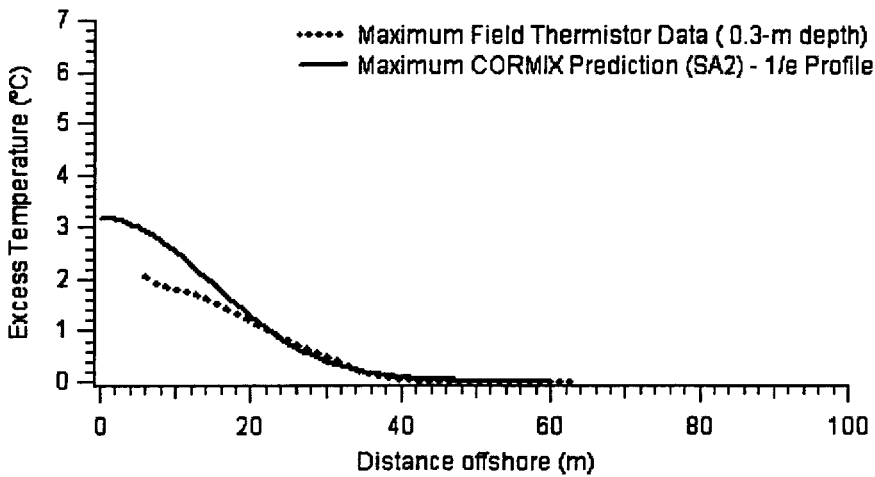
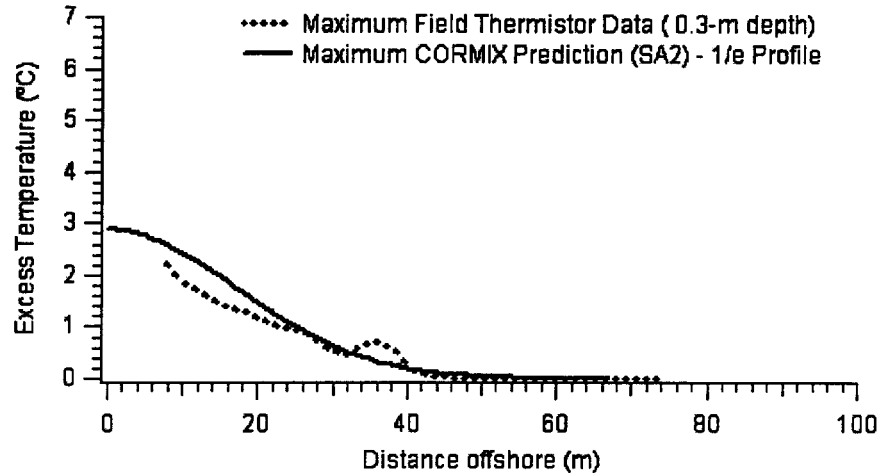
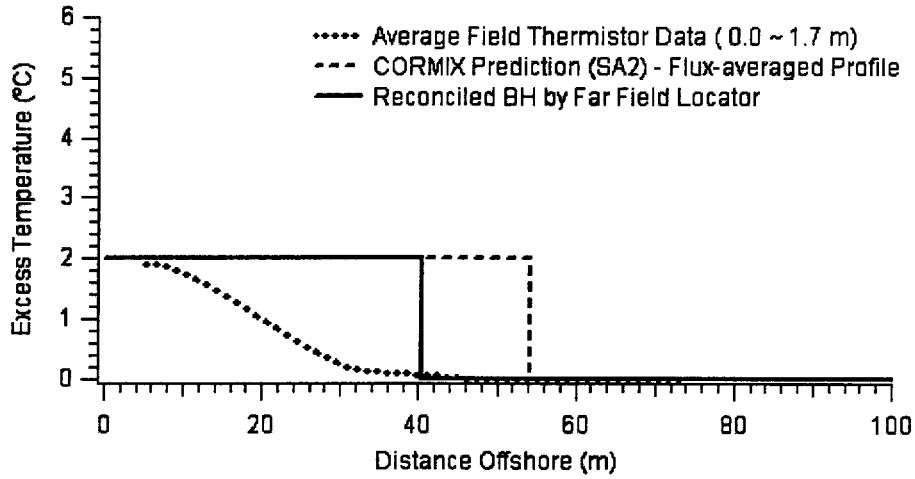


Figure 5.6 Excess Temperature Profiles in of Field Surveys and CORMIX Predictions (Nebraska City Power Station)

d) 180-m Transect (Buoyant Surface Jet)



e) 381-m Transect (Buoyant Ambient Spreading)



f) 762-m Transect (Buoyant Ambient Spreading)

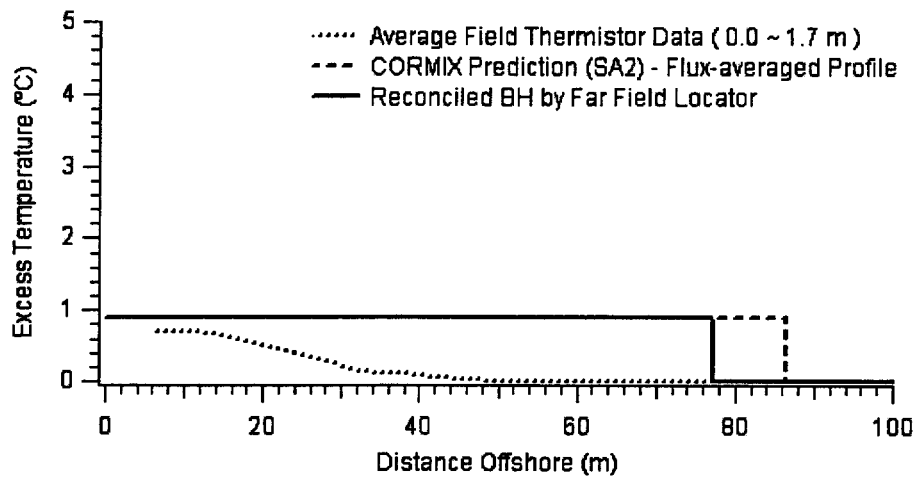


Figure 5.6 (cont'd)

g) 1524-m Transect (Passive Ambient Mixing)

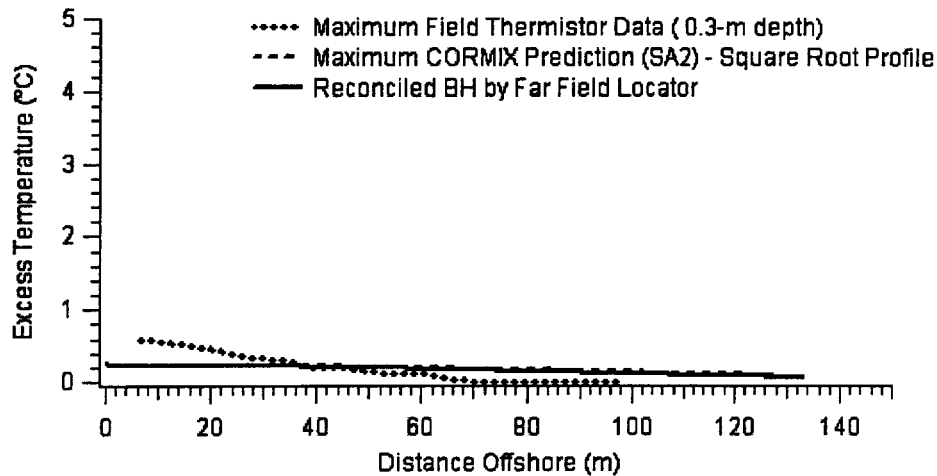


Figure 5.6 (cont'd)

5.4 North Omaha Power Station

On the sampling day, the one of the generator was down and the relatively low-temperature discharge was measured in the outlet of cooling system. As the concern of steady-state of the discharge, CORMIX simulation might not be significantly helpful for both validations and further decision-making. To simulate this discharge situation, the highest discharge temperature measured in the vicinity of outfall, 27.4 °C, was applied as the discharge temperature rather the temperature measured at the outlet of cooling system, 22.22 °C.

5.4.1 General Features of the CORMIX Flow Classification and Simulation

This flow is classified into Flow Class SA1, a shoreline attached jet in the “deep” water. The main feature the same as mentioned in SA1 flow class description previously.

For the detailed CORMIX simulation, a recirculation is formed in the near-field. The recirculating zone takes place from $x = 3$ m to $x = 60$ m downstream of the outfall with the maximum lateral extent at $y = 8$ m. Following the recirculation bubbles, flow is strongly deflected by the ambient currents and becomes the wall jet,

where the flow begins the bank attachment of which the plume centerline is set to follow the bank. The wall jet and near field both end at $x = 280$ m downstream. The vertical temperature distribution is uniform due to the full depth of the plume.

In the far field, the buoyant spreading process takes place between $x = 280$ m to $x = 942$ m downstream and starts to re-stratify. Thereafter, the passive ambient diffusion begins with the plume thickness of full water depth.

5.4.2 Comparison Thermistor String Data with CORMIX Predictions

5.4.2.1 Vertical Temperature Profiles at North Omaha Station

According to the modeling results, the nearly uniformity in vertical temperature is simulated in the near-field. Although the relevant uniform vertical distribution in temperature is not observed in the thermistor data, approximately, the 1 °C difference between the surface and subsurface layers simply represents the slightly weaker magnitude of bottom boundary interaction than predicted.

Though the plume vertical thickness predicted is slightly less than the water depths in the buoyant spreading region, the nearly uniform vertical distribution in temperature can still be observed in the buoyant spreading region because the turbulence at the bottom of the water column causes the internal mixing in adjacent plume.

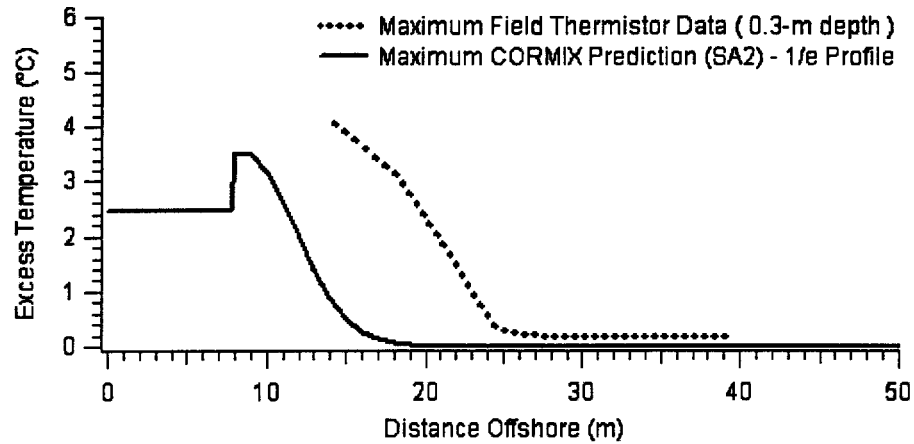
Farther downstream, similar to the previous cases, the temperature is always uniform vertically in both field data and modeling results.

5.4.2.2 Lateral Temperature Profiles at North Omaha Station

In near-field, the narrower plume width than actually observed is predicted consistently in the near-field by 15 m due to the arbitrary mixing occurring in the recirculation zone. Most the predicted plume width is improved in the far-field. It is important to note that in the field data, the plume lateral spreading observationally

slows down starting at 120 m downstream and thereafter the plume width remains 40 m. This could be explained by the existence of the weak buoyant spreading resulting from the less density difference in the stratified flow and the ambient turbulence starts to be the dominant factor that controls the dilution.

a) 30-m Transect (Buoyant Surface Jet)



b) 60-m Transect (Buoyant Surface Jet)

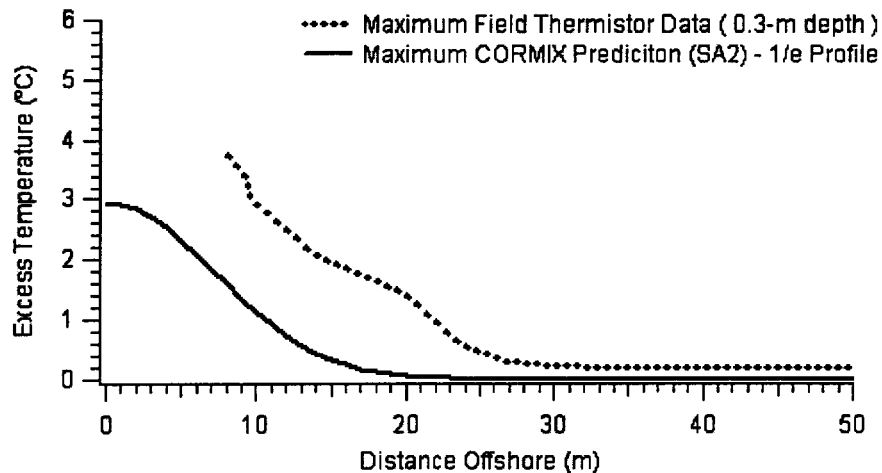
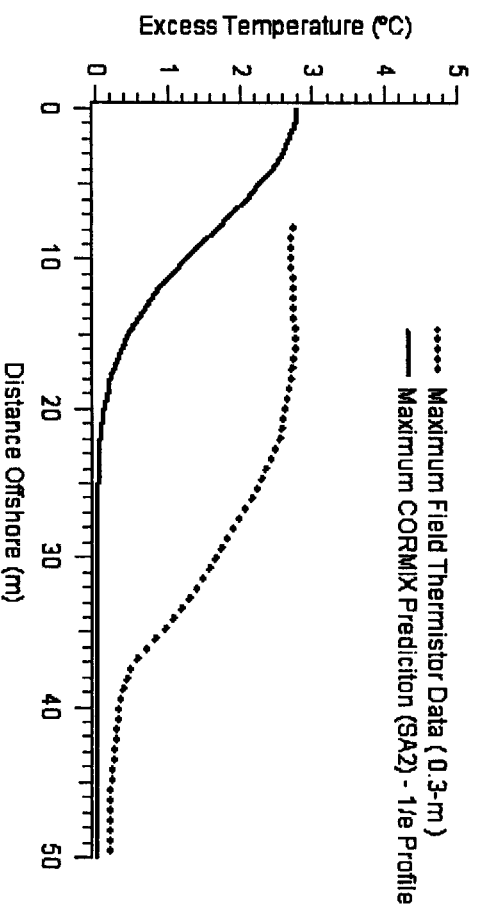
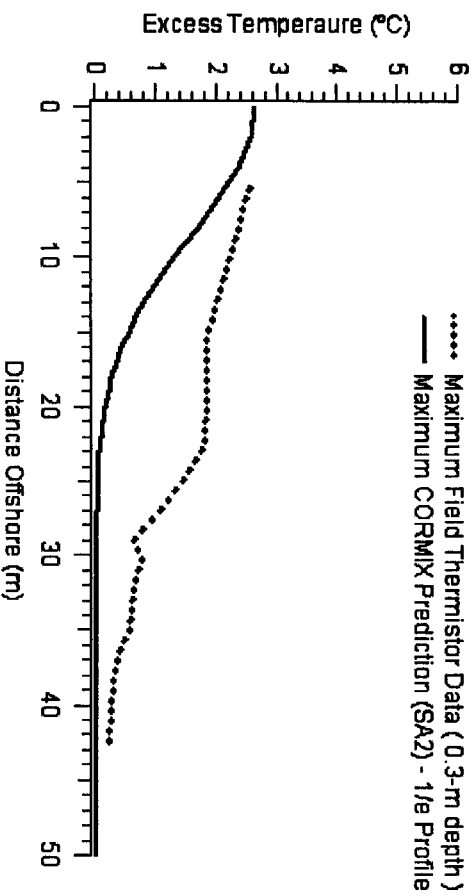


Figure 5.7 Excess Temperature Profiles of Field Surveys and CORMIX Predictions (North Omaha Power Station)

c) 120-m Transect (Buoyant Surface Jet)



d) 180-m Transect (Buoyant Surface Jet)



e) 381-m Transect (Buoyant Ambient Spreading)

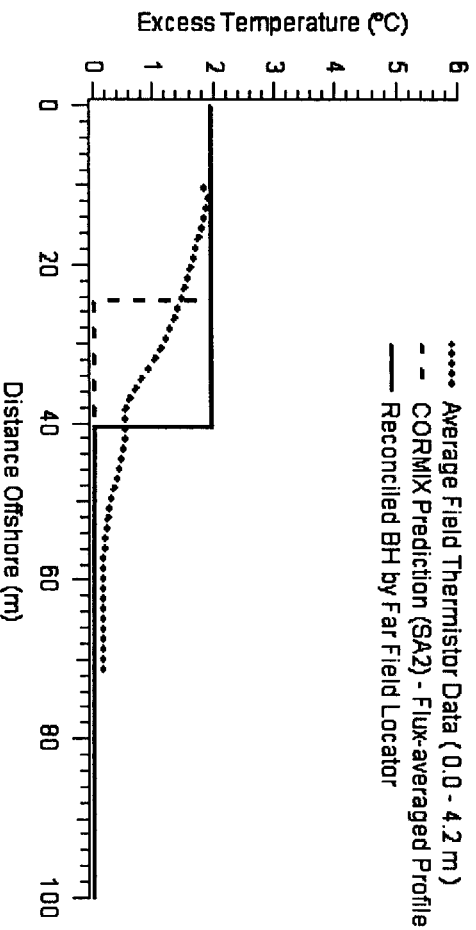
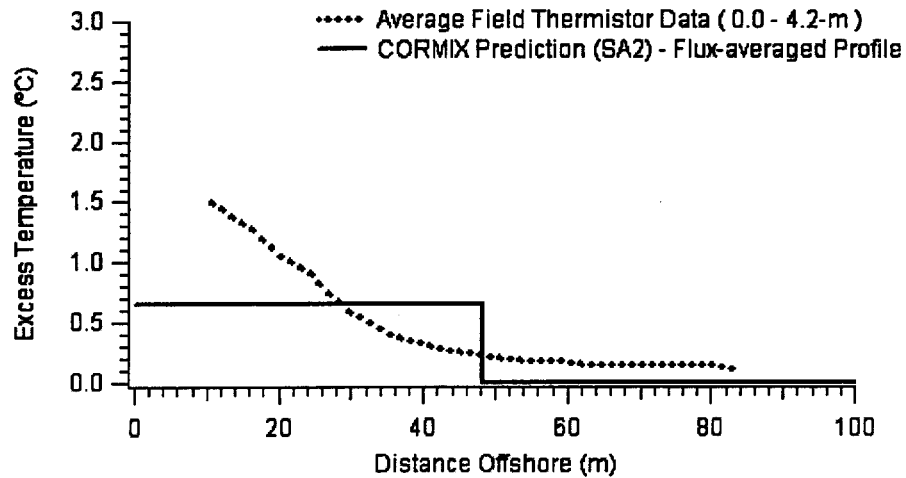
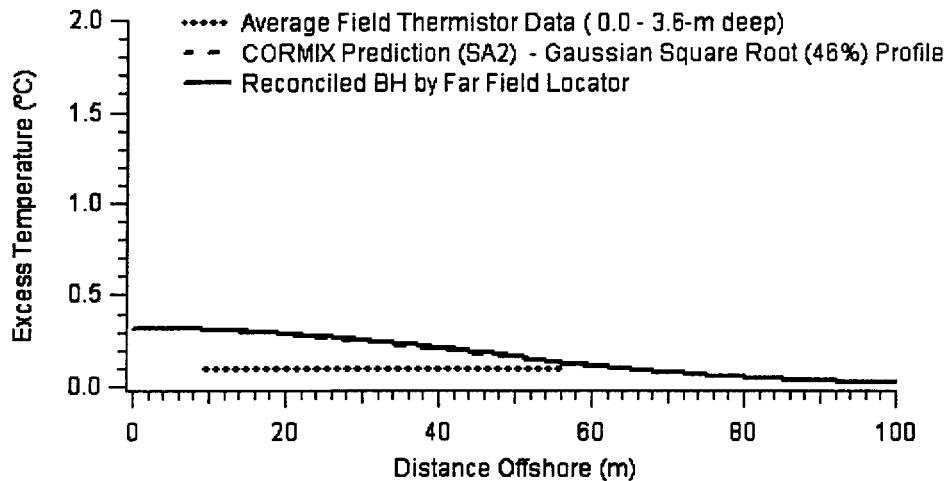


Figure 5.7 (cont'd)

f) 762-m Transect (Buoyant Ambient Spreading)



g) 1524-m Transect (Passive Ambient Mixing)

**Figure 5.7 (cont'd)**

5.4.2.3 Maximum Temperatures within Lateral Profiles at North Omaha Station

The predicted temperature also has good agreements with the thermistor data as shown in Figure 5.7. In some transect, the temperature is over predicted and under predicted in other ones. In general, the difference in the highest temperature between modeling results and thermistor data is less than 1 °C.

Like previous cases, the reconciled plume width is wider and is closer to the width measured. However, 15-m under prediction still remains in most of transects.

5.5 Overall Results and Statistics Analysis

For Cooper Nuclear Station, the predicted temperature is highly corresponded with the temperature measured in the near-field simulation and is slightly over predicted by approximately 1 °C (Figure 5.8). Similarly, the near-field modeling results also agree with the field observation in plume lateral extent and the plume width is over predicted by 20 m in far-field simulation. Regarding to the plume vertical thickness, model over emphasizes the duration of buoyant spreading motions and results in longer period of stratified flow.

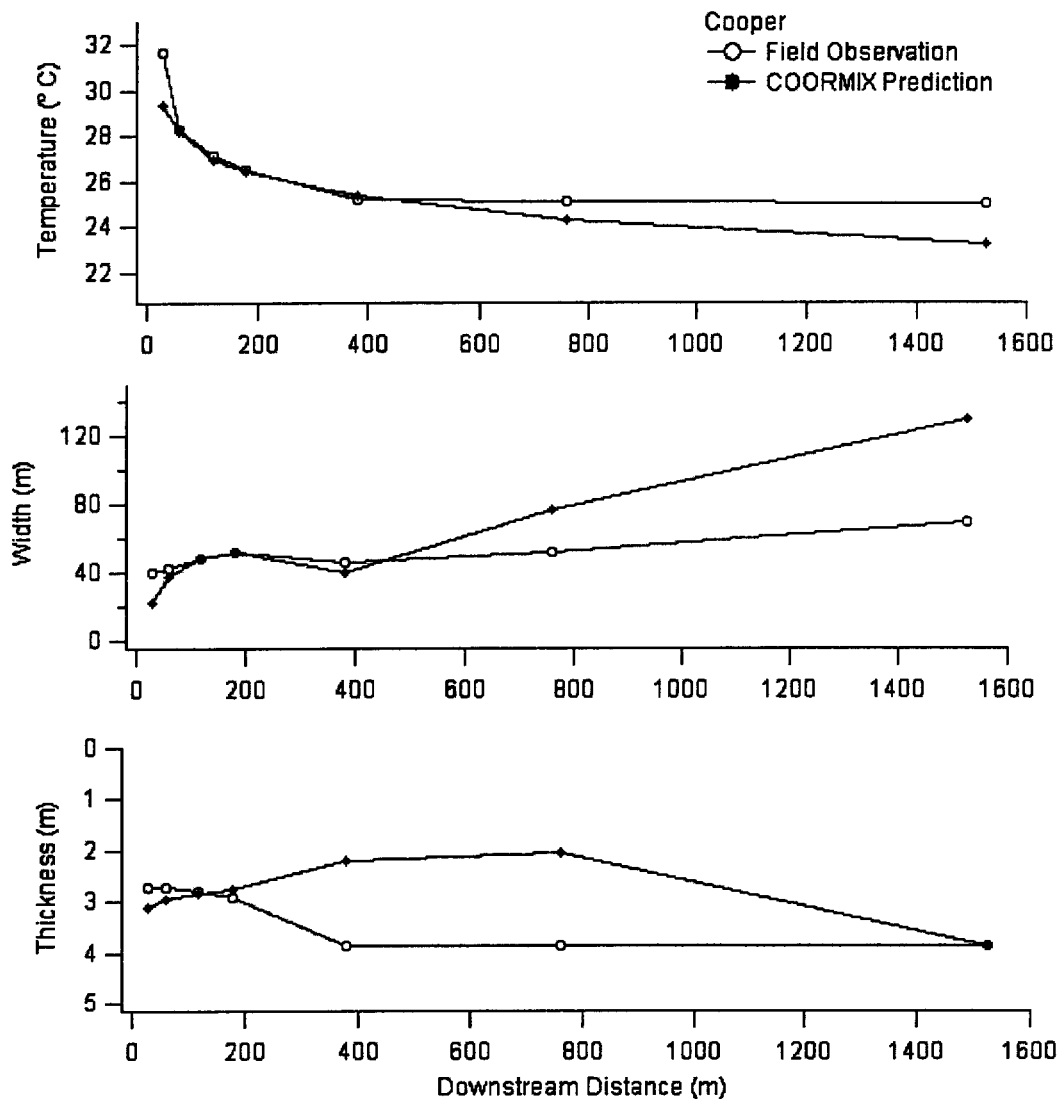


Figure 5.8 Overall Comparison of CORMIX Prediction and Field Observation in Temperature, Width, and Thickness – Cooper Station

For Ft. Calhoun Nuclear Station, the temperature is slightly over predicted by less than 1 °C in both near-field and far-field simulation, in general (Figure 5.9). The near-field modeling results show the under prediction in plume width and the plume width is slightly over predicted m in far-field simulation. Regarding to the plume vertical thickness, again the longer period of stratified flow is simulated whereas the discharge stratifies shortly and quickly collapses from the field observation.

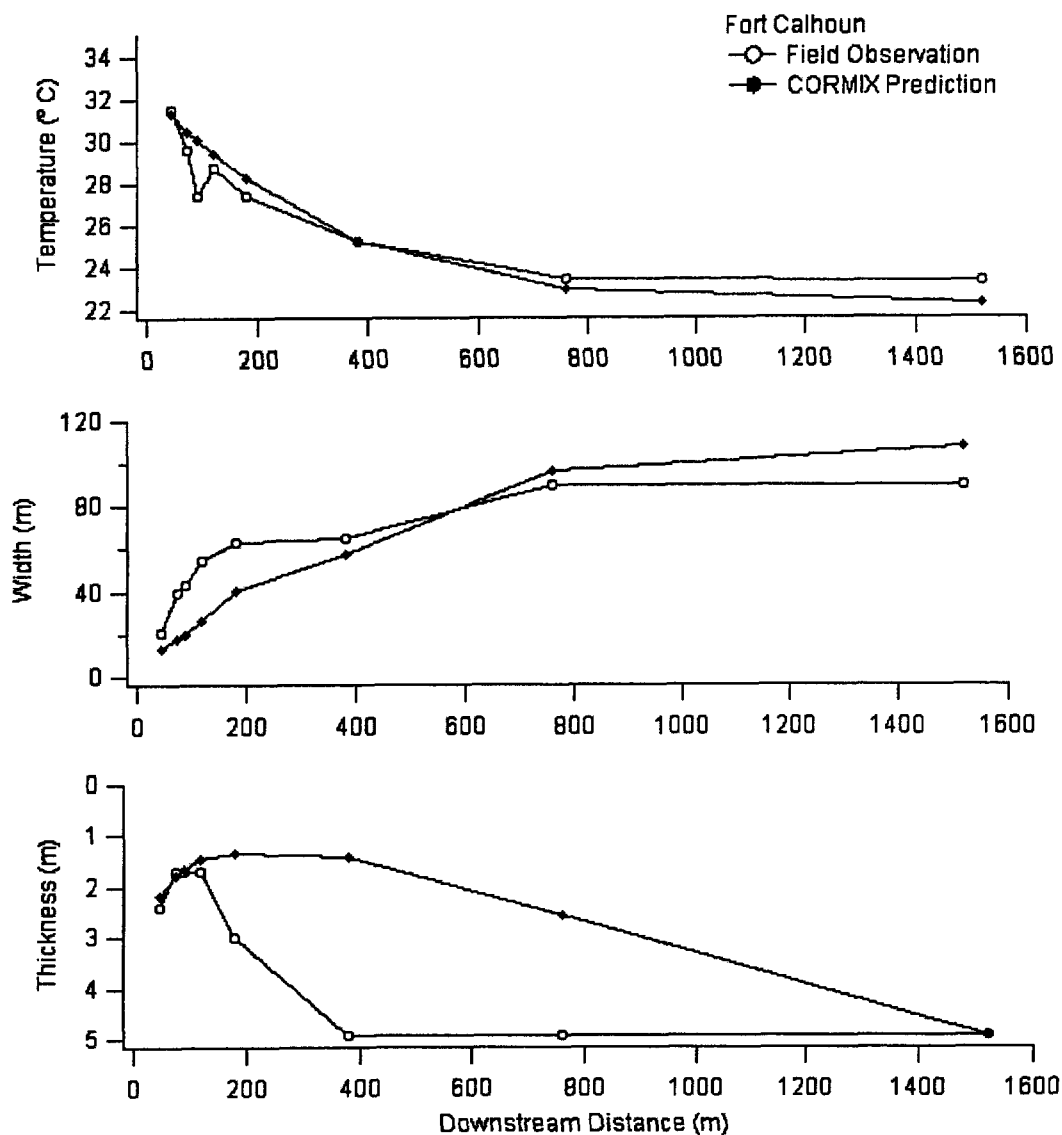


Figure 5.9 Comparison of CORMIX Prediction and Field Observation in Temperature, Width, and Thickness – Ft. Calhoun Station

For Nebraska Coal-fired station, the temperature is slightly over predicted by less than 1 °C in near-field and is generally well corresponded to field observation (Figure 5.10). The near-field modeling results agree with the field observation in plume lateral extent and the plume width is over predicted in far-field simulation with the increasing distance downstream. The discharge interacts with riverbed initially and stratifies for very shorter distance before being exposed to fully vertical mixing. However, model over emphasizes the degree of buoyancy for a longer distance.

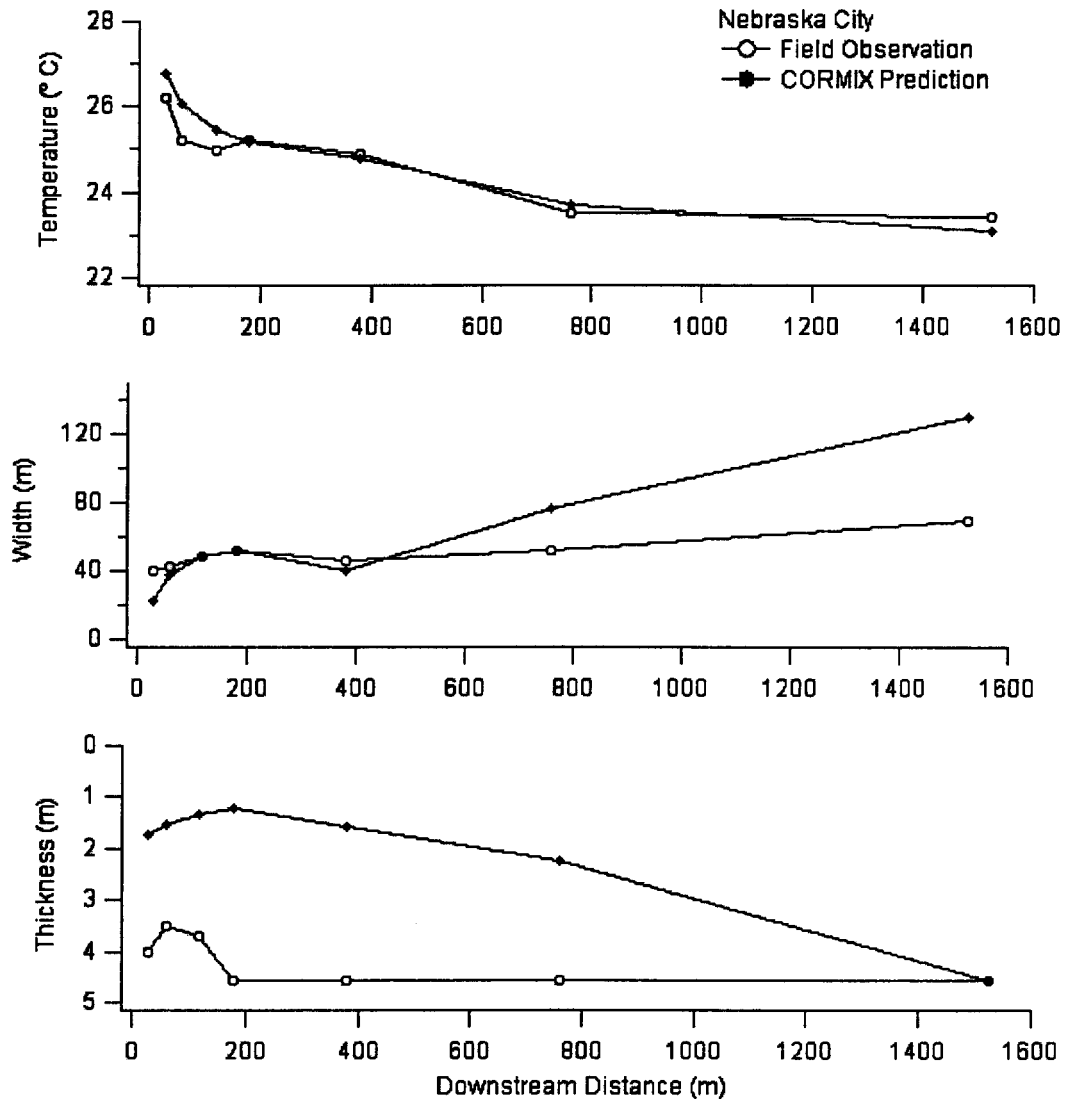


Figure 5.10 Comparison of CORMIX Prediction and Field Observation in Temperature, Width, and Thickness – Nebraska City Station

For North Omaha Coal-fired Station, the temperature is slightly over predicted by less than 1 °C in both near-field and far-field simulation, in general (Figure 5.11). The modeling results reveal the narrower plume than the actual plume in both near-field and far-field simulations. In terms of vertical motion, slightly longer period of buoyant spreading process is simulated.

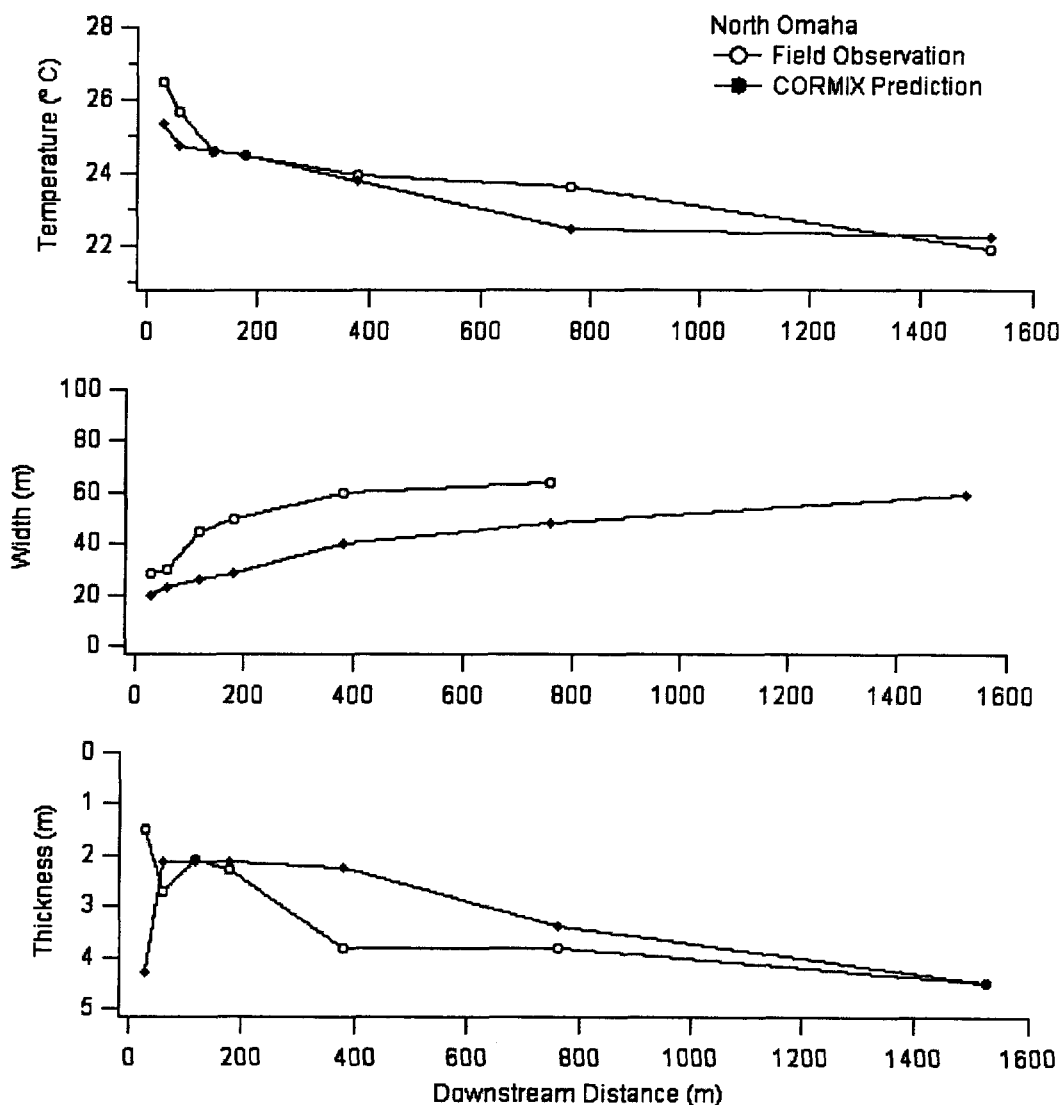


Figure 5.11 Comparison of CORMIX Prediction and Field Observation in Temperature, Width, and Thickness – North Omaha Station

In the statistic analysis, the verification is carried out by flow classes, including SA1 and PL2 flow class, in maximum temperature for the near-field and

far-field simulations individually. Besides, in order to compare different modeling results for the same flow class, normalized index, maximum temperature t_{\max} over excess discharge temperature t_0 is used to integrate different degrees of magnitude for the thermal discharge into the statistical processes. By doing so, it would be much more precise and indicative to distinguish the internal model errors and temperature fluctuation from the outcome of statistics analysis.

In PL2 flow class, the analysis is only presented in far-field because the plume-like discharge has extremely shorter near-field region due to the weaker initial source conditions and the existence of stronger buoyancy. All the data points are scattered around the slope 1 line, which is the standard line for one-to-one relationship in absolute value. The scatter could be mainly due to the temperature fluctuation that is commonly observed in natural environments. The temperature fluctuation is not the main focus of this study because the to determine subtle temperature fluctuation requires the long period of measure for a fixed location and field data collection was to map out the plume temperature distribution. In the general trend of the temperature dilution, the prediction is highly corresponded to the field observation (Figure 5.12). In notation of the correlation, the correlation coefficient (R^2) is 0.96 and indicates the data points are less scattered and there is a strong linear relationship between the prediction and the field observation. In terms of the regression, the linear relationship can be defined mathematically. The slope of the regression line is 1.15 and close to the standard slope, 1. The offset of the regression (3.58) is large, relative to the ideal offset (0).

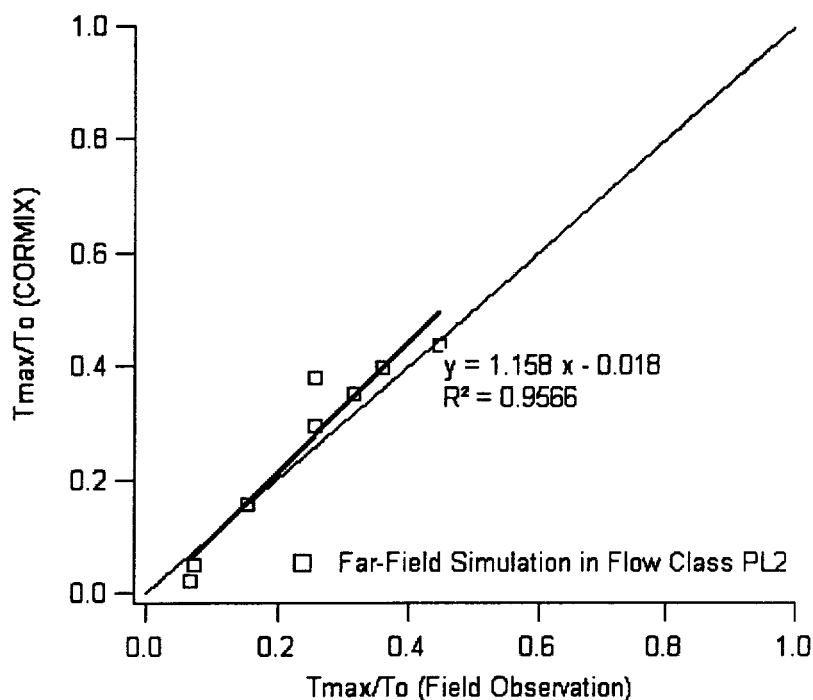


Figure 5.12 Regression and Correlation of Flow Class PL2

In SA1 flow class, both near-field and far-field statistics analyses are presented. All the data points are scattered around the standard line and however, the larger variation is observed in the far-field results than the near-field results. In the near-field results, a strong linear relationship between the prediction and the field observation is determined by the high correlation coefficient (R^2), 0.96. However, in terms of the regression, the linear relationship is not corresponded to the standard mathematically. The slope of the regression line is 1.158 and the offset of the regression is -3.85 . The poor slope and offset are significantly influenced by the displacement of the three points that are under predicted. Two of those are in North Omaha case and one in Cooper case. The explanation for North Omaha case could be the unsteady operation conditions during the field survey. As mention previously, the several generators were shut down and less warm water was discharged during the data collection. For the cooper case, the model internal error is the major source that results in the under prediction. The model simulates the deeper water in the vicinity of outfall as the lower boundary and however, the actual local depth at discharge is

shallower. Consequently, the model simulates more mixing the more dilution and temperature is under predicted.

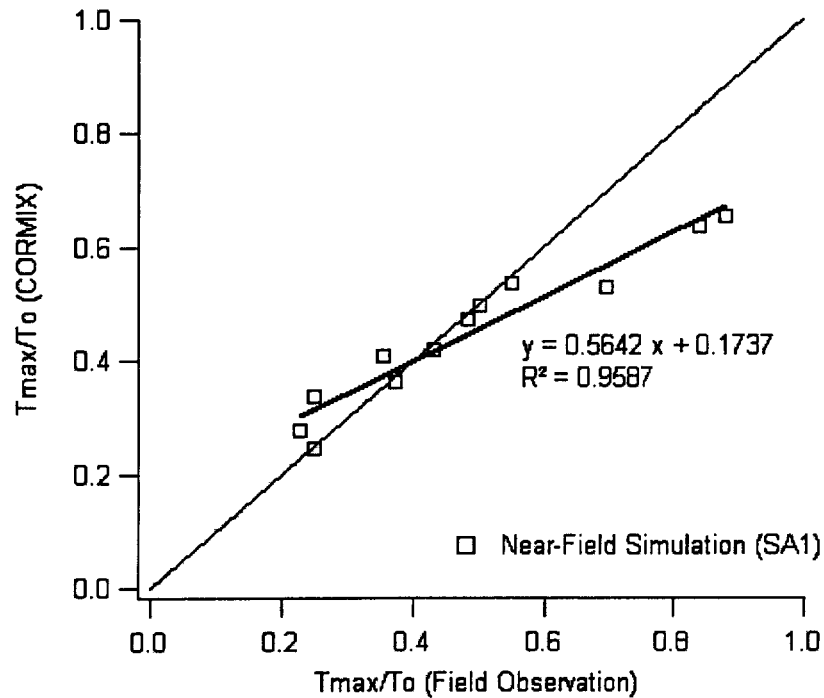


Figure 5.13 Regression and Correlation of Flow Class SA1 in Near-Field Simulation

On contrast, the far-field analysis shows that the data points are more scattered and less correlated. A less than 0.9 correlation coefficient represents the weak relationship between those to data sets and also implies the less reliability of regression. Although some problematic data and unknown on-site characteristics, such no temperature dissipation in a longer distance downstream and the unsteady operation in North Omaha Station, might result in low correlation coefficient, there still exist several problems regarding to the determination of transition between buoyant spreading motions and the passive diffusion and the over-emphasized buoyancy in the far-field simulation.

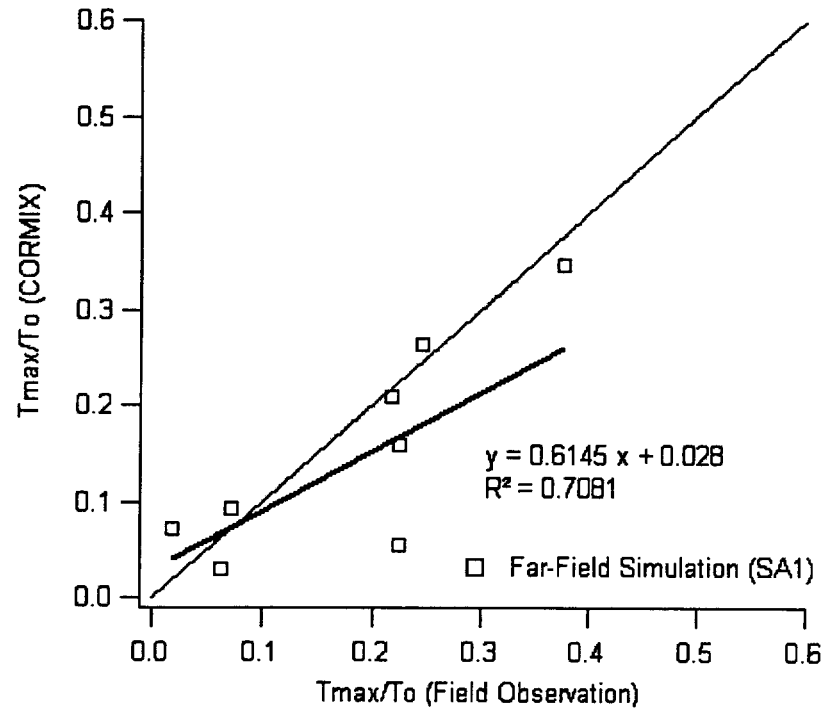


Figure 5.14 Regression and Correlation of Flow Class SA1 in Far-Field Simulation

Overall, the plume behaviors are appropriately simulated in most of the cases presented in maximum temperature, plume width, and the plume thickness. The statistics analyses also indicate that the rate the temperature dissipation is appropriately simulated in the range of the 10 °C excess temperature that is the general excess temperature of the cooling water discharged from power stations.

6

Regulatory Mixing Zones for Thermal Discharges at Study Sites

Seasonal changes in ambient flow conditions commonly result in critical conditions for water quality management of mixing zones under the regular operation of the power plant facility. Typically, the 7-Day average low flow with a 10-year return period (7Q10) is the ambient discharge specified as the critical design condition. However, for each the four sites, 3 cases representing different ambient conditions will be presented. Case 1 will be the 7Q10 (7-day average low flow, ten year return period) for the site. Case 2 will be a modified low summer flow based upon reservoir releases as proposed in the Missouri River Master Water Control Manual[31]. Case 3 will represent the winter time low flow condition. Table 7.1 summarizes the ambient discharges and depths used for the 3 cases at each site.

6.1 Interpreting the Mean Velocity, Average Water Depth, and Depth at Discharge

The operation of the power plants remains relatively constant throughout the year, so discharge conditions do not change seasonally. Therefore the model input for discharge parameters remain the same for the critical low flow conditions.

For the ambient and geometric parameterization, the mean velocity, river depth, and river width can change seasonally. Therefore, these parameters will be adjusted to reflect critical regulatory conditions. Particularly the lower water levels

due to low flow has tendency to create unstable near-field flow classes within CORMIX. conditions, the lower water level, due to low river flow, has tendency to form the unstable flows.

As mentioned previously, mixing within CORMIX is dependent on local current u_a velocity rather than ambient discharge Q_a . Because no ambient velocity measurements are available for the critical low flow conditions, representative velocities must be estimated. The approach given here is to estimate the mean velocities with the use of historical onsite USGS gage measurements for various river stages and the application of the Manning equation.

$$V_{(m/s)} = \frac{1}{n} R_h^{2/3} S^{1/2} \quad (6.1)$$

A typical channel roughness coefficient Manning's N for the Missouri River is $n=0.025$. The local river slope is documented in the outfall designs. The local cross-section area is important for determining the hydraulic radius as a function of stage (discharge). In general, changes in discharge are reflected directly in the average water depth H_A , depth at discharge H_D , local depth at discharge H_{D_0} , and the channel width BS . For below bankfull discharge (e.g 7Q10) in a typical very wide flat-bed cross-section like the Missouri River, the depth (stage) shows the most significant variation in response to discharge changes, while river width BS (and hydraulic radius) varies much less. Thus a reasonable assumption is that for different below bankfull discharges the river width BS remains relatively constant. Furthermore, a rectangular cross section is assumed as representative of the geometry. Thus, the hydraulic radius R_h is estimated as summation of the river width BS plus two average river depths H_A .

To estimate the actual mean water depth H_A , depth at discharge H_D , local depth at discharge H_{D_0} for critical conditions, historical gage measurements are employed. From the field observation, the actual H_A , H_D , and H_{D_0} are obtained by processing the ADCP river profiling measurements. In addition, the actual river discharges is known from the gage measurements near the power plants on the sampling dates. Using historical gage data, the corresponding gage heights can be found for the actual river discharges on the sampling dates and the low flows. The

difference in gage height between actual discharges and low discharge is simply thought to be the difference in water elevation. By subtracting the difference in gage height from the observed H_A , H_D , and H_{D_0} , H_A , H_D , and H_{D_0} in various flow conditions can be estimated, assuming the cross-section at the gage is representative of the site cross-section. Finally, with applying the Manning equation (Eqn. 6.1), the mean ambient velocity of critical river discharges can be calculated. Table 6.1 lists all the variables for velocity estimation in critical flow conditions.

Table 6.1 HA and HD under Different Discharges

	Fort Calhoun	Cooper *	Nebraska City	North Omaha
QA(cms)	886	966	957	884
QA(cfs)	31300	34100	33800	31200
Gage Height (ft)	7.50	8.21	8.92	16.20
HA(m)	4.91	4.23	4.57	3.83
HD(m)	4.67	4.75	4.21	4.15
HD0(m)	4.32	3.48	3.048	4.15
Slope	1.85E-04	1.96E-04	2.08E-04	1.33E-04
Rh	5.58	4.03	4.09	4.67
Ua(m/s)	1.00	1.24	1.29	1.41
QA_7Q10(cms)	818	902	881	818
QA_7Q10(cfs)	28888	31863	31094	28888
Gage Height (ft)	6.91	8.06	8.29	15.27
delta water elevation (m)	0.18	0.05	0.19	0.28
HA_7Q10(m)	4.73	4.18	4.38	3.55
HD_7Q10(m)	4.49	4.70	4.02	3.87
HD0_7Q10(m)	4.14	3.43	2.86	3.87
Slope	1.85E-04	1.96E-04	2.08E-04	1.33E-04
Rh	4.51	3.99	4.18	3.43
Ua_7Q10(m/s)	0.87	0.88	1.01	0.81
QA_mm7Q10(cms)	839	817	796	733
QA_mm7Q10(cfs)	29632	28863	28094	25889
Gage Height (ft)	7.10	7.34	7.59	14.64
delta water elevation (m)	0.12	0.27	0.41	0.48
HA_mm7Q10(m)	4.79	3.96	4.16	3.35
HD_mm7Q10(m)	4.55	4.48	3.80	3.67
HD0_mm7Q10(m)	4.20	3.21	2.64	3.67
Slope	1.85E-04	1.96E-04	2.08E-04	1.33E-04
Rh	4.56	3.79	3.98	3.24
Ua_mm7Q10(m/s)	0.87	0.85	0.98	0.78
QA_w7Q10(cms)	377	365	353	340
QA_w7Q10(cfs)	13318	12903	12478	12014
Gage Height (ft)	2.70	3.30	3.84	9.35
delta water elevation (m)	1.46	1.50	1.55	2.09
HA_w7Q10(m)	3.45	2.73	3.02	1.74
HD_w7Q10(m)	3.21	3.25	2.66	2.06
HD0_w7Q10(m)	2.86	1.98	1.50	2.06
Slope	1.85E-04	1.96E-04	2.08E-04	1.33E-04
Rh	3.33	2.65	2.92	1.71
Ua_w7Q10(m/s)	0.71	0.67	0.80	0.51

Note: 7Q10 represents summer low flow condition

Mm7Q10 represents annual low flow condition reported in Master Manual[31]

w7Q10 represents the winter low flow condition

* Gage measurement not available for Cooper site, use the average value of Ft. Calhoun and Nebraska City

6.2 Thermal Discharge Assessment based on the CORMIX Simulation

For the four survey sites, the edge the regulatory mixing zone (RMZ) is at 5000 ft (1524 m). Water quality criteria must be meet at the edge of this zone, however may be exceeded within the RMZ. The criteria are seasonally based, the summer criteria (7Q10 or mm7Q10) specifies a maximum temperature increase (ΔT) above ambient of 1.667 °C, while the winter criteria (w7Q10) is 2.78 °C.

For the Cooper site, under 7Q10 and w7Q10, the discharge is in SA1 (shoreline attached, stable near-field) CORMIX flow class. The maximum temperature predicted at the RMZ of $x = 1524$ m is 0.29 °C and 0.31 °C, respectively. Under mm7Q10, the discharge is classified SA2 flow class (shoreline attached, unstable near-field) and the maximum temperature predicted at the same location is 1.16 °C.

For the Ft. Calhoun site, under 7Q10 and mm7Q10, the discharge is a PL2 (plume like, shore-hugging) flow class. The maximum temperature predicted at the RMZ of $x = 1524$ m is 0.43 °C and 0.41 °C, respectively. Under w7Q10, the discharge is classified SA1 (shoreline attached, stable near-field) flow class and the maximum temperature predicted at the same location is 0.98 °C.

For the Nebraska City site, under all discharge conditions the discharge is a SA2 (shoreline attached, unstable near-field) flow class. The maximum temperature predicted at the RMZ of $x = 1524$ m is 0.27 °C for 7Q10, 0.29 °C for mm7Q10 and 1.05 °C for w7Q10. They are all below the WQ standard in both summer and winter conditions.

For the North Omaha City site, under all discharge conditions the discharge is a SA2 flow class (shoreline attached, unstable near-field). The maximum temperature predicted at $x = 1524$ m is 0.52 °C in 7q10, 0.53 °C in mm7Q10 and 2.45 °C in w7Q10. As well, they all meet the WQ standards in both the summer time and winter time.

Figure 6.1- 7.12 illustrate the general plume patterns and the excess temperature distribution by ArcView for each facility under 7Q10, mm7Q10, and w7Q10 discharge conditions.

Table 6.2 summarizes the WQ standard under various river discharge conditions and the predicted maximum temperature on the edge of the mixing zone.

Table 6.2 WQ Standards and the Predicted Temperature at 5000 ft (1524 m) Downstream of the Outfall

	Fort Calhoun	Cooper	Nebraska City	North Omaha
Predicted Temperature (°C)				
7Q10	0.43	0.29	0.27	0.52
mm7Q10	0.41	0.31	0.29	0.53
WQ Standard (°C)	1.67	1.67	1.67	1.67
w7Q10	0.98	1.16	1.05	2.45
WQ Standard (°C)	2.78	2.78	2.78	2.78

However, it is important to note that these simulations are run with only the given river discharge and actual ambient conditions such the water depths and velocities are based on calculations. These factors can significantly influence the plume trajectory and mixing characteristics in the simulation. If the calculated site conditions are inconsistent with actual ambient data for the critical flow conditions, then the simulations may not produce reliable results. From the previous chapters, the overall performance of the CORMIX model relies upon an adequate characterization of the source and ambient conditions. Thus, the results presented above should be considered carefully. To obtain more a higher degree of confidence in modeling results, detailed site data at low flow conditions should be obtained.

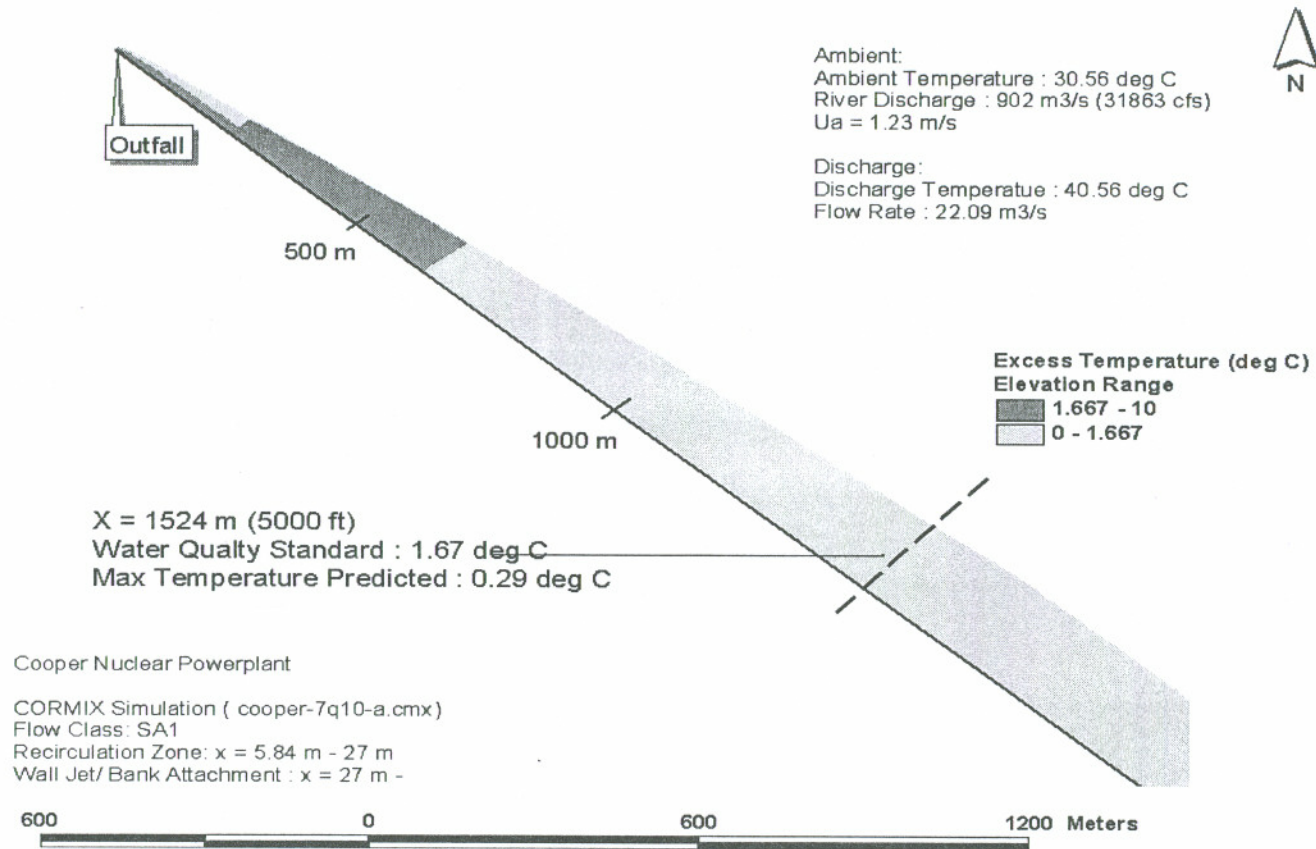


Figure 6.1 Illustration of the Thermal Plume Pattern and Excess Temperature Distribution in 7Q10 Discharge Condition at Cooper Nuclear Power Plant

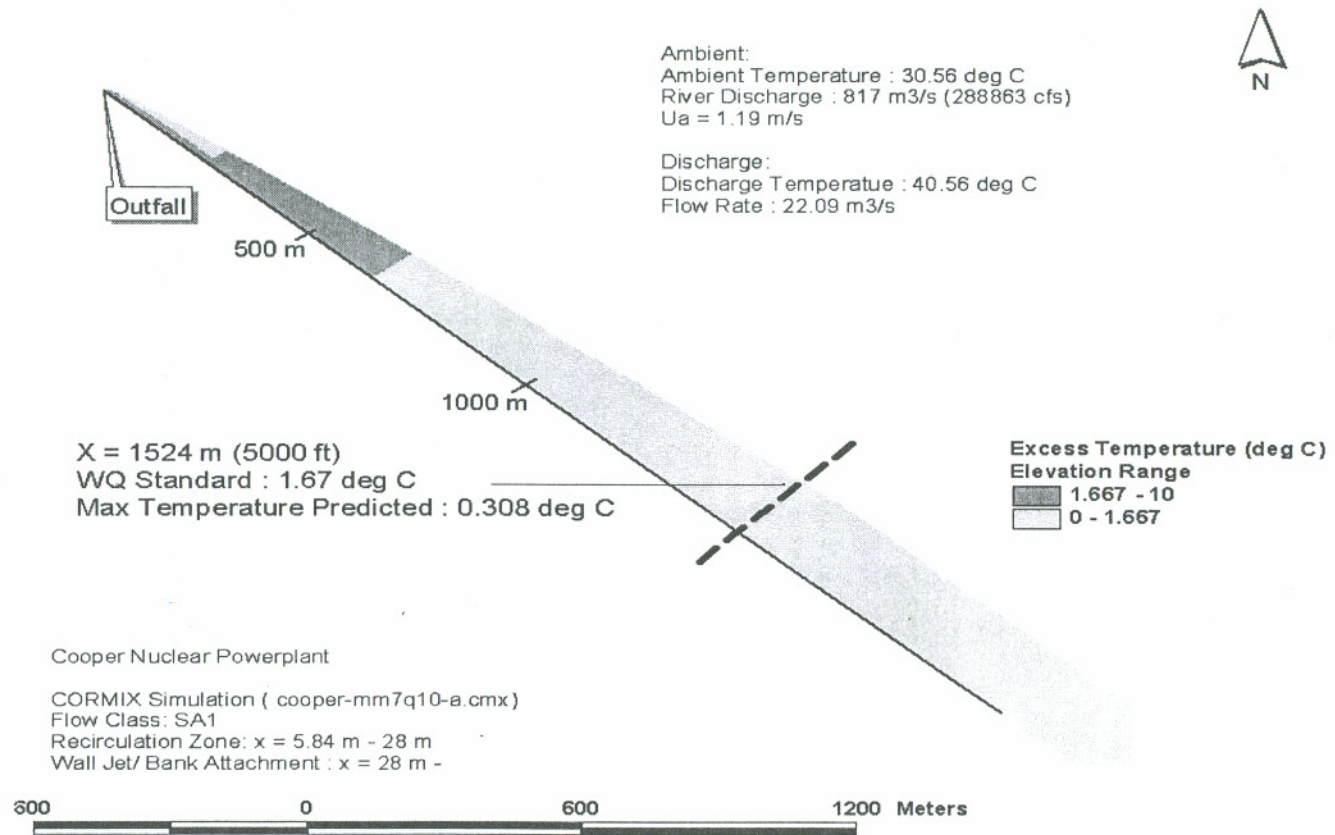


Figure 6.2 Illustration of the Thermal Plume Pattern and Excess Temperature Distribution in mm7Q10 Discharge Condition at Cooper Nuclear Power Plant

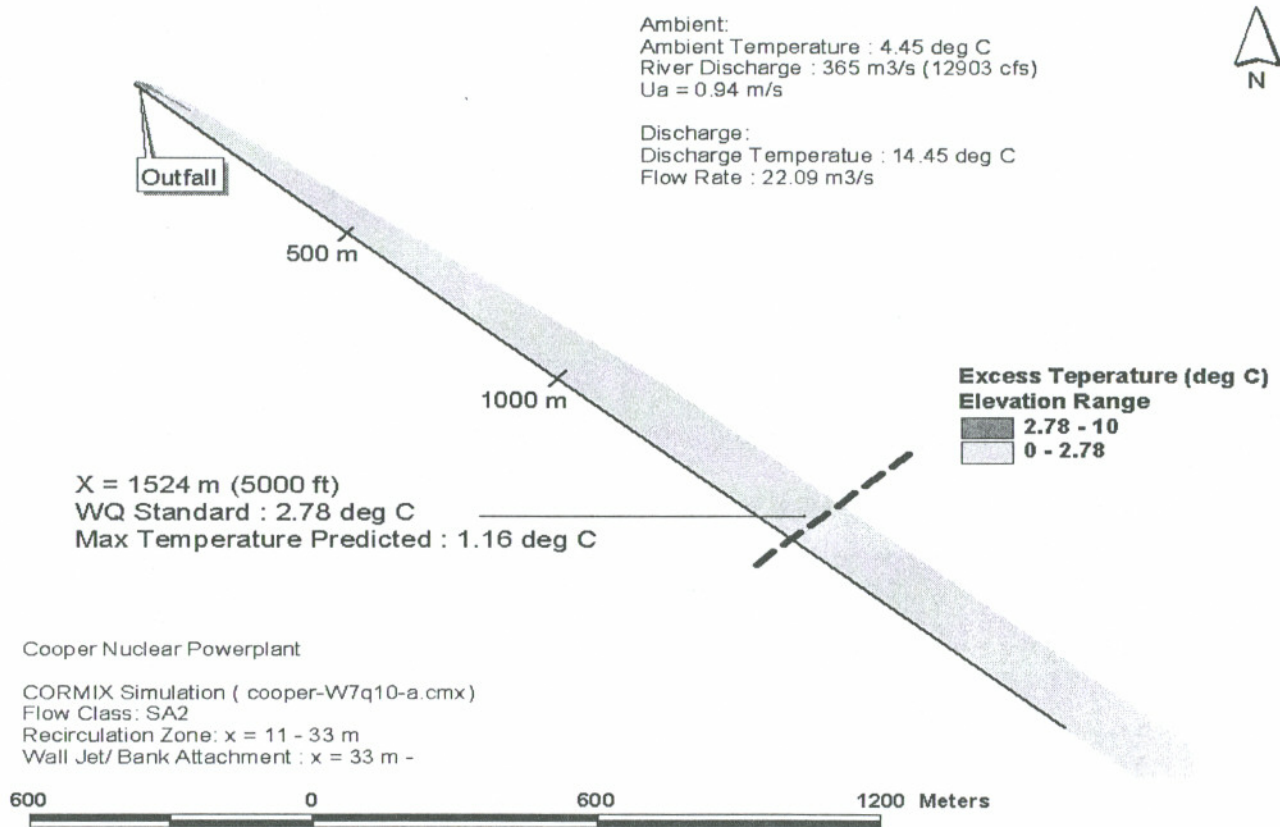


Figure 6.3 Illustration of the Thermal Plume Pattern and Excess Temperature Distribution in w7Q10 Discharge Condition at Cooper Nuclear Power Plant

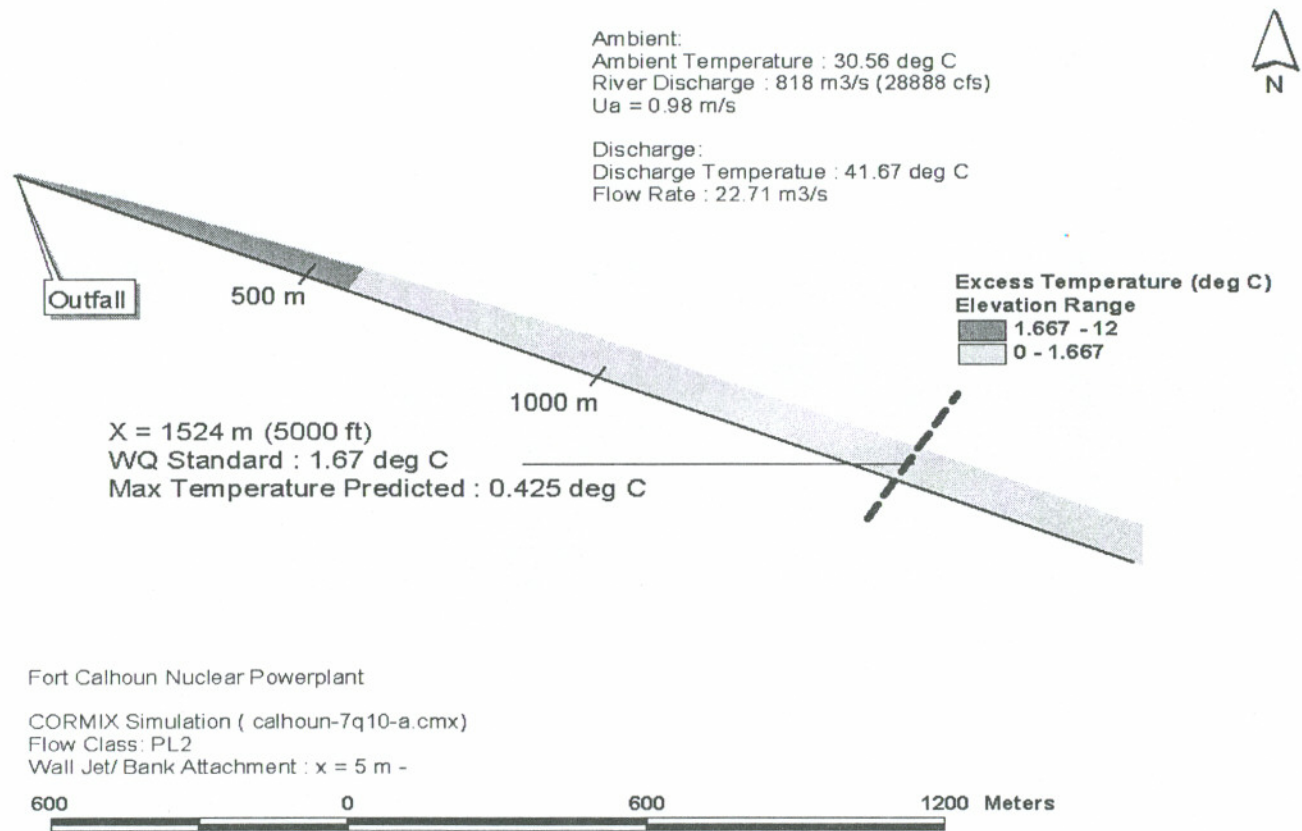


Figure 6.4 Illustration of the Thermal Plume Pattern and Excess Temperature Distribution in 7Q10 Discharge Condition at Ft. Calhoun Nuclear Power Plant

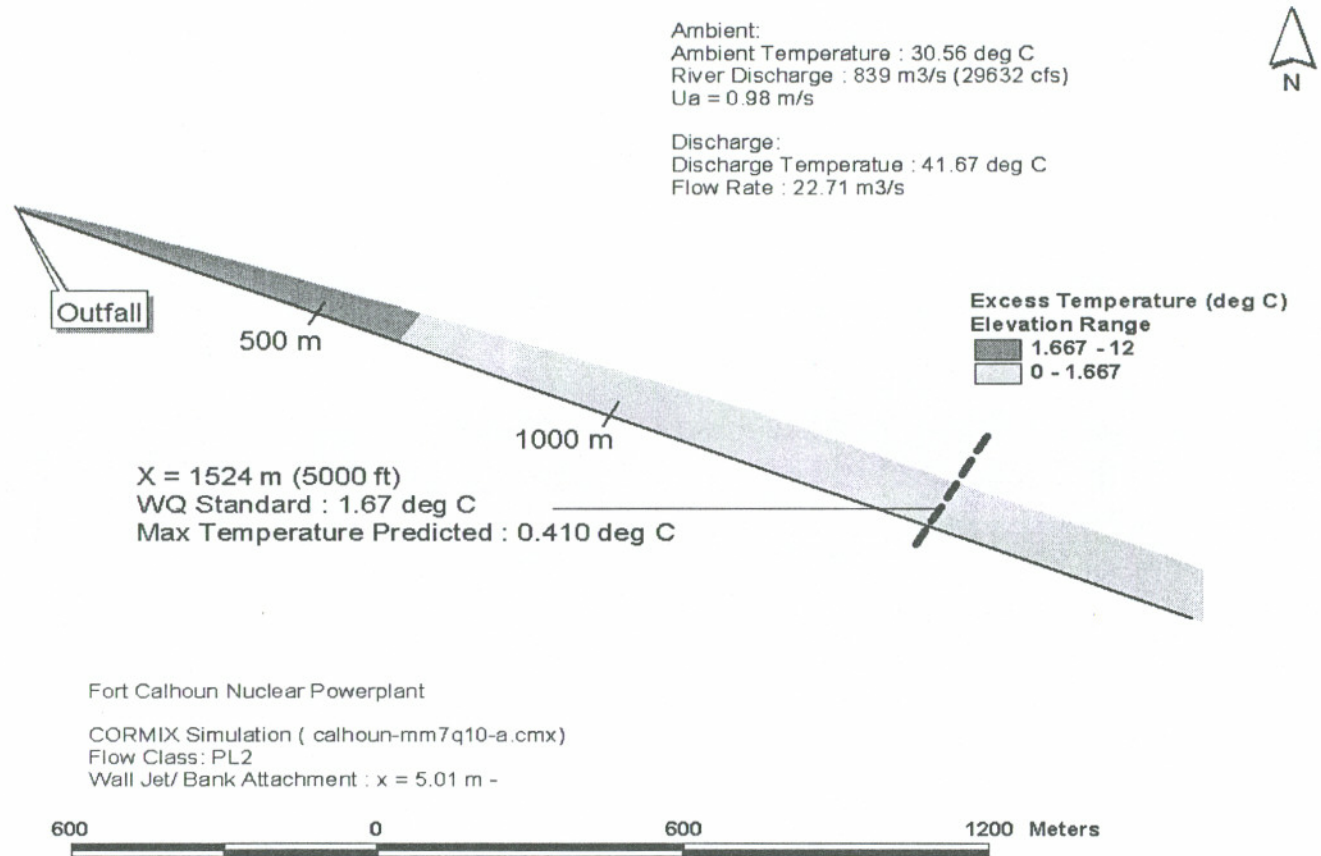


Figure 6.5 Illustration of the Thermal Plume Pattern and Excess Temperature Distribution in mm7Q10 Discharge Condition at Ft. Calhoun Nuclear Power Plant

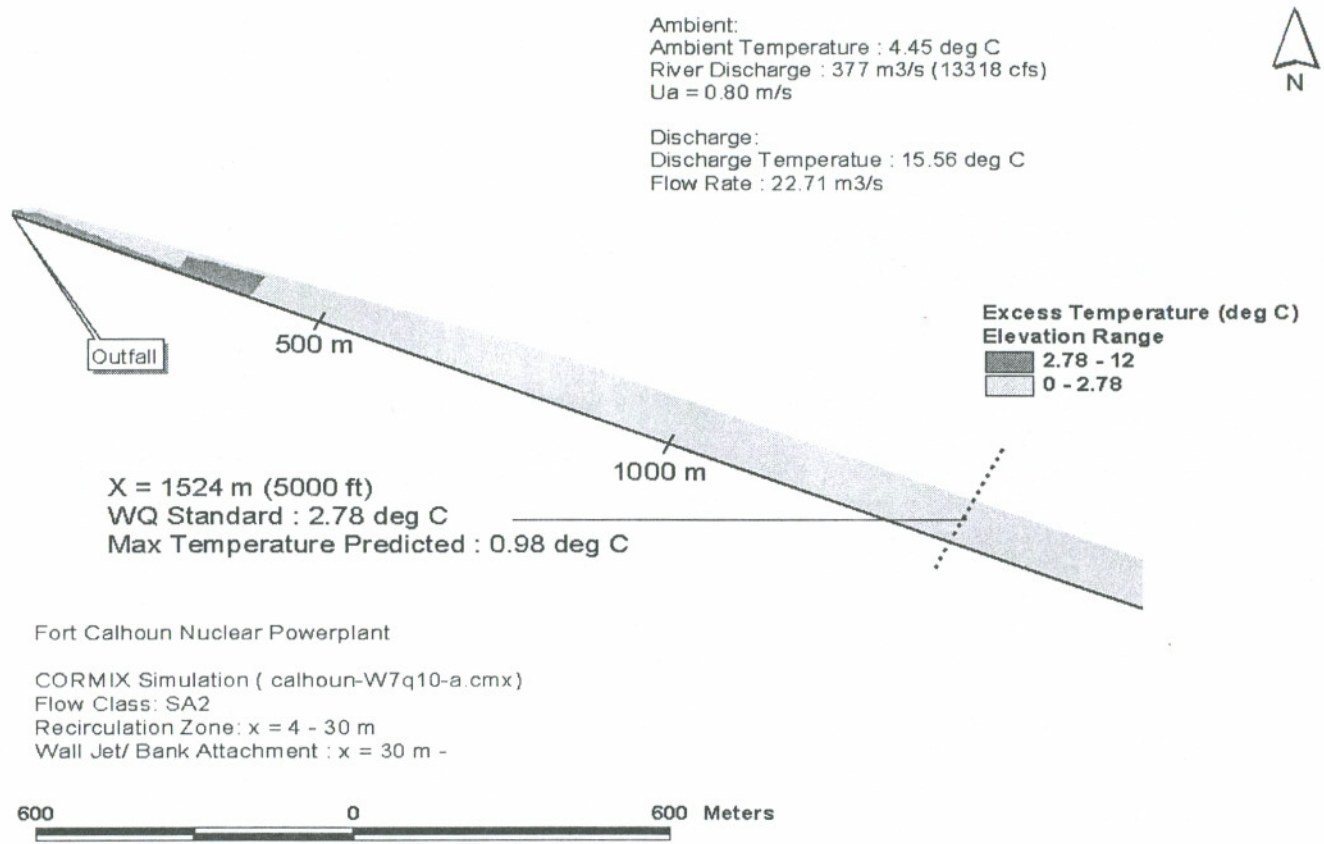


Figure 6.6 Illustration of the Thermal Plume Pattern and Excess Temperature Distribution in w7Q10 Discharge Condition at Ft. Calhoun Nuclear Power Plant

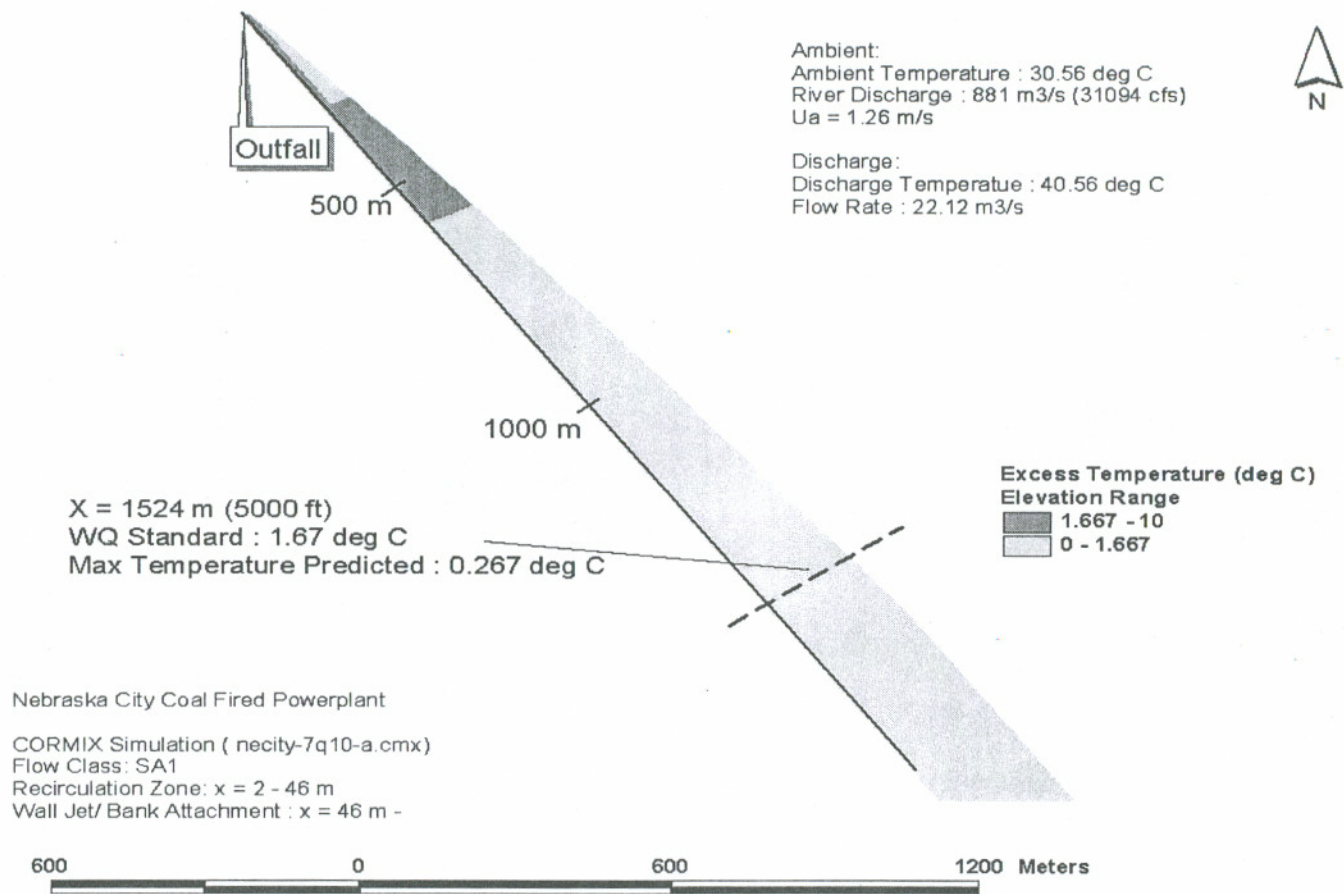


Figure 6.7 Illustration of the Thermal Plume Pattern and Excess Temperature Distribution in 7Q10 Discharge Condition at Nebraska City Coal Fired Power Plant

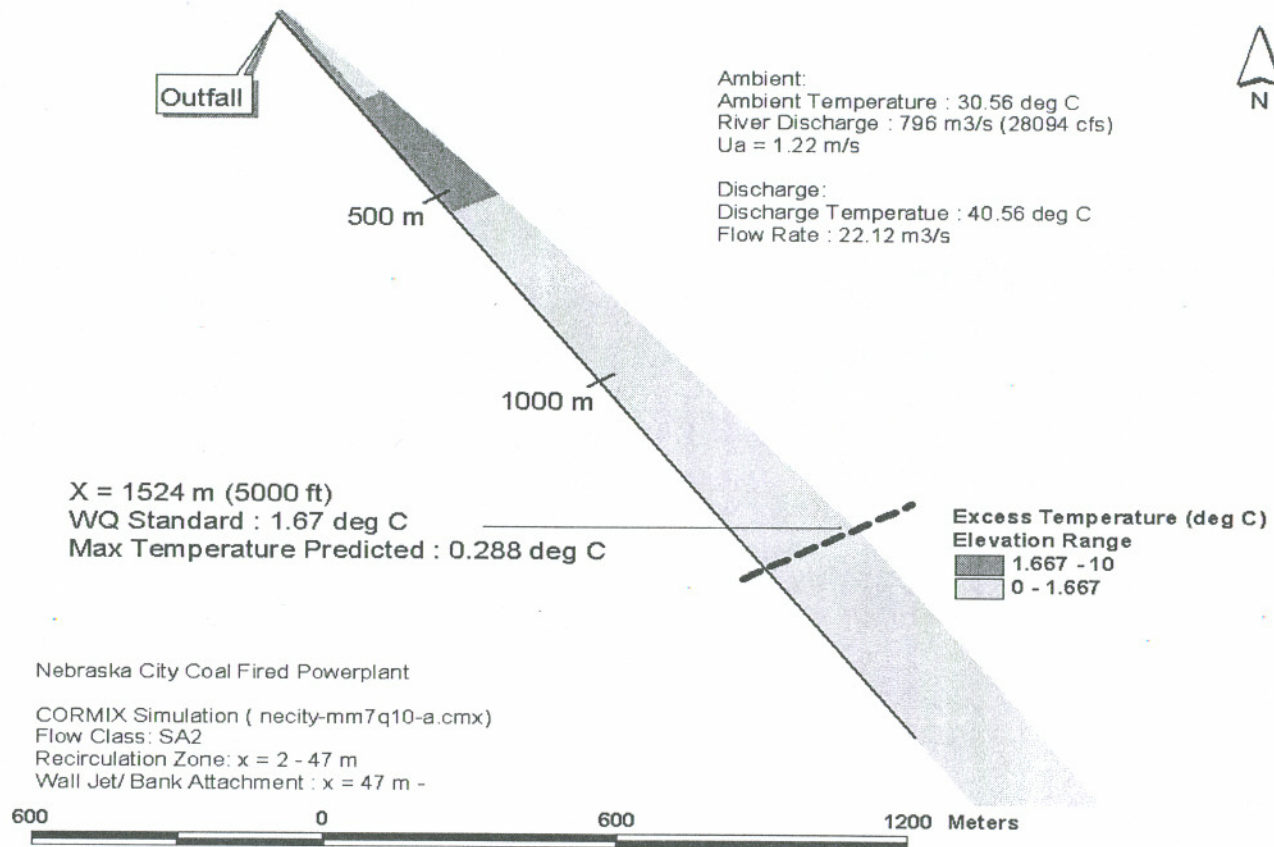


Figure 6.8 Illustration of the Thermal Plume Pattern and Excess Temperature Distribution in mm7Q10 Discharge Condition at Nebraska City Coal Fired Power Plant

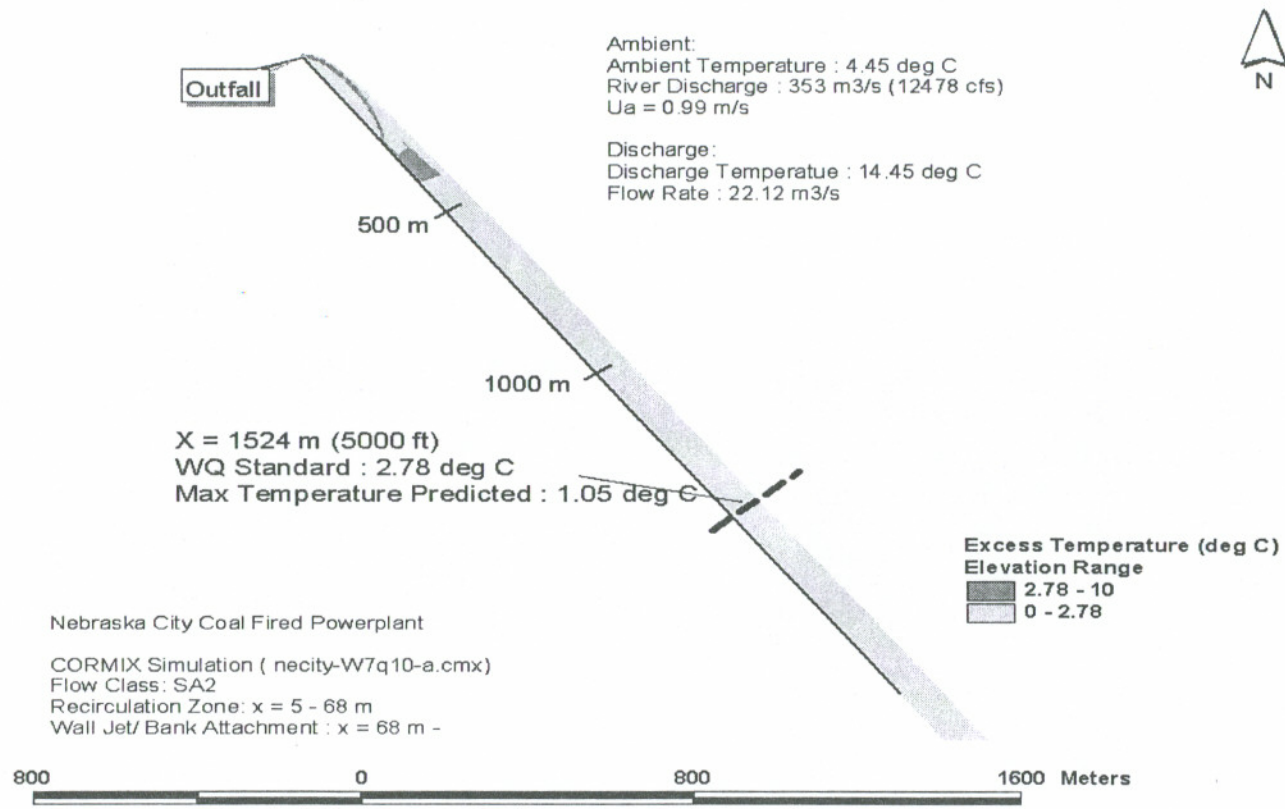


Figure 6.9 Illustration of the Thermal Plume Pattern and Excess Temperature Distribution in w7Q10 Discharge Condition at Nebraska City Coal Fired Power Plant

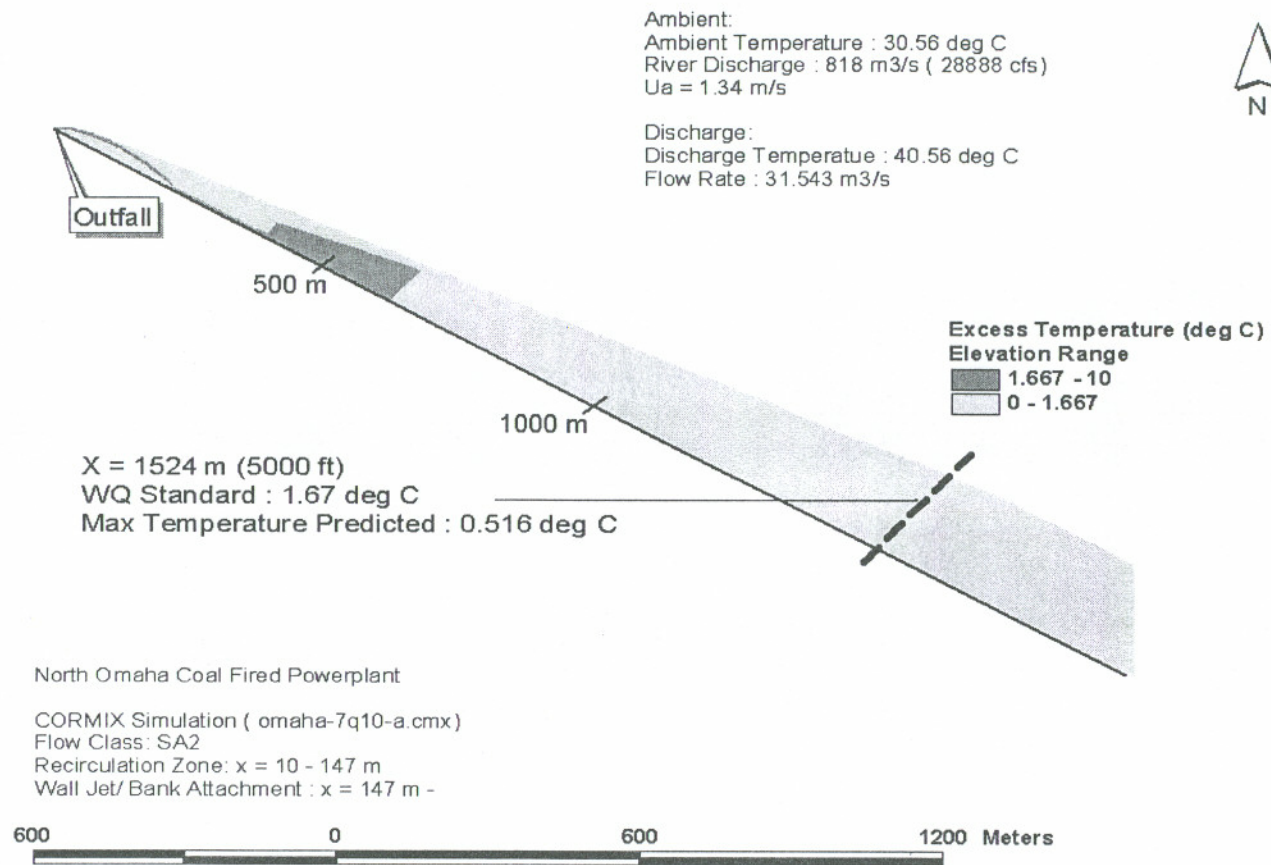


Figure 6.10 Illustration of the Thermal Plume Pattern and Excess Temperature Distribution in 7Q10 Discharge Condition at North Omaha Coal Fired Power Plant

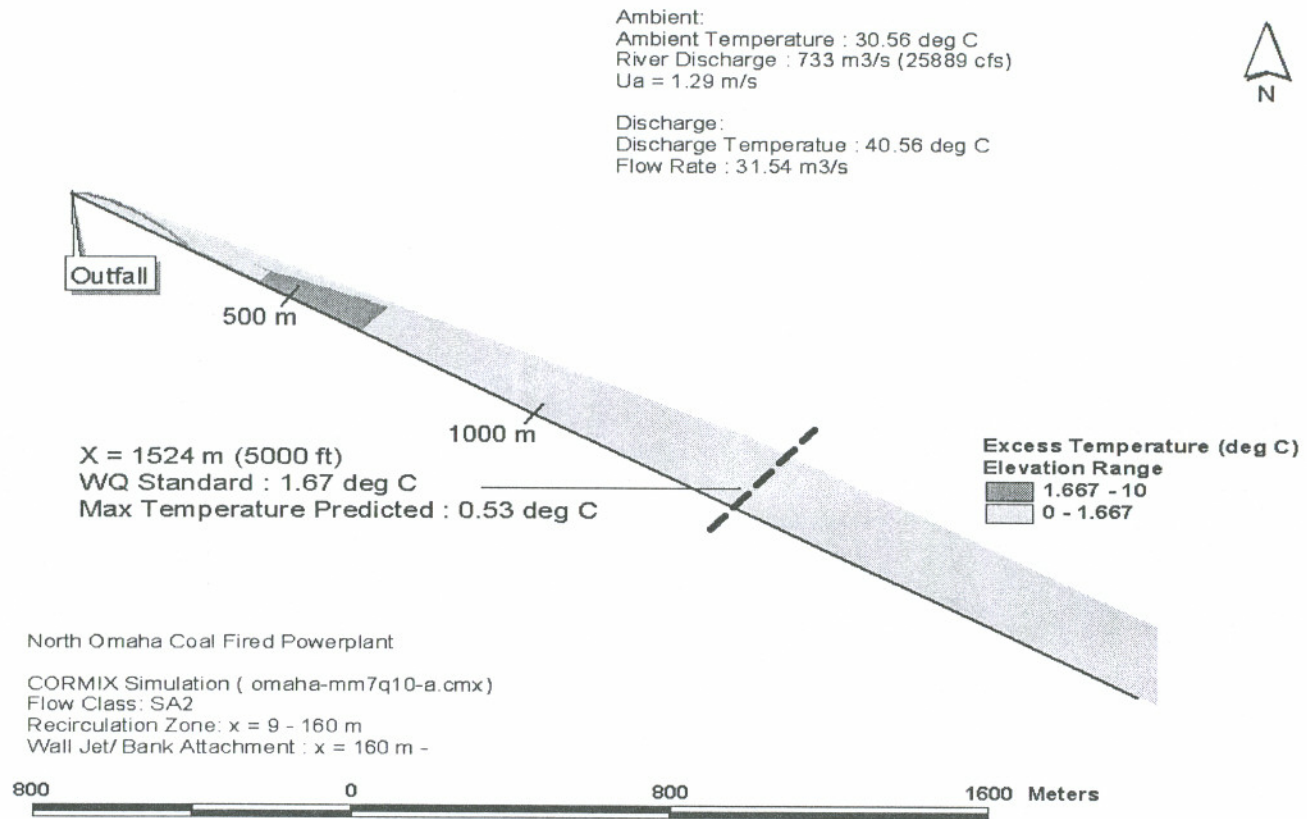


Figure 6.11 Illustration of the Thermal Plume Pattern and Excess Temperature Distribution in mm7Q10 Discharge Condition at North Omaha Coal Fired Power Plant

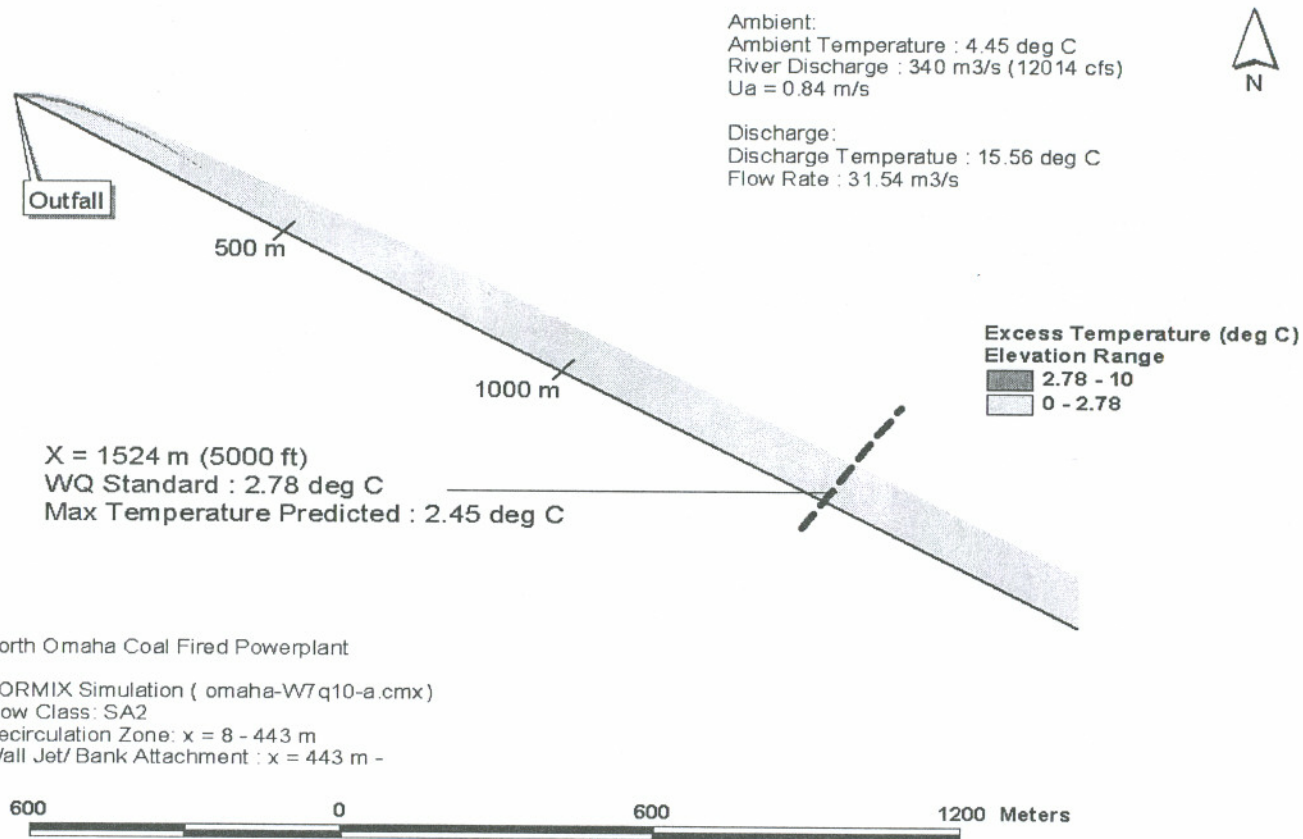


Figure 6.12 Illustration of the Thermal Plume Pattern and Excess Temperature Distribution in w7Q10 Discharge Condition at North Omaha Coal Fired Power Plant

Satellite Thermal Imagery

With significant recent progress in remote sensing, new technology with satellite sensor capabilities may offer an additional method for field data collection on thermal discharges. Considering the increased efficiency possible by utilizing advanced technology for thermal plume studies, remotely sensed satellite data was considered as a mixing model validation tool. Satellite thermal imagery was obtained to evaluate the feasibility of using remote sensed technology in power plant thermal plume surveys and to assess the use of remote sensed data for thermal mixing zone analysis and CORMIX model validation in a large Midwest river.

7.1 Introduction of Multi-Spectral Thermal Imager

Multispectral Thermal Imager (MTI) is analyzed and evaluated in this study for further model validation. MTI, a single military satellite with high-precision thermal sensors on board, is sponsored by Department of Energy (DOE) and executed by Sandia, Los Alamos National Laboratory and Savannah River Technology Center. The main goal of this project is to develop an evaluate advanced multispectral and thermal imaging, image processing and associated technologies for nonproliferation treaty monitoring[32].

Fifteen (15) spectral bands on the MTI's passive sensors range from visible to long-wave thermal infrared. It contains three visible bands, five near-infrared bands,

two short-wavelength infrared bands, two mid-wavelength infrared bands, and three long-wavelength thermal infrared bands. In visible bands, the ground resolution is 5 m however in thermal bands only 20 m ground resolution can be realized. These bands provide a broad range of data on surface temperature materials, water quality and vegetation stress. The imagery will be used to demonstrate enhanced capabilities in a variety of applications, including temperature retrieval, analysis of thermal and particulate pollutant transport in surface water systems and the atmosphere, waste and mining site monitoring, vegetation health and material identification. Verification of MTI's performance in these different applications requires independent radiometric measurements and the collection of necessary collateral data, such as atmospheric temperature and humidity profiles, direct water temperature measurements and target material samples for laboratory spectral analyses[32-34].

Atmospheric interferences have been a major problem in the history of remote sensing, particularly for passive sensors which only receive the reflected radiance without emitting the source radiance as the reference to normalized the reflected radiance. As is the case with all passive remote sensing systems, the atmosphere has a significant effect on the intensity and spectral composition of the energy recorded by a thermal system, particularly to the satellite-based sensors because of the longer travel distance for the reflected radiance passing through the atmosphere to the space. The atmosphere attenuation in the solar incoming radiation and reflected radiance from ground attributes varies temporally and spatially depending on the weather conditions and atmospheric constituents. The effect will depend on the degree of atmospheric absorption, scatter, and emission at the time and place sensing. Commonly, the atmospheric absorption and scattering by the water vapor and particles tend to make the signals from ground objects appear colder than they actually are, and atmospheric emission tends to make ground objects appear warmer than they are. Of course, the meteorological conditions can directly alter the composition of atmospheric constituents and have a strong influence on the form and the magnitude of the thermal atmospheric effects[35-37]. For MTI's atmospheric corrections, the atmospheric radiance and transmission model, moderate resolution

transmittance (MODTRAN), is used to derive the spectral transmission under various atmospheric conditions of temperatures, constituents, water vapor, and weather in different locations. The surface water temperature is retrieved by a radiative transfer model with the use of the MODTRAN results[38].

7.2 Analysis of the MTI Remote Sensed Data

In the process of remote-sensed data analysis, some difficulties arose regarding use of the thermal imagery in verification of CORMIX predictions and field data. First, the relatively low ground resolution of the MTI data of approximately 20 m was the primary problem with the remote sensed data. Thermal mixing zones for cooling waters discharges in rivers are likely to have significant variation within the 20 x 20 m grid. The large pixel size forces an averaging effect over the ground in which thermal attributes within 20 x 20 m grid are presented as one averaged temperature value that results in a rough plume pattern[39]. For example, thermal plumes near the four Missouri power plants are relatively in small scale, approximately less than 20 meters in total width in the near-field. As a result, the detailed lateral temperature distribution cannot be resolved due to the relatively low resolution (Figure 7.1).

Besides, the averaging used within the 20 m pixel grid therefore limits the feasibility of MTI thermal images in mixing zone model validation or field data verification. For instance, the 20 m x 20 m grid might cover partially both land and water along shoreline boundaries as a mixed pixel. If most of the sensor readings represent the land surface on the bank shoreline, then the reflectance detected by the sensor is not only composed of the radiance from the water surface but mostly from the ground. In late fall, the ground temperature is almost always remarkably higher than the water temperature because the soil has lower specific heat and tends to absorb heat and rise in temperature rapidly. Consequently the temperature converted from the reflectance data may be larger than the actual water temperature near the

bank in daytime and lower in nighttime. However, there is no consistent way to determine for each grid element what percentage represents land surface versus water surface within a pixel. In addition to the mixed pixels along the shoreline, shore hugging plumes are quite common for the surface discharge configurations used at the four study locations and high temperatures are often observed in the near-shore area. The averaging effect in a pixel is particularly problematic for shoreline-attached plumes in determining the high temperature in the dilution analysis (Figure 8.1).

Inconsistent atmospheric and radiometric corrections and the sensitivity of the sensors are other possible limitations of the MTI data obtained for riverine mixing zone analysis. Although the field data collection and satellite imagery acquisition were on different days, it was assumed that daily temperature variations are small enough to be negligible in study period. However, there can still be some significant differences between images that were shot on different dates, indicating the inconsistency of the atmospheric and radiometric correction in this technology.

Indeed, in some regions the thermal plume can be distinguished from the image by enhancing the image contrast (Figure 7.1). But in terms of absolute temperature, the difference between the temperatures within the plume and ambient temperature was less than 1°C in some cases and therefore plume temperature and dilution S cannot be explicitly calculated from the remote sensor temperature data for the riverine systems of this study.

In summary, due to all these platform features of relatively low resolution and averaging effects, inconsistent atmospheric and radiometric corrections and small-scale thermal discharges in this study, the MTI remote sensed data obtained was not taken into consideration in verification of field data and CORMIX modeling. However, with the more consistent correction algorithms, the technology can be applied on the thermal discharge monitoring for those large-scale thermal discharges in the ocean. For the small-scale thermal discharge, to validate thermal plume mixing models in large rivers, remote sensed data must be able to resolve plume features within 1-2 m and be calibrated appropriately. Some airborne-based sensors, such as Forward Looking Infrared (FLIR), have been used successfully to conduct a number

of related thermal studies and can be applied for the further model validation for surface thermal discharge in the large rivers[40].

a) Contrast Enhanced Imagery



b) Lateral Temperature Trend

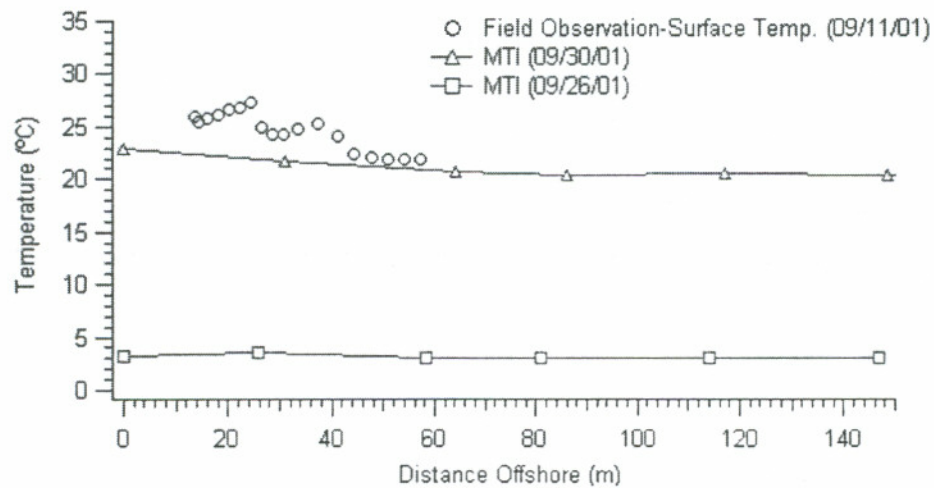


Figure 7.1 MTI Thermal Imagery at North Omaha Station, Sept. 9, 2001

- Processed by the histogram stretch, the shoreline-hugging plume can be observed in the vicinity of the North Omaha Station
- The temperature trends at 380 m downstream of Cooper station.

8

Conclusions and Recommendations

8.1 Conclusions

Ambient and discharge schematization is a fundamental component in modeling mixing zones with CORMIX. Schematization is the technique used to simplify site conditions into the parameter set needed for simulation model input. Schematized parameters in CORMIX mixing zone simulation capture essential discharge and ambient geometry information.

Discharge parameters, such as flow rate and excess temperature, are used to determine the sources conditions of mass flux, momentum flux, and buoyancy flux. The daily motoring records and plant construction documents can be a reliable source for discharge parameterization. Detailed field observations and reliable data source are required to complete ambient data parameterization.

Source conditions along with the strength of ambient crossflow and intensity of ambient turbulence are the predominant mechanisms that cause plume advection and mixing. In buoyancy dominated discharges, such as cooling water discharge, far-field density current mixing can trap the plume in a confined surface layer and limit entrainment except along lateral boundaries. Boundary interaction also influences the plume behaviors, particularly for shore-hugging plumes. Consequently for shoreline attached flows, the mixing and temperature dissipation can be limited in density current mixing in surface discharges.

In large rivers, due to the steep slope of banks, the rectangular river cross-section schematized by CORMIX is adequately representative of actual site conditions. In addition, the schematization of details of local discharge geometry is needed to assess plume bottom attachment and near-field discharge stability. For these reasons, detailed ADCP river profiling measurement is highly desirable for adequate source characterization.

With the application of the realistic input parameters, statistical analyses indicate that the CORMIX system and the CORMIX3 surface discharge hydrodynamic model can predict thermal plume mixing zone behavior in large rivers in general quantitative agreement with available data. Therefore CORMIX can be used to make reasonable predictions for regulatory management of thermal plumes in large rivers. With the data sets for critical low flow scenarios, several simulations were also conducted to assess thermal plume behavior for regulatory compliance. It is important to note that modeling results should be used carefully because the several ambient parameters, such as average water depth, discharge depth, and current velocity are derived upon engineering formula based on observed flows and site conditions. The actual critical conditions at low flows might be slightly different from the projected conditions so verification of the low flow model input is desirable.

In analysis of the available remote sensing data, the present technology is not applicable for the objectives of this study. The relatively low resolution of MTI platform becomes problematic for the shoreline-attached plumes observed in this study. Mixed pixels along the shoreline or in the near-bank area contain both ground temperature and water temperature information so the averaged temperature is not representative for near-shore plume temperature. However, this averaging effect is inevitable in remote sensing technology and it worsens with lower resolution. In addition, the inconsistency of the atmospheric and radiometric correction of the data obtained is another issue in resolving the water surface temperature from the imagery. In future model validation studies for relatively small-scale thermal discharges, airborne sensors which usually have higher resolution and more precise corrections should be considered.

8.2 Recommendations for Field Surveys

Overall the data collected at the four power plant facilities along the Missouri River was successful in model validation. The ADCP measurements provided sufficient information regarding ambient flow conditions, river geometries, and riverbed features to facilitate schematization and model input parameterization. In addition, the detailed data collected make possible optimizations of simulation model input based on local site conditions. However, some suggestions on the field sampling protocol are proposed based on experience in CORMIX parameterization and data analysis for these sites.

In the Missouri River sites, the rectangular schematization was created based upon the upstream profiling measurements. For relatively large streams, such as Missouri River, the stream width and depth tend to remain fairly consistent in the project area. However, sloping banks geometry may vary from location to location. For CORMIX3 schematization, the sloping bank may influence plume bottom attachment at the discharge entry. Furthermore, the bottom bathymetry might have changes downstream from upstream profiles used in data input parameterization and therefore might not be adequate if substantial changes occur. Therefore, profiles used to represent upstream conditions for schematization should be taken as close as possible to the discharge outlet. In addition, several downstream transects should be taken with include details of the near-bank shoreline region.

In CORMIX modeling, the temperature at discharge is the temperature at the outfall entry into the ambient, and the physical dilutions and concentrations are computed based on this initial temperature. For the Missouri River sites the discharge temperatures was measured at outlet of the cooling system in the power plant facility. Since the cooling water was not immediately discharged into the river but into the discharge canal, heat loss is expected to occur before discharge into the river. Moreover, because the heat loss is related to the local ambient temperatures and weather conditions, it is difficult to estimate heat loss during the transport to obtain the temperature right at the outfall. Therefore to more accurately characterize source

conditions, temperature profile data should be collected at the discharge outlet at the point of entry into the ambient.

For shoreline-attached flows, plumes remain attached to the bank and higher temperatures are likely to be observed near the discharge bank. Because of the shallow water and overgrown banks, the survey boat was not able to collect data close to the shoreline, resulting in the absence of near-shore thermistor data. Perhaps specialized boom-mounted equipment could be developed to gather near-shore ADCP and thermistor data.

References

1. Energy Information Administration, *Electric Power Annual 1997*. Vol. II. 1998a: US Department of Energy, Energy Information Administration.
2. Veil, J.A., Puder, M. G., Littleton, D. J., Moses, D. O., *Cooling water use patterns at US nonutility electric generating facilities*. Environmental Science & Policy, 1999(2): p. 477-487.
3. Veil, J.A., *Potential impacts of 316(b) regulatory controls on economics, electricity reliability, and the environment*. Environmental Science & Policy, 2000(3): p. S1-S6.
4. Edison Electric Institute. *Environmental Directory of US Powerplants*. 1996. Edison Electric Institute, Washington, DC.
5. Sweeney, B.W., *Factors influencing life-history patterns of aquatic insect*, in *The Ecology of Aquatic Insects*. 1984. p. 56-100.
6. Sweeney, B.W., et al., *Life Histories and Biogeography of Aquatic Insects*, in *Global Climate Change and Freshwater Ecosystems*. 1991.
7. Mason, C.F., *Thermal Pollution*, in *Biology of Freshwater Pollution*. 1991. p. 187-195.
8. Bamber, R.N., *The Influence of Rising Background Temperature on the Effects of Marine Thermal Effluents*. Journal Thermal Biology, 1995. **20**(1): p. 105-110.
9. Spicer, G., O'shea, T., Piehler, G., *Entrainment, impingement and BTA evaluation for an intake located on a cooling water reservoir in the southwest*. Environmental Science & Policy, 2000(3): p. S323-S331.
10. Melton, B.R. and G.M. Serviss, *Florida Power Corporation-Anclote Power Plant Entrainment Survival of Zooplankton*. Environmental Science & Policy, 2000(3): p. S233-S248.
11. *Guide for the Verification and Validation of Computational Fluid Dynamics Simulations*. 1998, American Institute of Aeronautics and Astronautics(AIAA).
12. EPA, U.S., *Water Quality Standards Handbook*. 1984, Washington, DC,.
13. *Title 117- Nebraska Surface Water Quality Standards*. 2000, Nebraska Department of Environmental Quality.

14. Martin, J.L. and S.C. McCutcheon, *Fundamental Relationships for Flow and Transport*, in *Hydrodynamics and Transport for Water Quality Modeling*. 1998, Lewis Publishers. p. 7-90.
15. Jirka, G.H., Doneker, R. L., Hinton, S. W., *User's Manual for CORMIX: A hydrodynamic Mixing Zone Model and Decision Support System for Pollutant Discharges into Surface Waters*. 1996.
16. Doneker, R.L., Jirka, G. H, *CORMIX-GI systems for mixing zone analysis of brine wastewater disposal*. *Desalination*, 2001(139): p. 263-274.
17. Doneker, R.L. and G.H. Jirka, *Expert Systems for Design and Mixing Zone Analysis of Aqueous Pollutant Discharges*. *Journal of Water Resources Planning and Management*, ASCE, 1991. 117(6): p. 679-697.
18. Jirka, G.H. and R.L. Doneker, *Hydrodynamic Classification of Submerged Single Port Discharges*. *Journal of Hydraulic Engineering*, ASCE, 1991. 117(6): p. 1095-1112.
19. Doneker, R.L. and G.H. Jirka, *CORMIX1: An Expert System for Mixing Zone Analysis of Conventional and Toxic Single Port Aquatic Discharges*. 1990, USEPA: Athens, GA.
20. Jones, G.R., J.D. Nash, and G.H. Jirka, *CORMIX3: An Expert System for Mixing Zone Analysis and Prediction of Buoyant Surface Discharges*. 1996, DeFrees Hydraulics Laboratory, Cornell University.
21. Jirka, G.H., E.E. Adams, and K.D. Stolzenbach, *Buoyant Surface Jets*. *Journ. Hyd. Div.*, 1981. 107(Hy11): p. 1467-1487.
22. Chu, V.H. and G.H. Jirka, *Chapter 25: Surface Buoyant Jets*, in *Encyclopedia of Fluid Mechanics*. 1986.
23. Martin, J.L. and S.C. McCutcheon, *Flow Models for Rivers and Streams*, in *Hydrodynamics and Transport for Water Quality Modeling*. 1998, Lewis Publishers. p. 199-220.
24. Akar, P.J. and G.H. Jirka, *Buoyant Spreading Processes in Pollutant Transport and Mixing. Part 2: Upstream Spreading in Weak Ambient Current*. *Journal of Hydraulic Research*, 1995. 33: p. 87-100.
25. Adams, E.E., Harlenman, D.R. F., Jirka, G. H., Stolzenbach, K.D., *Heat Disposal in the Water Environment*. 1981.
26. French, R.H., *Development of Uniform Flow Concepts*, in *Open-channel Hydraulics*. 1985, Mc-Graw-Hill Book Company. p. 111-162.

27. Sayre, W.W., Yeh, T., *Transverse Mixing Characteristics of the Missouri River Downstream from the Cooper Nuclear Station*. 1973, University of Iowa: Iowa City.
28. Chow, V.T., *Open Channel Hydraulics*. 1959, New York: McGraw-Hill Book Company.
29. Yotsukura, N. and W.W. Sayre, *Transverse Mixing in Natural Channels*. Water Resources Research, 1976. 12: p. 695-704.
30. Oppenheim, A.V., and R.W. Schaffer, *Discrete-Time Signal Processing*. 1999. pp.468-471.
31. *Missouri River Master Water Control Manual - Review and Update*. 2001, U.S. Army Corps of Engineers.
32. Decker, M.L., Kay, R. R., Rackley, N. G. *Multispectral Thermal Imager (MTI) Satellite Imaging Operations and Performance*. in 15th Annual/USU Conference on Small Satellites. 2001.
33. Garrett, A.J., et al., *Post-launch Validation of Multispectral Thermal Imager (MTI) Data and Algorithms*.
34. Kay, R.R., et al. *An Introduction to the Department of Energy's Multispectral Thermal Imager (MTI) Project Emphasizing the Imaging and Calibration Subsystems*. in 12th AIAA/USU Conference on Small Satellites. 1999.
35. Forster, B.C., *Derivation of atmospheric correction procedures for LANDSAT MSS with particular reference to urban data*. International Journal of Remote Sensing, 1984. 5: p. 799-817.
36. Gerstl, S.A.W., *Physics concepts of optical and radar reflectance signatures*. International Journal of Remote Sensing, 1990. 11(7): p. 1109-1117.
37. Lillesand, T.M. and R.W. Kiefer, *Multispectral, Thermal, and Hyperspectral Sensing*, in *Remote Sensing and Image Interpretation*. 1999. p. 309-372.
38. Borel, C.C., Clodius, W., *Recipes for Writing Algorithm for Atmospheric Corrections and Temperature/Emissivity Separation in the Thermal Regime for a Multi-Spectral Sensor*. SPIE Paper, Conf 4381-24, 1999.
39. Woodcock, C.E., Strahler, A. H., *The Factor of Scale in Remote Sensing*. Remote Sensing of Environment, 1987. 21: p. 311-322.
40. Davies, P.A., L.A. Mofor, and M.J. Neves, *Comparisons of Remotely Sensed Observations with Modeling Predictions for the Behaviour of Wastewater*

Plumes from Coastal Discharges. International Journal of Remote Sensing,
1997. **18**(9): p. 1987-2019.

Appendix A

**CORMIX Output for Validation of Thermal Plume Predictions at
Four Power Plants, Nebraska**

Efflux conditions:

X	Y	Z	S	C	BV	BH
0.00	0.00	0.00	1.0	0.102E+02	1.52	10.88

END OF MOD301: DISCHARGE MODULE

BEGIN MOD302: ZONE OF FLOW ESTABLISHMENT

Control volume inflow:

X	Y	Z	S	C	BV	BH
0.00	0.00	0.00	1.0	0.102E+02	1.52	10.88

VERTICAL MIXING occurs in the initial zone of flow establishment.

Profile definitions:

BV = Gaussian 1/e (37%) vertical thickness
 BH = Gaussian 1/e (37%) horizontal half-width, normal to trajectory
 S = hydrodynamic centerline dilution
 C = centerline concentration (includes reaction effects, if any)

Control volume outflow:

X	Y	Z	S	C	BV	BH	SIGMA =	
10.51	5.88	0.00	1.0	0.102E+02	4.46	6.98	2.86	
Cumulative travel time =							1. sec	

END OF MOD302: ZONE OF FLOW ESTABLISHMENT

BEGIN CORSURF (MOD310): BUOYANT SURFACE JET - NEAR-FIELD

Surface jet in deep crossflow with shoreline-attachment.

Profile definitions:

BV = water depth (vertically mixed)
 BH = Gaussian 1/e (37%) horizontal half-width, normal to trajectory
 S = hydrodynamic centerline dilution
 C = centerline concentration (includes reaction effects, if any)

X	Y	Z	S	C	BV	BH
10.51	5.88	0.00	1.0	0.102E+02	4.46	6.98
11.09	5.91	0.00	1.2	0.818E+01	4.46	7.00

Jet/plume RESTRATIFIES at the above position.

BV = Gaussian 1/e (37%) vertical thickness

Maximum lateral extent of recirculation bubble.

14.00	5.97	0.00	1.3	0.760E+01	4.41	7.77
-------	------	------	-----	-----------	------	------

End of recirculation bubble at the above position.

Dilution in recirculation bubble = 1.7

Corresponding concentration = 0.607E+01

Flow continues as WALL JET/PLUME.

39.63	0.00	0.00	1.6	0.623E+01	3.03	22.68
67.59	0.00	0.00	1.9	0.529E+01	2.93	25.65
95.55	0.00	0.00	2.2	0.468E+01	2.87	28.34
123.51	0.00	0.00	2.4	0.426E+01	2.82	30.83
151.47	0.00	0.00	2.6	0.394E+01	2.79	33.17
179.43	0.00	0.00	2.8	0.368E+01	2.75	35.40
207.38	0.00	0.00	2.9	0.347E+01	2.72	37.53
235.34	0.00	0.00	3.1	0.330E+01	2.69	39.58
263.30	0.00	0.00	3.2	0.314E+01	2.67	41.56
291.26	0.00	0.00	3.4	0.301E+01	2.64	43.47

Cumulative travel time = 372. sec

END OF CORSURF (MOD310): BUOYANT SURFACE JET - NEAR-FIELD

** End of NEAR-FIELD REGION (NFR**) **

Some bank/shore interaction occurs at end of near-field.

Efflux conditions:

X	Y	Z	S	C	BV	BH
0.00	0.00	0.00	1.0	0.123E+02	4.32	5.01

END OF MOD301: DISCHARGE MODULE

BEGIN MOD302: ZONE OF FLOW ESTABLISHMENT

Control volume inflow:

X	Y	Z	S	C	BV	BH
0.00	0.00	0.00	1.0	0.123E+02	4.32	5.01

RAPID DEFLECTION by ambient current:

Profile definitions:

BV = top-hat thickness, measured vertically
 BH = top-hat half-width, measured horizontally from bank/shoreline
 S = hydrodynamic average (bulk) dilution
 C = average (bulk) concentration (includes reaction effects, if any)

Control volume outflow:

X	Y	Z	S	C	BV	BH	SIGMA =
5.01	0.09	0.00	1.0	0.123E+02	4.52	5.02	16.80

Cumulative travel time = 5. sec

END OF MOD302: ZONE OF FLOW ESTABLISHMENT

** End of NEAR-FIELD REGION (NFR**) **

BEGIN MOD341: BUOYANT AMBIENT SPREADING

Profile definitions:

BV = top-hat thickness, measured vertically
 BH = top-hat half-width, measured horizontally from bank/shoreline
 S = hydrodynamic average (bulk) dilution
 C = average (bulk) concentration (includes reaction effects, if any)

Plume Stage 2 (bank attached):

X	Y	Z	S	C	BV	BH
5.01	0.00	0.00	1.0	0.123E+02	4.46	4.95
419.95	0.00	0.00	3.6	0.345E+01	1.50	52.50
834.88	0.00	0.00	10.6	0.116E+01	2.84	82.43
1249.82	0.00	0.00	24.0	0.514E+00	4.91	107.67

Cumulative travel time = 1215. sec

END OF MOD341: BUOYANT AMBIENT SPREADING

BEGIN MOD361: PASSIVE AMBIENT MIXING IN UNIFORM AMBIENT

Vertical diffusivity (initial value) = 0.612E-01 m²/s
 Horizontal diffusivity (initial value) = 0.765E-01 m²/s

Profile definitions:

BV = Gaussian s.d.*sqrt(pi/2) (46%) thickness, measured vertically
 = or equal to water depth, if fully mixed
 BH = Gaussian s.d.*sqrt(pi/2) (46%) half-width,
 measured horizontally in Y-direction
 S = hydrodynamic centerline dilution
 C = centerline concentration (includes reaction effects, if any)

Plume Stage 2 (bank attached):

X	Y	Z	S	C	BV	BH
1249.82	0.00	0.00	24.0	0.514E+00	4.91	107.67

Plume interacts with BOTTOM.

The passive diffusion plume becomes VERTICALLY FULLY MIXED within this prediction interval.

1499.88	0.00	0.00	24.0	0.495E+00	4.91	107.94
---------	------	------	------	-----------	------	--------

Efflux conditions:

X	Y	Z	S	C	BV	BH
0.00	0.00	0.00	1.0	0.967E+01	3.05	2.49

END OF MOD301: DISCHARGE MODULE

BEGIN MOD302: ZONE OF FLOW ESTABLISHMENT

Control volume inflow:

X	Y	Z	S	C	BV	BH
0.00	0.00	0.00	1.0	0.967E+01	3.05	2.49

VERTICAL MIXING occurs in the initial zone of flow establishment.

Profile definitions:

- BV = Gaussian 1/e (37%) vertical thickness
- BH = Gaussian 1/e (37%) horizontal half-width, normal to trajectory
- S = hydrodynamic centerline dilution
- C = centerline concentration (includes reaction effects, if any)

Control volume outflow:

X	Y	Z	S	C	BV	BH	SIGMA =
2.12	2.35	0.00	1.0	0.967E+01	3.50	4.67	19.18

Cumulative travel time = 1. sec

END OF MOD302: ZONE OF FLOW ESTABLISHMENT

BEGIN CORSURF (MOD310): BUOYANT SURFACE JET - NEAR-FIELD

Surface jet in deep crossflow with shoreline-attachment.

Profile definitions:

- BV = water depth (vertically mixed)
- BH = Gaussian 1/e (37%) horizontal half-width, normal to trajectory
- S = hydrodynamic centerline dilution
- C = centerline concentration (includes reaction effects, if any)

X	Y	Z	S	C	BV	BH
2.12	2.35	0.00	1.0	0.967E+01	3.50	4.67
2.57	2.47	0.00	1.2	0.795E+01	3.52	4.68

Jet/plume RESTRATIFIES at the above position.

BV = Gaussian 1/e (37%) vertical thickness

24.24	5.94	0.00	2.0	0.473E+01	1.81	6.61
-------	------	------	-----	-----------	------	------

Maximum lateral extent of recirculation bubble.

36.88	6.31	0.00	2.3	0.429E+01	1.64	7.58
-------	------	------	-----	-----------	------	------

End of recirculation bubble at the above position.

Dilution in recirculation bubble = 1.9

Corresponding concentration = 0.513E+01

Flow continues as WALL JET/PLUME.

46.25	0.00	0.00	2.4	0.405E+01	1.59	15.85
68.26	0.00	0.00	2.6	0.368E+01	1.50	17.40
90.27	0.00	0.00	2.8	0.343E+01	1.42	18.88
112.27	0.00	0.00	3.0	0.325E+01	1.36	20.29
133.82	0.00	0.00	3.1	0.311E+01	1.32	21.63
155.83	0.00	0.00	3.2	0.300E+01	1.28	22.94
177.83	0.00	0.00	3.3	0.290E+01	1.24	24.22
199.84	0.00	0.00	3.4	0.282E+01	1.21	25.45
221.38	0.00	0.00	3.5	0.275E+01	1.18	26.63

Cumulative travel time = 226. sec

END OF CORSURF (MOD310): BUOYANT SURFACE JET - NEAR-FIELD

** End of NEAR-FIELD REGION (NFR**) **

The initial plume WIDTH/THICKNESS VALUE in the next far-field module will be CORRECTED by a factor 1.41 to conserve the mass flux in the far-field!

BEGIN MOD301: DISCHARGE MODULE

Efflux conditions:

X	Y	Z	S	C	BV	BH
0.00	0.00	0.00	1.0	0.560E+01	2.13	2.44

END OF MOD301: DISCHARGE MODULE

 BEGIN MOD302: ZONE OF FLOW ESTABLISHMENT

Control volume inflow:

X	Y	Z	S	C	BV	BH
0.00	0.00	0.00	1.0	0.560E+01	2.13	2.44

VERTICAL MIXING occurs in the initial zone of flow establishment.

Profile definitions:

BV = Gaussian 1/e (37%) vertical thickness
 BH = Gaussian 1/e (37%) horizontal half-width, normal to trajectory
 S = hydrodynamic centerline dilution
 C = centerline concentration (includes reaction effects, if any)

Control volume outflow:

X	Y	Z	S	C	BV	BH	SIGMA =
2.64	2.58	0.00	1.0	0.560E+01	2.80	4.46	23.63

Cumulative travel time = 1. sec

END OF MOD302: ZONE OF FLOW ESTABLISHMENT

 BEGIN CORSURF (MOD310): BUOYANT SURFACE JET - NEAR-FIELD

Surface jet in deep crossflow with shoreline-attachment.

Profile definitions:

BV = water depth (vertically mixed)
 BH = Gaussian 1/e (37%) horizontal half-width, normal to trajectory
 S = hydrodynamic centerline dilution
 C = centerline concentration (includes reaction effects, if any)

X	Y	Z	S	C	BV	BH
2.64	2.58	0.00	1.0	0.560E+01	2.80	4.46
30.58	8.34	0.00	1.6	0.356E+01	4.28	4.79
Maximum lateral extent of recirculation bubble.						
58.44	5.35	0.00	1.9	0.299E+01	3.51	5.07
59.63	5.08	0.00	1.9	0.298E+01	3.44	5.08
End of recirculation bubble at the above position.						
Dilution in recirculation bubble = 2.3						
Corresponding concentration = 0.248E+01						
Flow continues as WALL JET/PLUME.						
85.89	0.00	0.00	1.9	0.288E+01	2.13	10.61
113.99	0.00	0.00	2.0	0.280E+01	2.13	11.06
141.47	0.00	0.00	2.0	0.273E+01	2.13	11.47
169.56	0.00	0.00	2.1	0.267E+01	2.13	11.86
197.04	0.00	0.00	2.1	0.261E+01	2.13	12.23
225.14	0.00	0.00	2.2	0.256E+01	2.13	12.58
252.62	0.00	0.00	2.2	0.252E+01	2.13	12.90
280.10	0.00	0.00	2.3	0.248E+01	2.13	13.20

Cumulative travel time = 162. sec

END OF CORSURF (MOD310): BUOYANT SURFACE JET - NEAR-FIELD

 ** End of NEAR-FIELD REGION (NFR**) **

The initial plume WIDTH/THICKNESS VALUE in the next far-field module will be CORRECTED by a factor 1.24 to conserve the mass flux in the far-field!

Appendix B

Far Field Locator Outputs

FFLOCATR RESULTS FILE:

FFLOCATR: FAR-FIELD PLUME LOCATOR Version 2.1, AUGUST 2002

Far-field data values from CORMIX3 prediction:

FILE NAME: C:\...\Desktop\slope cases\NebCity_9_12_ave_velocity.prd
 Site Name: NebCity Power Station_Missouri River
 Design Case: CORMIX 3- Surface Discharge (Heated)
 Time Stamp: Tue Oct 8 17:53:38

Channel characteristics (metric):
 BS = 182.00 HA = 4.57 UA = 1.21
 BANK = right DISTB = 0.00
 STRCND= U uniform density environment

Pollutant data:
 C0 = 9.67 CUNITS= deg.C

CUMULATIVE DISCHARGE DATA (m):
 FFL INPUT FILE NAME: \\W...\CORMIX Simulations\CORMIX Simulation\Nebcity.ffi
 Data label: Cumulative Discharge

Cumulative discharge measured from right hand bank.

Number of Cross-sections(XS): 3

XS'Label-'	Dist.	10%	20%	30%	40%	50%	60%	70%	80%	90%	100%
1 '381-m'	381.	18.7	29.1	40.5	53.7	67.8	75.0	90.0	110.0	125.0	140.0
2 '762-m'	762.	19.2	35.2	48.8	64.4	81.1	90.0	120.0	135.0	150.0	170.0
3 '1524-m'	1524.	28.0	49.6	79.4	106.3	125.0	140.0	155.0	170.0	183.0	190.0

FAR-FIELD PLUME PROPERTIES (m):

Plume location measured in XS from right hand bank.

XS #	'Label-'	Distance downstream	Left edge	Plume centerline	Right edge	Dilution	Conc.
1	'381-m'	381.00	40.35	0.00	0.00	4.8	0.200E+01
2	'762-m'	762.00	77.10	0.00	0.00	10.9	0.885E+00
3	'1524-m'	1524.00	157.01	0.00	0.00	33.2	0.290E+00

END OF FFLOCATR: FAR-FIELD PLUME LOCATOR

